NOTE TO USERS

DISSERTATION

MODELING REGIONAL CLIMATE CHANGE IMPACTS ON AVAILABLE WATER FOR AGRICULTURE

Submitted by

Elgaali Attalla Elgaali

Department of Civil Engineering

In partial fulfillment of the requirements
for the degree of Doctor of Philosophy
Colorado State University
Fort Collins, Colorado
Spring 2005

COLORADO STATE UNIVERSITY

December 5, 2004

WE HEREBY RECOMMEND THAT THE DISSERTATION PREPARED UNDER OUR SUPERVISION BY ELGAALI ATTALLA ELGAALI ENTITLED MODELING REGIONAL CLIMATE CHANGE IMPACTS ON AVAILABLE WATER FOR AGRICULTURE BE ACCEPTED AS FULFILLING IN PART REQUIREMENTS FOR THE DEGREE OF DOCTOR OF PHILOSOPHY.

Committee on graduate work

Co-advisor

Advisor

Department Head

ABSTRACT

Modeling Regional Climate Change Impacts on Available Water for Agriculture

There is mounting evidence that increasing amounts of atmospheric carbon dioxide may lead to significant changes in global climate during this century. Global warming may have tremendous consequences for irrigated agriculture around the world; and the welfare of the communities in regions that depend on irrigation may be critically affected by climate change. The possible effects of such climatic changes on water resources for agriculture in the Arkansas River basin in Colorado, U.S., have been investigated. My aim is to improve the estimates of the potential impacts of climate change on the availability of irrigation water by using higher resolution climate scenarios, smaller temporal and spatial analysis scale and provide results that will be useful for the water planning and management decision-making processes.

Results from general circulation models indicate that the potential impacts of climate change on this region include changes in winter snowfall and snow melt, seasonal rainfall amounts and intensities and winter and summer time average temperatures. Therefore, a framework was developed to quantify the effects of these seasonal impacts on the availability of irrigation water. Monthly surface water supplies, consumptive use, and water balance are estimated using neural networks, consumptive use, and water balance models respectively.

As part of this study I used two transient climate scenarios extracted at high resolution from two General Circulation Models (GCM's); the HAD (Hadely center) and the CCC (Canadian Center). The high resolution was obtained by downscaling the output of the two GCM's to half-degree spatial resolution. Each GCM transient climate scenario was generated assuming 1% annual increase in CO_2 concentrations.

The methodology and results described in this study are contributing to the national analysis of impacts of climate change on the water sector.

The frame work developed as part of this research will help a region plan for changes in water supply and demand and will give decision-makers a tool for evaluating the impacts of climate change. The data driven nature of the frame work makes it flexible so that it can be applied to different areas.

Elgaali Attalla Elgaali
Department of Civil Engineering
Colorado State University
Fort Collins, CO 80523
Spring, 2005

ACKNOWLEDGEMENTS

Over the past several years numerous people contributed to help me finish this dissertation. These people have shaped my work and my life and helped to make me who I am. My appreciation goes to them all.

My thanks to my academic advisors **Dr. Luis Garcia**, **Dr. Dennis Ojima** – and committee members – **Dr. Jim Loftis** and **Dr. Jose Salas**. Special thanks and appreciation are due **Dr. Luis Garcia** for his contributions. Each contribution has been a blessing: the personal, scholar, financial, and professional support. Thank you **Dr. Garcia** for the dedication, the stimulating ideas, the words of encouragement, the commitment to excellence, the constructive critiques, the tolerance, the friendship. I am forever indebted to **Dr. Ojima** for his frequent and candid input, and his unselfish support.

I would also like to express my deep gratitude and appreciation to the members of my graduate committee **Dr. Jim Loftis** and **Dr. Jose Salas** for their valuable comments and suggestions during the course of the research, and their invaluable comments on this manuscript.

A number of others made extraordinary contributions toward the completion of this work. David Patterson of the Colorado State University, Integrated Decision Support group (IDS), Civil Engineering Department made invaluable contributions to my computer works. I am also thankful to Leslie Patterson at IDS for helping edit this manuscript. The assistance of Steve Knox and Suzy Lutz at Colorado State University,

Natural Resources Ecology Laboratory (NREL) is very much appreciated. Their help in extracting climate and crop data was priceless.

Much appreciation to a number of special friends at IDS for providing a healthy and pleasant environment throughout the years of this research.

To my wonderful family, my wife Omaima, son Khalid, and daughters Amel and Raghd thanks for your support, inspiration, and encouragement.

To my big and small family to whom I am most indebted

TABLE OF CONTENTS

LIST OF TABLES

LIST OF FIGURES

1. INTRODUCTION

1.1 Background

Extent of Climate Change

In many areas of the world, agricultural production is threatened by water supply shortages. Currently, about 17% of the world's cropland is under irrigation (Rosenzweig and Hillel 1998). In the United States, irrigation represents about 81% of the total water demand and consumes 41% of the water supply (Solley et al. 1993). In the Great Plains of the United States, surface water supplies have been declining since 1980 forcing 12% of the cropland in the region to be retired from irrigation (Dugan et al., 1994). Due to the shortage in surface water supply the use of groundwater for irrigation has expanded and aquifer depletion is becoming a serious issue. The Ogallala aquifer, a main source of water in the Great Plains, has been pumping about 16.6 million acre-feet each year since 1940 without enough recharge to compensate for withdrawals (Rosenberg et al. 1999). Moreover, changes in water utilization are making the competition for water between agriculture and other uses (e.g. urban development) more intense (Ojima et al., 1999).

There is mounting evidence that increasing amounts of carbon dioxide (CO2) may lead to significant changes in global climate during this century (IPCC 2001). Increasing amounts of CO2 and other greenhouse gases will raise global temperatures causing what is known as global warming. Global warming, if it occurs as projected, might have important impacts on water resources and agriculture. The change in temperature is

expected to alter precipitation and evapotranspiration, the prime drivers of water availability and agricultural production. Naturally, climate-water-agriculture interactions are of concern not only to the scientific community but to policy makers as well. Proper understanding of these interactions under climate change might help to mitigate the adverse impacts of global warming while selectively reinforcing the positive impacts. Indeed, potential climate change impacts have been assessed for decades. As our understanding about the extent and magnitude of climate change has improved, the need for accurate and detailed predictions of what might occur in the future has become increasingly urgent.

Climate change is expected to further stress water resources. It might widen the gap between the demand for, and supply of, water for irrigation. The changing climate and elevated atmospheric CO_2 are expected to influence irrigation by changing evapotranspiration, precipitation, and available water supplies. The combined effect of these changes would impact the supply and the demand of water. Generally, under warmer conditions the water supply is expected to decrease as demand increases due to rising rates of evaporation and transpiration (Peterson and Keller 1990). Also, in an environment of increased temperature and evaporation, the lack of available water can further stress soil moisture. Stress in soil moisture can greatly reduce agricultural yield (Rosenzweig and Hillel, 1993; Rosenzweig and Hillel, 1998; Ojima et al., 1999).

On the other hand, the physiological effects of high levels of CO_2 on plants, may affect irrigation demand. Generally, high levels of CO_2 enhance stomata closure (the pores in the plant leaf through which water vapor and CO_2 are exchanged with the atmosphere) and increase the plant foliage (increase plant leaf area). Increase in stomata

closure reduces the transpiration in the plant. Meanwhile, an increase in leaf area means a greater number of stomata and hence an increase in transpiration.

1.2 Need for Study

There are many regions around the world that depend mainly on irrigation to provide most of the water required for crop growth. By impacting irrigation, climate change may critically affect the future economical and societal activities in these regions. Therefore, it is an imperative task to project the combined effects, on irrigation, of both the general warming and specific physiological responses of crops to the elevated levels of atmospheric CO_2. Such projections can contribute to assessments of future water resources for agriculture. Currently, the increasing competition between agricultural and other water users provides stimuli for conducting such assessments.

The future availability of water for agriculture will depend on possible changes in hydrological regimes at the watershed and river basin scales. An effective model of climate change that combines weather scenarios with supply and water demand simulations will help the region plan for water supply changes and will give policy-makers a tool for evaluating impacts of climate change.

Potentially, climate change will decrease the supply of water available for agriculture while it increases the demand. As both factors are critical to projecting regional water budgets, both must be considered (Frederick 1993). Water supply is a key factor in determining agricultural potential. In scientific studies of models dealing with irrigation water budgets, water supply is usually assumed sufficient. Such an assumption leads to uncertainties in the projections of the water budgets. The water supply may be affected by changes in quantity, type (snow or rain) and timing of precipitation.

Therefore, detailed regional studies are needed on the relation of climate variables such as snow and rain to surface water supply and the sensitivities of water supply to changes in these climatic variables (Ojima et al., 1999).

Evapotranspiration (ET) is the prime variable in estimating irrigation demand, and the overall effect of climate change on irrigation is to increase crop evapotranspiration (Allen et al., 1991). Integrated assessment studies of climate change impacts on ET at a regional scale are helpful for decision-making (Rosenberg, 1993). Therefore, estimation of regional ET is required in assessing the regional impacts of climate change on irrigation. Current methods of estimating regional crop ET usually ignore the spatial and temporal variability of its parameters thus producing incorrect estimates of irrigation demand (Hashmi and Garcia, 1998). In the past, few studies estimated regional ET and considered its temporal and spatial variability (Hashmi et al., 1993; Mauser and Schadlich, 1998). To study the impacts of climate change on water resources, studies are still needed to reproduce the spatial complexity of actual and projected demand for irrigation water.

A number of studies have used historical analogues and projected climate scenarios to assess the risk to agriculture from climate change (Rosenberg et al., 1990; Peterson and Keller, 1990; Allen et al., 1991; Rosenberg et al., 1993; Peart et al., 1995). These studies have succeeded in providing estimates of the effects of climate change. However, these studies have used results from large- scale climate models that only give reasonable estimates of the consequences of climate change over large geographic areas. Large- scale models, due to coarse resolution (200 km X 200 km), lack precision, and

were found to be unreliable in simulating smaller spatial and temporal scale features (Rosenzweig and Hillel, 1998).

Recent works by Eheart and Tornil, 1999; Ojima et al., 1999; and Jones, 2000 represent a further step in modeling climate change impacts. These studies simulated the climate impacts on areas of smaller scales using models of higher spatial resolution. These studies used a modeling structure that accounts for interacting processes at river basin or regional-scale and subregional-scale (10^3 km^2 or finer). These scales are very supportive to decisions for integrated water management.

Information Needs Identified

Previous research has drawn widespread attention to areas of concern and has helped to foster constructive dialogue on the magnitude and direction of climate change. Previous studies have provided:

- Convincing evidence that amounts of atmospheric carbon dioxide (CO_2) are increasing, and that this increase may lead to significant change in global climate (IPCC, 2001).
- Valuable data establishing that estimates of responses to climate change can be made using climate models such as General or Global Circulation Models (GCM) (e.g. McFarlane et al., 1992; Jonns et al., 1997).
- Demonstration of the utility of using simulation models to estimate the risk climate change poses to water resources and agriculture and to identify the related vulnerable regions (Peterson and Keller, 1990; Allen, 1991; Peart et al., 1995; Ojima et al., 1999).

Research results have identified a number of key issues that must be addressed in order to improve water and land management choices. Future studies need to:

- Build the capability to better address the current competition among the water needs of agriculture and other users as a baseline for potential changes.
- Achieve a detailed understanding of the water budget and cycle for agriculture at a regional scale.

- Quantify the regional water budget so that temporal and spatial distribution of water availability is better understood.
- Address all components of the water cycle including evaporation, transpiration, soil water content, and surface and ground water in the water budgets.
- Link the interaction between these components to current and future climate regimes.

1.3 The Problem and Study Objectives

Careful consideration of prior studies leads to the following statement regarding the research needs; around the world, climate change may have a significant impact on the timing and amount of water that will be available for irrigated agriculture. The welfare of farmers and rural communities in regions that depend on irrigation may be critically affected by climate change. This makes answering the following questions very important:

1. What are the extent and magnitude of the impacts of both the general warming and elevated levels of atmospheric CO_2 on the availability of irrigation water?
2. How does the temporal and spatial complexity of the demand for and supply of water for irrigation vary as a result of variations in climate, soil type, and land cover?

Answering these questions can contribute to assessments of the amount and timing of water that might be available for irrigated agriculture.

Previous studies have used a variety of projected climate change scenarios to estimate a range of potential impacts. Different climate, ecosystem, and water balance models have been developed to estimate the parameters of the soil-vegetation-atmosphere interactions. However, many of these models are of limited use because they lack precision due to their coarse spatial resolution. In addition, the precipitation and hydrological cycles that are especially critical for agriculture are often poorly simulated (Rosenzweig and Hillel, 1998). Furthermore, models must be available for evaluation of

large-scale planning targets in view of detailed design and management issues that arise at smaller scales (Ojima et al., 1999).

The research described here provides a modeling methodology for linking agriculture water potentials to climate change on a scale useful to addressing the distributed nature of the problem. The main goal of this research is to improve the estimates of potential impacts of regional climate change on irrigation water by improving key features of previous research. The improvements include: resolution of climate scenarios (higher), spatial representation of the problem, scale of analysis (monthly and seasonal) of responses and sensitivities to climate changes, and use of multiple crops.

To model the regional climate impacts on crops and water supply a modeling framework will be developed consisting of a water supply and spatial consumptive use model. The use of spatial approach for estimation of irrigation demand is to minimize errors and achieve higher accuracy level. Conversion of precipitation data into water supply estimates is a complex and difficult process using the traditional methods. Artificial Neural Network (ANN) models hold the possibility of facilitating these difficulties by training the network to map the relationship between precipitation and water supply estimates. In this study the potential of ANN models will be demonstrated for simulating the relationship between precipitation and water supply. For this scale of analysis, smaller spatial and temporal resolutions produce more accurate results. This framework will develop a modeling structure that accounts for interacting processes at basin or regional-scale. First, these models will be calibrated using historical data and then applied using different climate scenarios.

Studies of climate change impact assessments, generally, use historical and scenario-driven approaches to design and conduct simulations of climate change impacts. The majority of these approaches have been using equilibrium scenarios those representing stable climate at some point in the future when CO_2 is doubled. In practice, climate is expected to increase gradually (transient) as a function of gradual increase in CO_2. Even though there have been very few studies based on transient scenarios. Arnell, 1996 reported that, there are three reasons why it would be useful to study the effect of transient climate change. First, transient studies give insights into the effects of climatic change trend and year-to-year variability. Second, transient projections give an indication of the potential rate of change, which may be very important in terms of adaptation to change. Finally, transient simulations could provide information on when certain critical thresholds are likely to be crossed. Therefore, in this study a transient scenario-driven approach is used to design and conduct the simulations of climate change impacts.

Research Objectives

The questions that have been raised in this research will be answered by meeting the following objectives for the Arkansas River Basin in Colorado:

1. Develop an artificial neural network (ANN) based methodology to estimate water supply for agriculture.
2. Using the ANN reproduce the approximate magnitudes of historical and future water supply available for irrigation as compared to the measured water supplies (baseline).
3. Develop a spatial model to estimate crop ET and water demand.
4. Reproduce the spatial complexity of actual and projected demand for irrigation water.

5. Quantify the impacts of climate change and elevated atmospheric CO_2 on the supply and demand of irrigation water.
6. Generate current and potential regional irrigation water budgets.
7. Evaluate the climate impact on regional agricultural water availability and consumptive use.

2. STUDY AREA DESCRIPTION

2.1 Arkansas River Basin General Description

2.1.1 Location and Physiography

This study focuses on a portion of the Arkansas River Basin known as the Arkansas valley in southeastern Colorado. The Arkansas River Basin refers to the Great Plains area bounded on the west by the Rocky Mountains and by Kansas, New Mexico and Oklahoma on the east and the south (Fig 2.1). It covers approximately 72,742 km^2 (28,415 square miles) about 27 percent of the state of Colorado. It is about 400 km (250 miles) long (east to west) and average about 240 km (150 miles) wide (north to south).

The Arkansas River itself heads near Leadville, at an elevation over 3,050 m (10,000 feet) above sea level. The river drops rapidly until it emerges from the mountains near Pueblo, then runs in an easterly direction until it reaches the Colorado-Kansas border near Holly at an elevation of approximately 1,036 m (3,400 feet).

2.1.2 Climate

Temperature

Temperature and precipitation vary widely in response to topographic differences and the areal extent of the region. Average annual temperatures range from 2 °C at Leadville near its head waters in the Rocky Mountains to 12 °C at Lamar in the lower valley. Seasonal variations in temperature are very large, and high temperatures characterize the region as a whole in the summer and low temperatures in the winter and spring. Table 2.1 shows mean temperatures for selected locations in the basin.

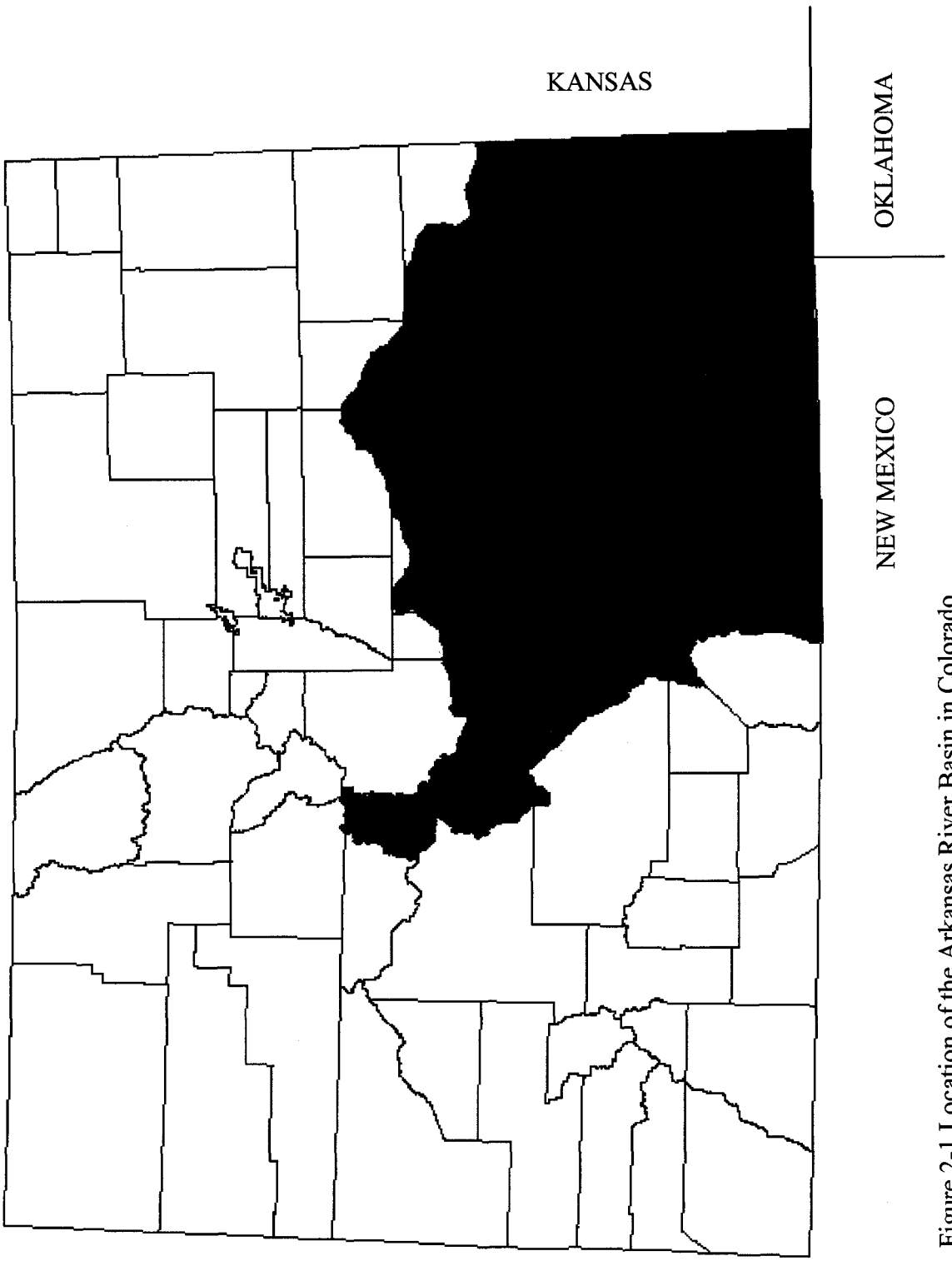

Figure 2-1 Location of the Arkansas River Basin in Colorado

Table 2-1 Mean Air Temperature (Average 1971-2000)

Month	Leadville	Canon City	Las Animas	Lamar
	Mean Temperature °C			
January	-9.5	1.4	-0.9	-1.5
February	-8.0	3.4	2.7	2.0
March	-4.5	6.4	7.3	6.6
April	-1.8	10.3	12.1	11.6
May	3.9	15.2	17.5	16.9
June	8.8	20.4	23.0	22.4
July	11.6	23.4	25.8	25.2
August	10.8	22.3	24.6	24.2
September	6.9	17.9	19.8	19.4
October	2.3	12.2	12.7	12.1
November	-5.2	5.3	4.3	3.7
December	-9.7	1.9	-0.3	-0.8
Annual	0.6	11.8	12.4	11.9

Precipitation

Precipitation is distributed unevenly throughout the year and amounts range from 9 to 12 inches per year in the middle and the eastern part of the region, 16 to 20 inches in the western part, and as much as 45 inches in the highest mountain ranges. Much of the precipitation at high elevations occurs as snow. Runoff from this snowfall is at a maximum in late spring and early summer (May – June). This runoff constitutes the water supply for different water uses such as recreation. Figure 2.2 shows the distribution of the annual precipitation over the whole basin.

Growing Season

Summers are cool in the mountains and warm in the plains portion of the basin. A maximum temperature over the last thirty years of 35° C has been recorded at Las Animas during July. An average January minimum temperature of -13° C has also been recorded in Las Animas, which implies that large temperature variations occur. The average frost-free season (of 0 °C (32 °F) threshold) varies from 85 days at Leadville to 167 days at Canon City, 161 days at Las Animas and 162 days at Lamar.

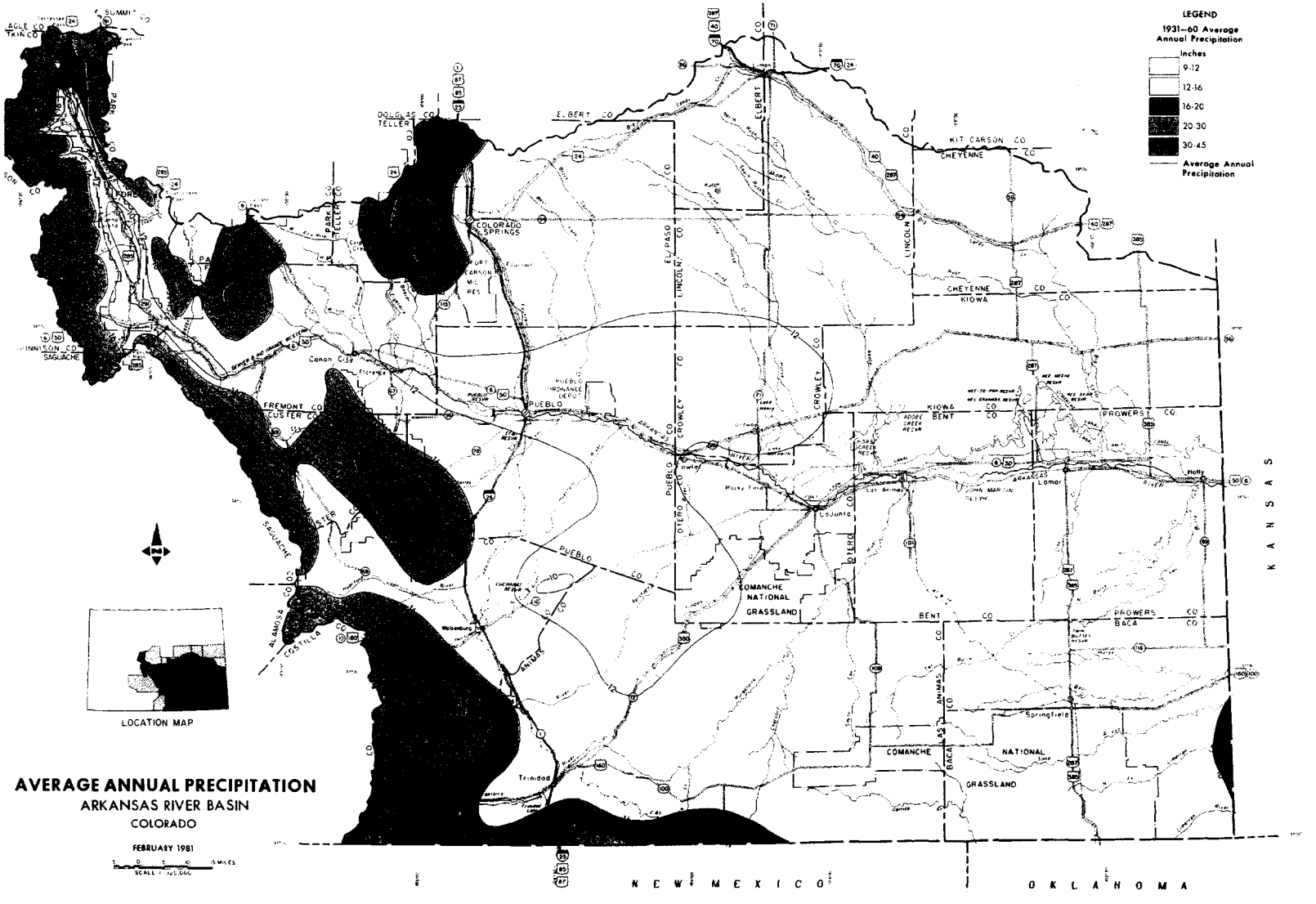

Fig 2.2 Average annual precipitation in the Arkansas River Basin (source: SCS-USDA, 1981)

2.1.2 Water

Surface Water

The greatest runoff in the basin comes from snowmelt in the large mountain systems at the western border of the region. Water supply varies from year to year depending on the winter snow pack in the mountains. In general, more than 60 percent of the average annual runoff occurs during April through July, and 20 percent during August through October.

Trans-Basin Diversions are a significant addition to the basin water supply. There is an extensive system of canals, tunnels, and reservoirs for collecting and transporting water from the west side of the Continental Divide to the Arkansas Basin.

Lakes and reservoirs in the basin serve the important function of controlling natural runoff. Runoff from snowmelt usually peaks during May and early June, but peak demand for water generally occurs in July and August. Reservoir storage is used to meet part of the demand, which is mainly for irrigation. In addition, some reservoirs and lakes also serve as recreation areas, fish and wildlife habitat, and flood control structures.

Diversions

Diverted water is applied to crops and pastureland in the basin through a huge system of ditches and canals. Twenty-one of these canals are used in this study. These are the major canals serving the farmlands in the valley that extends from Pueblo west to the Kansas State border east. Table 2.2 shows the total diversions for those canals being studied. In general, the amount of water diverted to these systems average 1.07 hectare-meter for 106,515 hectares (3.5 acre feet for 263,000 acres) served (21 canals). The surface diversion data was summarized from records of the Colorado State Engineer Office in Denver.

Table 2-2 Irrigation Diversions (Average 1950-2000)

Ditch	Hectares Served	Diversions (ha-m)
Bessemer	7,028	7,760
Booth	1,89	497
Excelsior	8,75	293
Collier	2,03	86
Colorado	9,279	10,680
RF Highline	8,020	10,284
Oxford	1,910	3,067
Otero	1,159	838
Catlin	6,943	10,990
Holbrook	5,286	5,274
Rocky Ford	2,184	5,381
Ft Lyon	3,5602	29,900
Las Animas	2,637	3,898
Fort Bent	1,768	2,067
Keese	754	660
Amity	1,5252	9,890
Lamar Manvel	3,180	5,086
Hyde	499	284
XY Graham	1,764	1,107
Buffalo	1,984	2,437
Total	10,6515	7,760

Groundwater

There are three major aquifers in the basin: (1) the Valley fill in the valleys of the Arkansas River and its major tributaries, (2) the Ogallala formation underlying the high plains, and (3) the Dakota Sandstone underlying the major portion of the basin east of the foothills. The valley fill along the Arkansas River is the main source of supplemental groundwater for irrigation (Arkansas River Basin, Cooperative Study Report, 1981). This aquifer generally consists of sand and gravel to depths up to 30 m (100 feet) along the main stem near Holly. The aquifer is very productive with some large capacity wells producing nearly 2,000 gallons per minute. There are about 2,500 large capacity wells between Pueblo and the state line.

2.1.3 Land

Soils

The general soil map (USDA, NRCS) shown in Fig. 2.3 locates soils with similar characteristics and suitability within the basin. Broad characteristics and relationships are then used to interpret the potential of soils for agricultural and other uses.

The general soils map was prepared by delineating 42 mapping units that differ from each other in the kinds of soils that are present. Soils in each mapping unit form patterns that are repeated from place to place. Soil mapping units are placed in seven major groups. The parent materials of the soils in the basin are a mix of weathered materials and wind deposits and others are alluvium. Generally, the slopes range from very steep at the high mountains to nearly level down the river valley. The farmlands are characterized by slopes ranging from nearly level to gentle and steep.

Geology

The Arkansas River Basin lies in the southern Rocky Mountain province and the Great Plains province. The western portion of the basin, southern Rocky Mountain province, is composed mainly of ancient granitic and metamorphic rocks, but includes also Paleozoic sediments, Tertiary intrusive and extrusive rocks and sediments, and glacial lake and stream deposits.

The eastern portion, Great Plains province, include portions of three sections; the Colorado Piedmont, the Raton section and the High Plains.

The Piedmont and Raton sections are composed of Cretaceous shale, chalk, limestone, and sandstone, but adjacent to the mountains are upturned beds of older Mesozoic and Paleozoic sediments and there are small areas of Tertiary and Quatenary sediments and volcanic rocks.

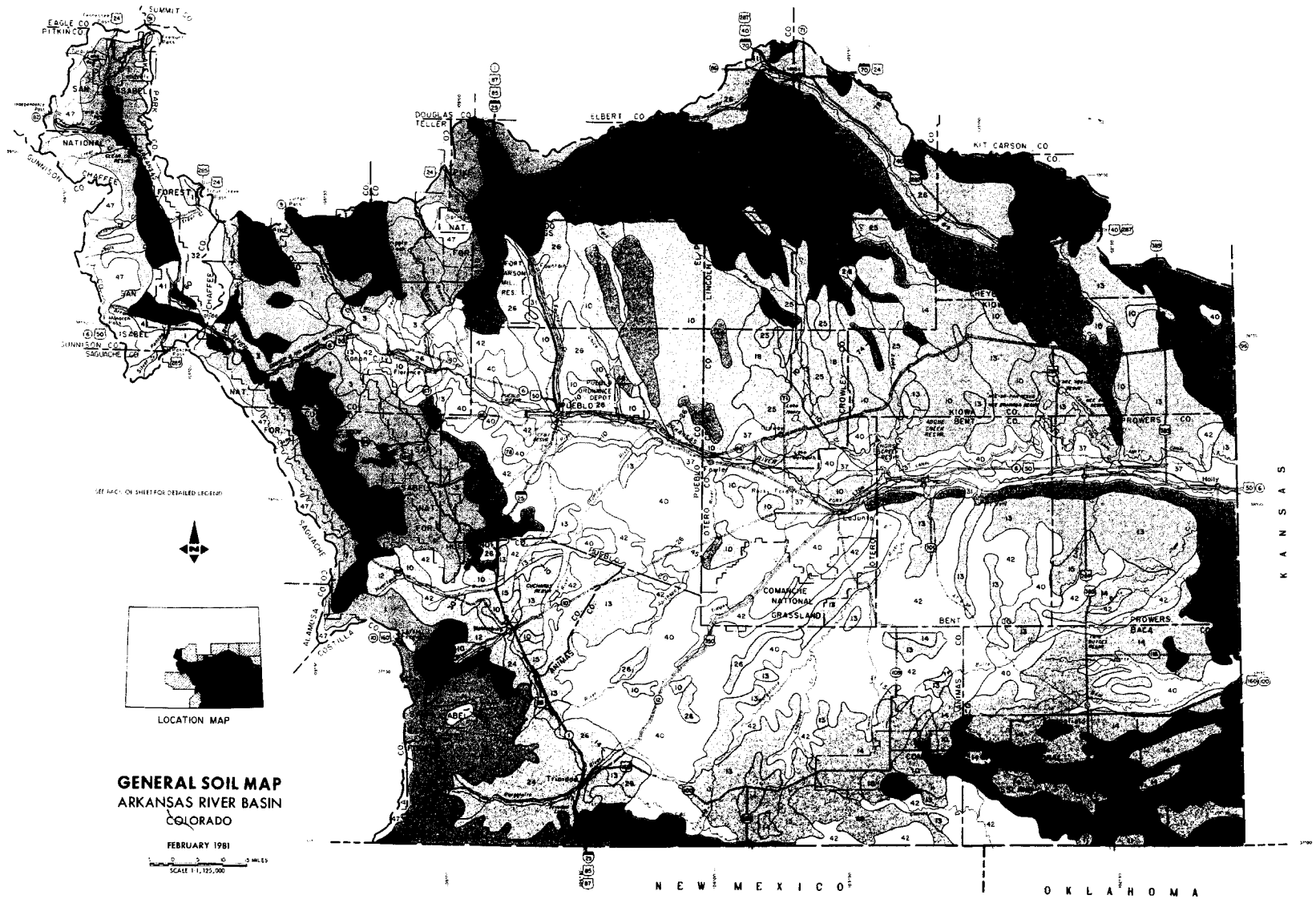

Fig 2.3 Distribution of soil type in the Arkansas River Basin (source: SCS-USDA, 1981)

LEGEND

GROUP I — ALFISOLS

BORALFS

1 Typic Cryoboralfs, skeletal-Rock Outcrop: sloping to steep

3 Typic Eutroboralfs, clayey-Rock Outcrop: steep

4 Psammentic Eutroboralfs-Aridic Haploborolls: loamy; gently sloping and sloping

GROUP II — ARIDISOLS

ARGIDS

10 Ustollic Haplargids: loamy; nearly level and gently sloping

11 Ustollic Haplargids-Ustic Torriorthents (shallow): loamy; gently sloping to steep

12 Ustollic Haplargids, loamy-Rock Outcrop: gently sloping to steep

13 Ustollic Haplargids, silty-Ustollic Haplargids, loamy-Ustic Torriorthents, silty: nearly level to sloping

14 Ustollic Haplargids, clayey-Ustollic Haplargids, silty-Ustollic Paleargids, clayey: nearly level and gently sloping

15 Ustollic Haplargids, clayey-Ustic Torriorthents, loamy (shallow): gently sloping to steep

18 Ustollic Natrargids, clayey-Ustollic Haplargids, loamy: nearly level to sloping

ORTHIDS

24 Lithic Camborthids-Lithic Ustic Torriorthents: loamy; steep

25 Usteric Camborthids: clayey; nearly level

26 Ustollic Camborthids-Ustic Torriorthents (shallow): clayey; nearly level to sloping

GROUP III — ENTISOLS

FLUVENTS

30 Ustic Torrifluvents: loamy; nearly level and gently sloping

31 Ustic Torrifluvents-Typic Fluvaquents: loamy; nearly level

ORTHENTS

37 Ustic Torriorthents-Ustollic Calciorthids: loamy; nearly level

40 Ustic Torriorthents, silty-Lithic Ustic Torriorthents, loamy: gently sloping

42 Lithic Ustic Torriorthents, loamy-Rock Outcrop: gently sloping to steep

GROUP IV

ORTHENTS

32 Lithic Cryorthents, skeletal-Rock Outcrop: steep

41 Lithic Ustic Torriorthents-Ustic Torriorthents: loamy; sloping to steep

GROUP V

PSAMMENTS

45 Ustic Torripsamments: gently sloping to steep

46 Ustic Torripsamments-Ustollic Haplargids, loamy: gently sloping to moderately steep

GROUP VI — INCEPTISOLS

UMBREPTS

47 Pergelic Cryumbrepts, skeletal-Pergelic Cryochrepts, skeletal-Rock Outcrop: sloping to steep

GROUP VII — MOLLISOLS

AQUOLLS

49 Typic Cryaquolls-Argic Cryaquolls, loamy-Cumulic Cryaquolls: loamy; nearly level and gently sloping

BOROLLS

50 Aridic Argiborolls-Lithic Argiborolls: skeletal; sloping to steep

53 Aridic Calciborolls, skeletal-Aridic Calciborolls, loamy: sloping to steep

55 Typic Cryoborolls, loamy-Rock Outcrop: sloping to steep

56 Typic Cryoborolls, clayey-Typic Cryoborolls, skeletal: moderately steep and steep

57 Typic Cryoborolls-Typic Cryothents: clayey; sloping to steep

58 Argic Cryoborolls-Typic Cryoborolls: loamy; gently sloping to steep

60 Aridic Haploborolls, loamy-Torriorthentic Haploborolls, loamy-Aridic Argiborolls, clayey: gently sloping to steep

61 Lithic Haploborolls, skeletal-Rock Outcrop: moderately steep and steep

GROUP VIII

USTOLLS

64 Aridic Argiustolls-Ustollic Haplargids: loamy; nearly level to sloping.

67 Aridic Argiustolls-Aridic Haplustolls: loamy; gently sloping to moderately steep

68 Aridic Argiustolls-Lithic Haplustolls: loamy; gently sloping to steep

69 Aridic Argiustolls, loamy-Torriorthentic Haplustolls, sandy: nearly level and gently sloping

70 Aridic Argiustolls, loamy-Aridic Paleustolls, clayey: nearly level and gently sloping

71 Aridic Argiustolls, clayey-Ustollic Haplargids, loamy: nearly level

74 Pachic Argiustolls-Aridic Argiustolls: clayey and silty; nearly level

75 Torrertic Argiustolls-Ustic Torriorthents (shallow): clayey; gently sloping to steep

77 Aridic Paleustolls-Ustollic Haplargids: clayey; nearly level to sloping

78 Aridic Paleustolls, clayey-Ustollic Paleargids, silty-Ustic Torriorthents, silty: nearly level to gently sloping

The soil bodies delineated on the "General Soil Map of Colorado" are called "Soil Map Units." Each one of these map units represents an area containing more than one different kind of soil. Only the major or important soils in each map unit are described. Different kinds of soils are closely associated and characteristically occur together within particular types of landscape settings. It is very important to remember that the soil map units are not grouped according to similar or like soils.

The first part of the name of a soil map unit is that of a Soil Subgroup. A Subgroup is one of the classes of soils described and defined in "Soil Taxonomy, A Basic System of Soil Classification for Making and Interpreting Soil Surveys." Terms describing the broad soil textural classes, amounts of rock fragments and slopes complete the name.

This map was made by combining delineations on more detailed soil maps available from the Soil Conservation Service and by predicting soil boundaries in areas where more detailed maps are not available.

Various temperature regimes are represented by using two shades of a color.

Most of the geologic material covering the Great Plains has been stripped by erosion from Piedmont and Raton sections. The remaining portions are composed mainly of the Ogallala formation (Arkansas River Basin, Cooperative Study Report, 1981).

Land Use

Land use refers to the kind of activity for which any given parcel of land is being utilized. The majority of the acreage of land in the Basin is used as native range, cropland, and pastureland with livestock being the significant source of income throughout. The other land uses including urban and built up areas, transportation (federal, state and county roads, and railroads), military installations and land designated for recreation and wildlife habitat. Water covers portions of the area in the form of lakes, reservoirs, canals, wetlands, and streams. Figure 2.4 shows the kinds and distribution of land uses over the whole river basin.

Many areas, particularly in the eastern two thirds of the Basin, are used for nonirrigated cropland production of winter wheat, forage and grain sorghum and to a lesser extent, corn, beans and silage corn.

The wide benches along the Arkansas River are irrigated with river water and produce a variety of cash and forage crops. Figure 2.5 shows the prime farmlands in the region. Primary irrigated crops in the region include alfalfa, corn for grain or silage, with significant amounts of grass hay, and beans. Other crops, including various vegetables, barley, and irrigated wheat are also grown. Irrigation methods used include open furrow and sprinkler. Water for irrigation is supplied by a complex surface distribution system and small amount by pumping from alluvial deposits.

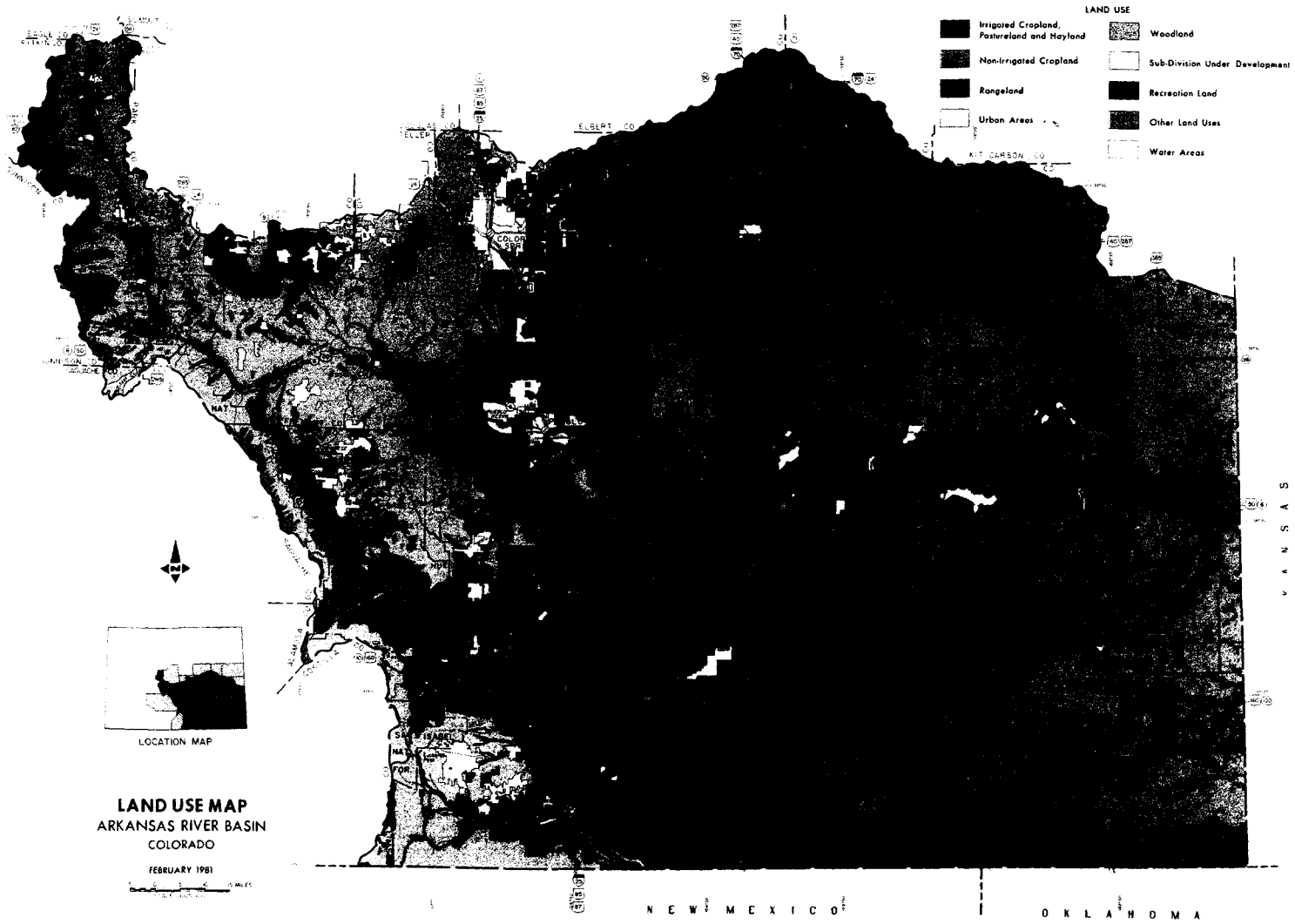

Fig 2.4 Landuse types in the Arkansas River Basin (source: SCS-USDA, 1981)

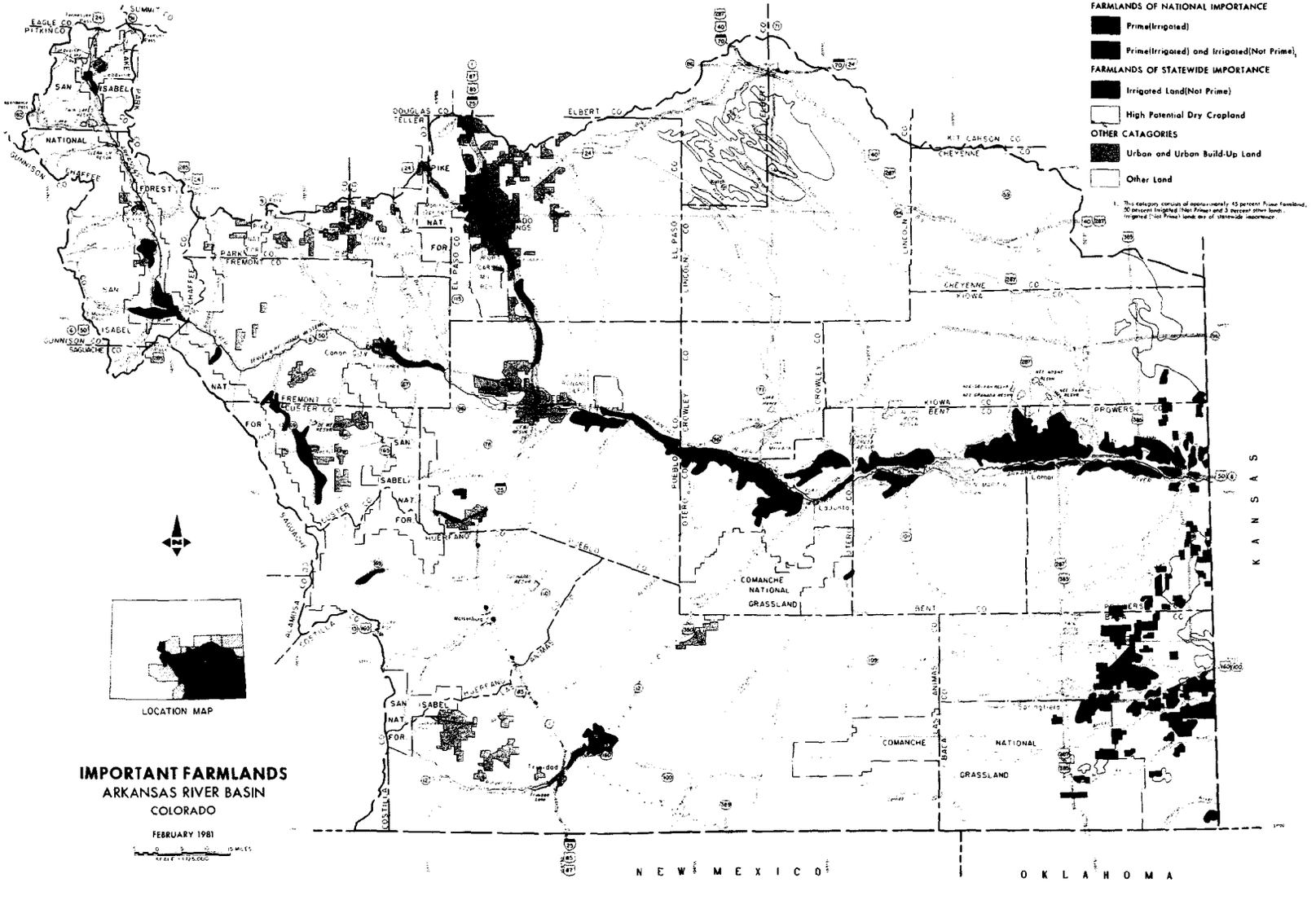

Fig 2.5 Main farmlands in the Arkansas River Basin (source: SCS-USDA, 1981)

3. LITERATURE REVIEW

3.1 Introduction

There is a growing awareness of the extent to which atmospheric processes influence ecological systems and society. Several scientific issues involving the atmosphere have been identified as being crucial to society, but the most important issue so far is climate change. Scientists from diverse disciplines have been working together to assess the potential impacts of climate change. This chapter is a brief presentation and discussion of the fundamental concepts of the various topics involved in climate change studies.

3.2 Aspects of Climate Change

The changing climate and elevated atmospheric CO_2 are expected to change regional precipitation and evapotranspiration. Water supply and use in semi-arid lands are very sensitive to changes in precipitation and evapotranspiration, because the fraction of precipitation that runs off or percolates is small (IPCC, 1992).

Higher temperatures may also have an impact on winter snow. Under a warmer climate scenario, most of the winter precipitation is expected to be in the form of rain instead of snow, leading to an increase in winter and spring runoff and a decrease in summer snowmelt flows (IPCC, 1992).

3.2.1 Change in Water Supply

Surface water supply (runoff) is the main hydrologic variable affected by climate change, especially in water-short regions like the Midwestern United States. The water

supply may be affected by changes in quantity, type (snow or rain), and timing of precipitation. The impacts of climate change on surface water supply need to be quantified since it is a key factor in determining agricultural potential. A number of studies have been carried out to investigate the influence of climate change on water supplies. Their main purpose has been to quantify the sensitivity of water supply to climate change through the use of simulation models.

Stockton and Boggess (1979) used four arbitrary climate scenarios (present average temperature $\pm$ 2°C, accompanied by a $\pm$ 10 percent change in annual precipitation) to estimate the effect of climate change on runoff and water supply in 18 water resource regions in the United States. They found that the most severe scenario (2°C increase combined with a 10 percent precipitation decrease) would have serious effects on all regions west of the 100th meridian except for the Pacific Northwest and the Great Basin where demand is low and ground water reserves are relatively high. Applying the same severe scenario to averages of temperature and precipitation from 1931 to 1976 in the upper Colorado River basin area, Revelle and Waggoner (1983) estimated that annual river flows would be reduced by 40 percent. Based on a study they conducted on twelve basins in Arizona, Idso and Brazel (1984) questioned the results of the Revelle and Waggoner's study and they attributed the high results to the fact that Revelle and Waggoner didn't consider the direct effects of CO_2 enhancement on stomatal closure which would reduce the plant transpiration. However, Idso and Brazel themselves, failed to consider snowmelt, which is the main source of water for the Colorado River (Irmgard et al., 1987).

For the entire United States, Peterson and Keller (1990) estimated a 25% decrease in available surface water as a result of 3°C warming. Most of their results show a decrease in summer runoff and an increase in winter runoff. To evaluate the hydrologic effects of climate change, Rango (1992) applied a snowmelt-runoff model to over 50 basins in different climatic regions around the world. With an average R^2 of 84%, he anticipates that the water supply for all purposes will be at high risk of decreasing.

As part of an integrated assessment of the regional impacts of the climate change on the region of Missouri, Iowa, Nebraska, and Kansas (MINK Study), Frederick 1993 tested historical (1951-1980 and 1930s) climate analogues, on three different river basins in this area. The warmer scenario (1930s) was found to reduce the mean flow in all three basins by a range of 7 to 28 percent.

Bergstrom et al. (2001) used downscaled scenarios to study the impacts of climate change on water supply in Sweden. They analyzed changes in runoff totals and regimes with a focus on the uncertainties introduced by GCMs. They forecasted a decline in water supply especially in the drier part of the country (the southern part).

In some areas like the Western United States, snowmelt is an important source of surface water. Therefore several studies investigated the effect of changes in snowmelt on surface water supply especially in areas where irrigated agriculture relies mainly on surface water (Cooly, 1990; Rango and Van Katwijk, 1990; Rango, 1995; Fyfe and Flato, 1999; Li PJ, 1999).

Most of the above mentioned studies were carried out assuming that changes in surface water supply will follow changes in precipitation, temperature and other climatic variables. Several assessments found that even where precipitation increases, warmer

temperatures may cause surface water supply to decline (Schaake 1990; Nash and Gleick 1993; Leavesley 1994). Using data from two GCMs scenarios (CCC, HAD), Wolock and MaCabe (1999) projected runoff for the 18 major water-resource regions in the conterminous United States. They found that the annual runoff in the major river basins in the Central Great Plains region, namely the Missouri and the Arkansas-White-Red river basins, tends to decline under the CCC scenario for the decade 2025-2034, while it is highly variable under the HAD scenario for the same decade.

Abu-Taleb (2001) conducted an integrated assessment in Jordan. He used water supply and demand forecasts to project deficits for the year 2020. The study concludes that some of the deficits might be compensated for by water management practices, illustrating the significance of considering climate change in water management planning, especially for countries already experiencing water imbalances.

Recently, climate change impacts on water supply have been investigated in several parts of the world including Sweden (Bergstrom et al., 2001); the Czech Republic (Dvorak et al., 1997); China (Li PJ, 1999); Australia (Chew et al., 1995); Jordan (Abu-Taleb, 2000); Eastern Europe (Hartig et al., 1997); Africa (Meigh et al., 1999); and the USA (Frederick, 1997; Lane et al., 1999; Hurd et al., 1999; Strzepek et al., 1999). Almost all of these predictions point to potentially worsening conditions for water supply in general and specifically in semiarid climates currently dependent on spring snowmelt.

3.2.2 Change in Plant Physiology and Transpiration

Global warming and increases in CO_2 are expected to alter ET by altering several factors such as temperature, cloud cover, wind, humidity, and plant growth (Rosenberg et. al, 1990). Changes in these factors can change atmospheric water demand as well as

plant water requirements (Rosenberg et. al, 1990; Raupach, 1998). Water requirement, the difference between precipitation and ET, determines the amount of water available at the root zone and the amount that can be transpired.

Carbon dioxide (CO_2) alters ET by altering the plant function and physiology (Wilson et. al, 1999). In environments enriched with CO_2, more CO_2 enters the plant leaf through stomata (the pores in the plant leaf through which water vapor and CO_2 pass) increasing stomata resistance (stomata closure, plant function) and decreasing transpiration (amount of water passing from plant to air) (Mott, 1990). On the other hand CO_2 enrich the photosynthesis process causing increases in the leaf area of the plant (physiological change) (Wilson et. al, 1999). Stomata number per leaf increases due to increase in leaf area. Hence, plant transpiration increases offsetting the decrease in transpiration due to stomata closure (Hileman et. al, 1994).

A few researchers have studied the impact of elevated CO_2 on transpiration. Kimbal and Idso (1983) reviewed 46 studies on the effect of doubled CO_2 on transpiration and found an average of 34% decrease in transpiration. Cure and Acock (1986) compiled 90 research reports on the effect of CO_2 on the transpiration of major crops and they estimated that for all crops transpiration was reduced by 23%. Under double CO_2 (700 ppm), Hileman et al. (1994) observed no change in seasonal transpiration despite an increase of 13-14% in stomatal resistance, and they attributed this to an increase in the plant leaf area. Henderson et al. (1995) conducted a study to estimate the effect of elevated CO_2 on transpiration using crop and climate models. They doubled the stomatal resistance for doubling the CO_2 level and the outcome was an average decrease of 18% in transpiration. Many other studies similarly noted; a decrease in

transpiration due to an increase in CO_2: Pollrad and Thompson (1995) noted a 28% decrease; Carlson and Bunce (1996) a 25% decrease; and Grossman et al. (1999) a 5% decrease.

3.2.3 Change in Water Demand

Due to an increase in temperature and therefore an increase in evaporative demands, the overall effect of climate change on irrigation is to increase crop evapotranspiration (Allen et al., 1991). Evapotranspiration (ET) is the prime variable in estimating irrigation demand. Hence estimation of regional ET is required in assessing the regional impacts of climate change on irrigation.

Rosenberg et al. (1990), using the Penman-Monteith equation, conducted a detailed sensitivity study of the biophysical effects of climate change on grassland in Kansas. They projected a 4 to 8% increase in evapotranspiration as a result of 1°C warming. By doubling CO_2 they estimated a 15% reduction in evapotranspiration as a result of a 40% gain in plant stomatal resistance, and a 5% increase in evapotranspiration as a result of a 15% increase in Leaf Area Index (LAI).

Peterson and Keller (1990) conducted a study to estimate the potential irrigation requirement (the amount of water needed to irrigate a crop) for the United States. Using a number of climate change scenarios (3°C warming, 3°C warming and a 10% increase in precipitation, and 3°C warming and a 10% reduction in precipitation) they estimated the irrigation requirement (evapotranspiration minus effective rainfall). In all cases, irrigation requirements increased under warmer conditions due to increase in evapotranspiration, which was always greater than the effective rainfall. Moreover, they found that due to the effect of CO_2 enrichment (closure of stomata, which reduce evapotranspiration) the same

irrigation requirements (as with only global warming) would be required with a warming of 4°C instead of 3°C.

Allen et al. (1991) used two GCMs scenarios (GISS and GFDL) to assess the combined effect of climate change and CO_2 on irrigation requirements for three crops (alfalfa, maize, and wheat). They used dynamic models with changing plant canopies and aerodynamic resistance. The study projected an increase in the evapotranspiration of alfalfa due to an increase in the length of the crop life cycle and a decrease in the evapotranspiration of maize and wheat due to a reduction in the crop life cycle. As part of the MINK study Rosenberg et al. (1993) used climate analogues scenarios (1931-1940 and 1951-1980) to forecast the region's water demand. The first scenario was found to make the water use for irrigation higher by 39% in Nebraska and 14% in Kansas compared to the second one, and the elevated CO_2 reduced the crop water use by 4 to 12%. Still the region would experience water scarcity under the 1930s climate.

Ropert et al. (1995) used crop dynamic models to project the water demand and the associated amount of energy consumed in the southeastern U.S. in the year 2040. They used 40 years of historical weather data to predict the average weather in the year 2040. In general, the study resulted in a greater demand for irrigation water and lower efficiency of energy production.

Eheart and Tornil (1999) investigated the relation between irrigation demand and stream flow under climate change in the Midwest (U.S.). They used a farm-scale model, EPIC (Williams, 1994), to predict irrigation demand. Then, they integrated those results using a basin-scale model to determine the effects of the predicted irrigation on stream

flow. Under drier conditions, they showed that the irrigation demand would increase, putting the surface water supply at risk of being short.

Several international efforts have been initiated to investigate the impact of climate change on agricultural water resources. These efforts include South Africa (Schulze et al., 2001); Taiwan (Chen et al., 2001); the United Kingdom (Mitchell, 1999); Australia (Jones, 2000); and the U.S (Quinn et al., 2001; Loaiciga et al., 2000; Ritschard et al., 1999; Ojima et al., 1999).

3.3 Assessment of Climate Change Effects

Climate change impact assessments are estimates of what might happen under specified climate scenarios. Generally, the conditions under climate change are projected and compared to conditions (baseline) in absence of climate change.

3.3.1 Climate Change Scenarios

Climate change scenarios have been generated as a first step in understanding global warming. A climate scenario can be defined as "a coherent, internally-consistent and plausible description of a possible future state of the world" (Carter et al., 1994). Different scenarios types being used in analysis of climate change impacts include:

Arbitrary scenarios: In this type of scenarios pre-selected values are added or subtracted from current or historical records of precipitation and temperature to simulate climate change (Waggoner, 1983).

Historical analogs: This type of scenario use climate information from the past as a scenario for future changes (Jager and Kellogg, 1983). For example, in the USA, the climate conditions that prevailed during 1930s (dust bowel) are used as scenario for the future.

General Circulation Model's scenarios: These scenarios are derived from global climate model experiments with specified forcing mechanisms (e.g. doubling atmospheric CO_2). General Circulation Models (GCMs) are physically based models developed to produce equilibrium and transient climate projections. The main disadvantage of GCMs is that they lack accuracy to make projections of surface climatic conditions over smaller regional-scale domains (Rosenzweig and Hillel, 1998).

Equilibrium scenarios: In this type of scenarios the average climate conditions (annual average conditions) are assumed to change and then to stabilize at some point in the future when CO_2 is doubled (Wang et al., 1992).

Transient scenarios: In this type of scenarios climate is assumed to change gradually over time, transient, (IPCC, 1996). The rate of climate change is a function of the assumed rate of change of CO_2 concentration (usually 1% compound per year).

To minimize the uncertainties associated with the outputs of the GCMs, investigators have tended to downscale GCMs scenarios to regional scales or use climate analogues.

Over the last decade climate scenarios have been improved through better physics and higher resolution within GCMs (IPCC, 1996a). Such improvements have also led to better simulations of climate behavior and better projections of climate parameters (Jones, 2000). Some of the more famous climate scenarios are: Geophysical Fluid Dynamics Laboratory (GFDL) (Manabe and Wetherald, 1987); Goddard Institute for Space Studies (GISS) (Hansen et al., 1984); Canadian Center for Climate Prediction and Analysis (CCC) (McFarlane et al., 1992, and Flato et al., 1999); Hadley Center for Climate Prediction and Research (HAD) (Johns et al., 1997).

As decisions for integrated management are made at a regional scale, climate scenarios need to be designed for use at the regional scale (Kellog and Zhao, 1982). Moreover, regional climate models need to have a spatial resolution fine enough to yield a realistic representation of mid-latitude synoptic system (Giorgi et al., 1994).

3.3.2 Modeling Climate Change Impacts

During the past decade, extensive research was conducted to study climate change and to assess its impacts (Rosenberg et al., 1993; Rosenzweig and Hillel, 1998; Ojima et al., 1999; Jones, 2000). Simulation models have played an important role in this regard, particularly those that integrate the effects of climate change with increasing levels of atmospheric CO_2 (White et al., 1996). The various approaches that have been followed in the assessment of the impacts of climate change can be classified into three categories (Carter et al., 1994).

- The *impact* approach is a straightforward linear analysis of cause and effect. Data from projected climate scenarios are used to determine the responses of different biophysical systems to changes in climate. Most climate impact studies have followed this approach.
- The *interaction* approach links climate change with other changes and with the feedback of a system affected by climate change. Studies of interactive effects of climate change under different water regimes and landuses (Allen et al., 1990 and Manne et al., 1993) would fall in this category.
- The *integrated* approach examines the societal impacts of, and responses to, climate change. The interactions within each sector and the interactions and feedback

between sectors in the society are considered (Adams et al., 1990 and Rosenberg, 1993).

Numerous investigators have examined the impacts of climate change using case studies, statistical models, and physical simulations. Despite the uncertainties, these studies illustrate how different physical and biophysical systems respond to climate change.

In recent years, Artificial Neural Network (ANN) methods have been successfully applied to a number of forecasting problems in the field of engineering. In this approach a network is trained to capture the interrelationships, between the training data sets that closely approximate target values. The training (learning) process is accomplished by presenting known pairs of inputs and outputs to the ANN in an orderly manner. This study will explore the effects of climate change on water supply for agriculture using an Artificial Neural Network. The input parameters considered in this study are the precipitation (rainfall and snow) while the output is the amount of surface water available for irrigation. A detailed description of an ANN will be presented in the subsequent section.

3.4 Neural Networks

3.4.1 Background

Artificial Neural Networks (ANN) are computational methods inspired by studies of the brain and nervous systems in biological organisms (Karunanithi et al., 1994). The interest in neural networks has been growing for their excellent performance in modeling nonlinear relationships (Goh, 1995).

Artificial Neural Networks (ANN) are able to model poorly understood relationships between dependent and independent variables. ANNs are mapping functions that can be trained to map any non-linear complex relation. Sets of input data and their corresponding output vectors are needed to train the network. Once properly trained, the network provides a data driven model which is capable of giving reasonable answers when presented with input vectors that have never been encountered during the training process. The key to successfully training an ANN is choosing the right network structure and training algorithm. In this research, a feedforward ANN will be used to approximate the relation between the surface water supply and snow water equivalent and rainfall.

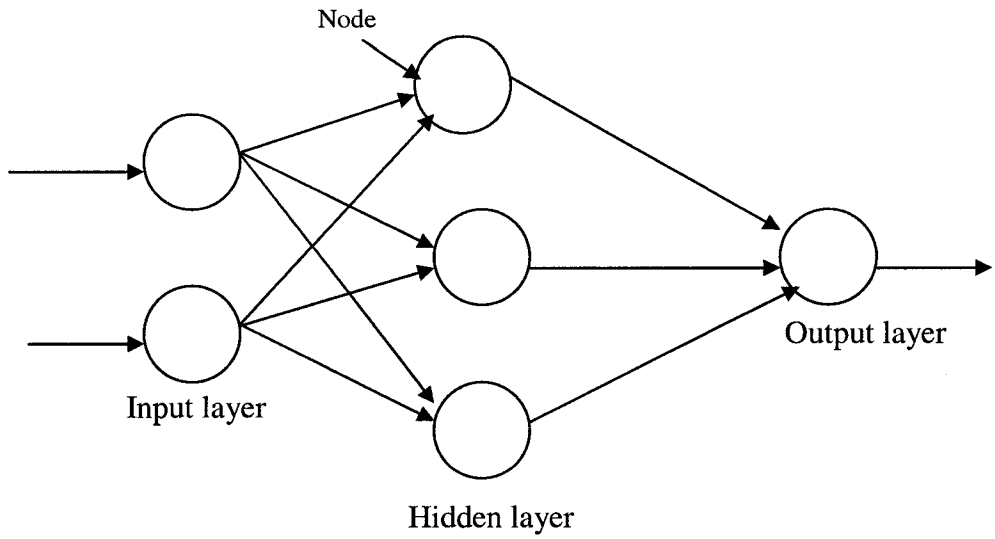

Figure 0-1 A feedforward 2-3-1 neural network

Feedforward ANNs are among the most common neural networks in use. The feedforward process involves presenting an input pattern to neurons (nodes) that pass the values into the first hidden layer. Each of the hidden layer nodes (neurons) computes a

weighted sum of the inputs, passes the sum through the transfer (activation) function, and presents the results to the next layer until the output layer is reached.

3.4.2 Neural Networks Applications

In their two-paper series, Flood and Kartman (1994) provided insight into the usage and potential applications of artificial neural networks within the field of civil engineering. Whether evaluating the bending moment for a cantilever or selecting the optimum cable tensions for guyed communication towers, the authors gave examples of civil engineering problems that were successfully solved by artificial neural networks. In the subsequent paragraphs, a number of applications in which artificial neural networks were used will illustrate the versatility of the technique.

Karunanithi et al. (1994) used neural network algorithms to estimate flows at an ungaged site on the Huron River in Michigan. Flows in streams and rivers are complex processes that are influenced by many factors such as watershed topography, vegetation cover, soil types, channel characteristics, groundwater aquifers, precipitation distribution, snowmelt, urban activities, and so on. In this case, daily stream flow records for the ungaged site were extended by the power model as well as by neural networks. Comparison of the results of the power model and neural networks to the available station records suggest that the predictions of the neural network models closely followed the observed daily stream flows and were more accurate than the power model predictions.

Kuligowski and Barros (1998) used a back propagation neural network to estimate missing rainfall data from nearby gages. The results of the neural network algorithm compared favorably to other techniques such as arithmetic and distance-

weighted averages of the values from nearby gages, and also to linear optimization methods such as regression.

Sureerattanan and Phein (1997) used a back propagation neural network algorithm to forecast the daily stream flow of the Mac Klong River Basin in Thailand. The input to the network consisted of rainfall and the past stream flow for the station under consideration. The output was a forecast of the stream flow. The pattern of the neural network forecast closely followed the observed data for the five stations considered with an accuracy of more than 90%. The results demonstrate that neural networks are capable of simulating highly non-linear relations without the need to understand the intricacies of that relation.

Smith and Eli (1995) used a back propagation neural network algorithm to obtain the runoff for a river basin given the rainfall patterns. The network was trained and tested on a simple synthetic watershed consisting of a 5x5 square grid configuration. The resulting neural network was capable of predicting the discharge peak and time of peak of the resulting runoff hydrographs when given the rainfall pattern. The network was thus able to simulate a highly non-linear, time varying, spatially distributed process.

Hsu et al. (1995) used an artificial neural network to model the rainfall-runoff relationship of the medium-size Leaf River Basin near Collins, Mississippi. The neural network model was compared to the linear ARMAX (Autoregressive Moving Average with Exogenous inputs) time series approach and the conceptual SAC-SMA (Sacramento Soil Moisture Accounting) model. The artificial neural network model was capable of effectively modeling the rainfall-runoff relationship, and its results were superior to both the ARMAX and the SAC-SMA models.

Goh (1995) used neural networks to estimate the relative density of soil samples from cone penetration test (CPT) results. The relation between the two parameters is highly non-linear and can only be described empirically. The back propagation algorithm used was successful in modeling the non-linear relationship, and it provided better results than the other standard empirical relations did. The trained network was used to synthesize charts that reliably relate the cone penetration test results to the relative density of the soil sample.

One of the complex problems solved by civil engineers is determining reservoir operation procedures for the efficient management of available water. The problem is complicated by the involvement of random hydrological events. Raman and Chandramouli (1996) used a neural network to determine the reservoir operating policies for the Aliyar Dam in India. The input for the network consisted of initial storages, inflows, and demand, while optimal releases represented the output. The operation policy was also determined by using a multiple linear regression model, a stochastic dynamic programming model, and a standard operating policy. By comparing the performance of the four different policy making methods for three years, the authors concluded that the operating policies generated by the neural network model, perform better than the three other methods under consideration.

Maier and Dandy (1996) used a neural network algorithm to forecast the salinity in Australia's Murray River 14 days in advance. The transport of salinity down the river stream is dependent on flow and upstream salinities. The flow in the river is complicated by the presence of storages, locks, weirs, and barrages. The back propagation algorithm was used with upstream salinities, water level at locks and weirs and upstream flow at

some gauging stations used as input for the neural network. The inputs were measured at one-day lags with each measurement used as an independent input for the neural network. Measurements of salinity at the point of interest for the days before the forecast date were also used as inputs. The only output of the network was the salinity at Murray Bridge at the date of interest. The trained neural network was able to predict the salinity at Murray Bridge 14 days in advance for all of 1991 with an accuracy of more than 90 %.

In water resources and hydrology, ANNs were used successfully to model rainfall and runoff (Smith and Eli, 1995; shamseldin, 1997; Tokar and Johonson 1999), to forecast river floods (Campolo et al., 1999; Zealand et al., 1999), to predict and analyze flow data (Sureerattanan and Phien, 1997; Hsieh and Tang, 1998; Eldaw, 2001), to model soil moisture correlation (Goh, 1995), to model water quality (Maier and Dandy, 1996), and to estimate missing rainfall data (Kuligowski and Barros, 1998). Artificial Neural Networks were used in conjunction with GIS to generate a subsurface profile and material distribution (Gaangopadhyay et al., 1999).

These are some examples where neural networks have been successfully employed to solve a variety of engineering problems. Neural networks are now being increasingly applied in many branches of science. Neural networks are attractive because of their ability to map complex relations without needing to understand the laws that govern that relation.

4. THEORY AND METHODOLOGY

The methodology developed in this study followed the impact approach to assess the climate change impacts. The impact approach is a straightforward linear analysis of cause and effect. Climatic data sets are used to run models to estimate the changes that happen in a biophysical system as a response to climate change. Figure 4.1 shows the steps that are carried out to analyze climate change impacts. The study used the historical period 1960-1990 as a baseline, and data from two climate scenarios (described below) to quantify the responses of water for irrigation to changes in climate. A water balance approach was used to determine the effect of the postulated climatic change on irrigation water budget. This approach is comprised of two parts. In the first part a model is developed to quantify the responses of the surface water supply. Artificial Neural Network (ANN) methodology was used to model the surface water supply system. The ANN was trained to approximate the relation between irrigation water diversions and river flow and precipitation on the river basin being modeled. In the second part the responses of the water consumptive use were quantified using a consumptive use model. The model uses climate and plant parameters to estimate the crop consumptive use and irrigation water requirement over the whole river basin. Then the outputs of the two models were used to estimate the water budget.

This chapter outlines, describes, and explains the methods and computational tools used to model the problem. Generally, in developing databases for assessment of

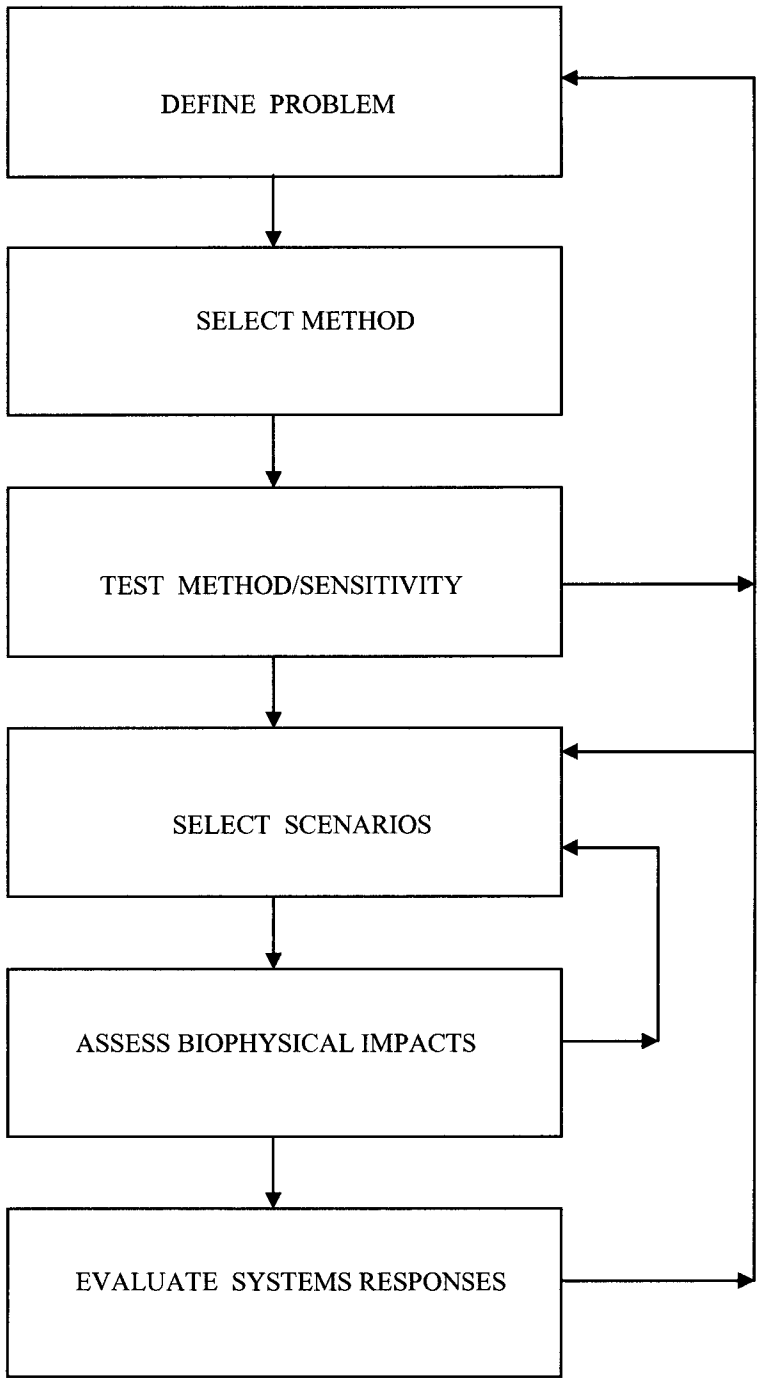

Figure 4-1 Steps in climate impacts assessment

climate change studies, considerations should be given to issues such as scale of analysis, the availability, accuracy, and adequacy of the data for the modeling and validation processes.

Such considerations eventually lead to selection of a study area, which best fulfills the above criterion. The area selected for this study is the Arkansas River basin, Colorado. The work reported here concerns the possible effects of several climatic change scenarios on water supply and demand for irrigation in the Arkansas River basin. In order to meet the research objectives the following steps were involved:

1. Selection of a region vulnerable to climate change with reliable data records.
2. Selection of representative climatic stations for the whole river basin.
3. Selection of climate scenarios with high spatial resolution to meet the objectives of this study.
4. Development of a model from existing climatic and runoff records that adequately simulates water diversions.
5. Development of a model from existing climatic and plant parameters that adequately simulates irrigation demand.
6. Use these models to determine the effects of climate change.

4.1 Scale of Analysis

4.1.1 Regional Scale

Usually, the coarse resolution of the global-scale climate models used in climate change analysis limits their ability to reproduce the spatial complexity of the system being modeled, and the assumptions made degrade the quality of the results and make them unreliable. Therefore, assessments of the potential impacts of climatic changes over smaller regional-scale domains are required. Region, usually is used to describe a large

area ranging from a river basin may be up to an entire country. Regional analysis involves a complex system of spatially distributed nature with multiple land uses, soil types etc. Some studies used region to describe small areas of dimensions in the order of 10^2 square kilometers (Hashmi 1993). But those areas were found to be representative of the complexity of a region. The methodology developed in this study will be applied on a river basin scale. River basin systems are of manageable size, and detailed information can be obtained. The area can be divided into homogeneous units helping in the modeling process. Higher resolution can be used to model the systems in the area. The models developed can reproduce the spatial complexity of the study area with reliable and manageable outputs. Thus, the area chosen for this study is large enough to account for the spatial variation and yet of manageable size for the methodology being developed.

4.1.2 Spatial Scale

The coarse resolution (average $4^{o}X4^{o}$) of the general circulation models that have been used for climate change projections limits their ability to reproduce the spatial complexity of the actual climatic variables and specifically precipitation at a regional scale. Therefore, climate scenarios over smaller region-scale domains are required. To meet the main objective of this research, modeling climate change impacts at small scales, we used high resolution ($0.5^{o}X0.5^{o}$) climate scenarios generated by the VEMAP project (see section 4.2.3). To represent the spatial distribution of the characteristics of the study area we divided the whole area into several sub-areas each one with uniform properties. To reflect the spatial distribution within each sub-area, the soil type and landcovers were extracted from historical records of data and then used in the CU model.

4.1.3 Temporal Scale

Monthly time steps were used to evaluate the changes in the water and crop systems following the climatic changes. However, crop conditions and consumptive use change daily. Therefore, the water consumptive use for crops is estimated daily and aggregated to monthly values. Finally, water budgets can be estimated monthly, seasonally, and annually.

4.2 Selection of Study Area

4.2.1 Basin Selection

The basin was selected to fulfill a number of criteria required for development and testing of the modeling system. It is especially important that the basin:

1) Have enough records of diversions and river flow for modeling and validation.
2) Have a surface irrigation system adequate for reproducing the surface water supplies under historical, current and climate change effects.
3) Have an area that encompasses a variety of land covers and acreages that will allow us to evaluate a number of different responses to climatic effects.

The selected region is in southeastern Colorado and is shown in Fig 4.2. The region is known as the Arkansas River valley and extends from the city of Pueblo upstream (west) to the border with Kansas downstream (east). Irrigated agriculture is the dominant landuse in the area. The study area contains two major reservoirs and twenty one ditches that deliver water to irrigate 106,515 ha (263,000 acres) out of a total area of 157,950 ha (390,000 acre) (Fig 4.3). A large number of crops are grown in the region. The crops grown in the study area are dominated by alfalfa and corn however a large number of other crops are grown including sorghum, winter wheat, and vegetables. Five dominant

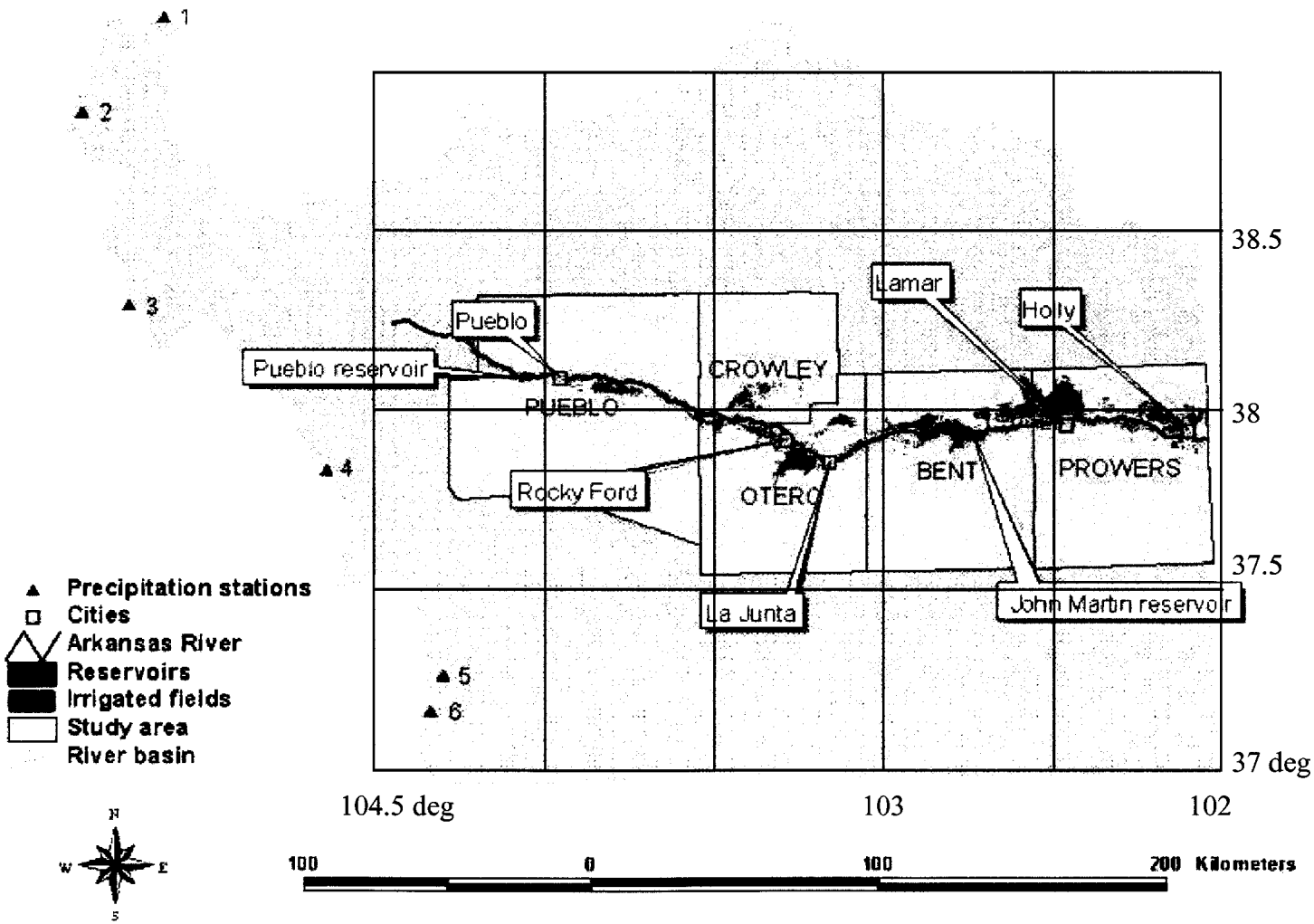

Figure 4-2 Location of the study area in the Arkansas River basin

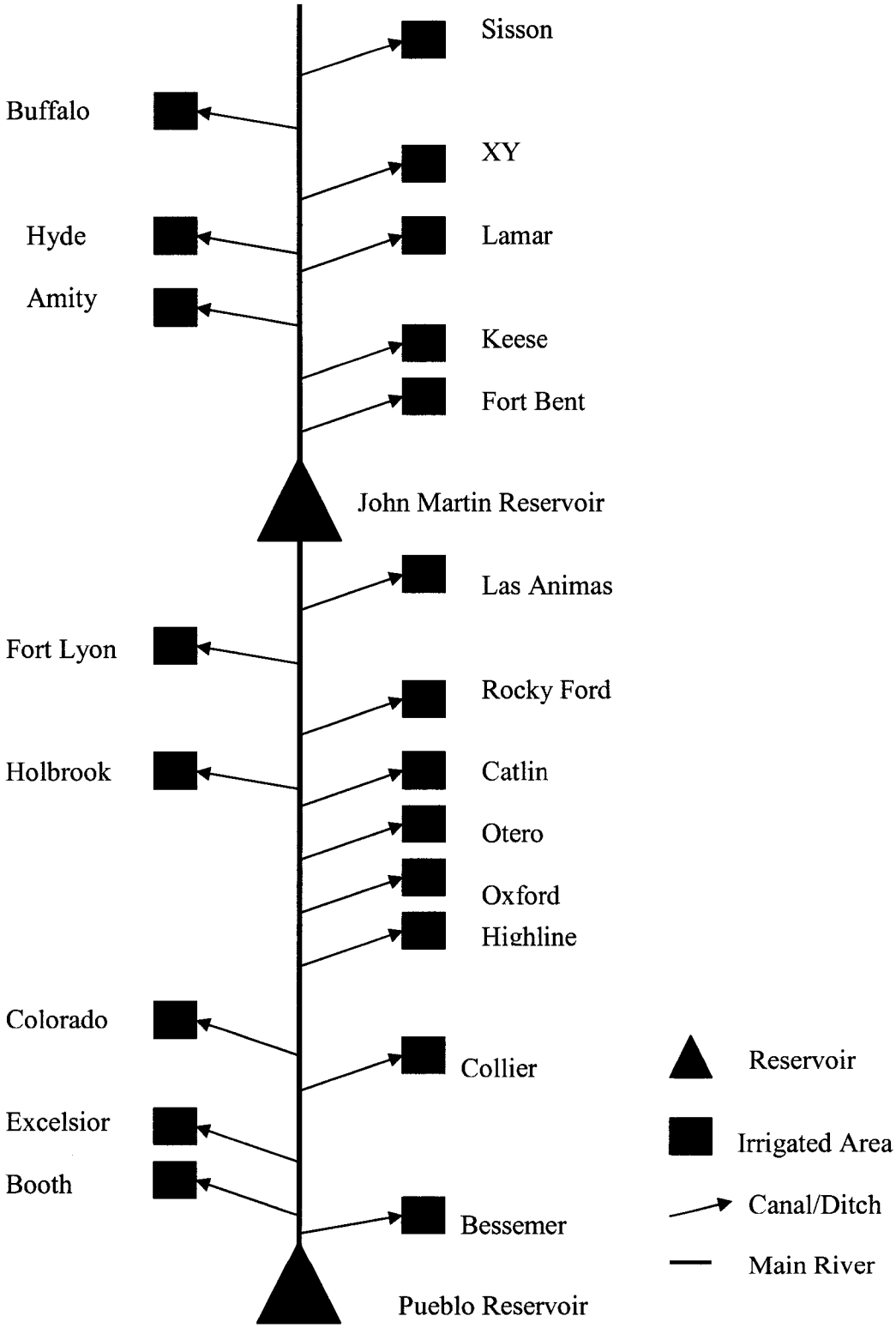

Figure 4-3 Surface irrigation system in the Arkansas River basin

crops namely alfalfa, corn grain, corn silage, wheat, and sorghum were used to estimate the region consumptive use.

Climate varies considerably over the river basin and accordingly the responses to climatic change are expected to vary. Hence, to reflect this spatial variation in the analysis process, the basin was divided into several sub-areas. The following five counties were selected as sub-areas to reflect the spatial variation along the region being modeled. The selected counties are:

1. Pueblo (2455).
2. Bent (2572).
3. Crowley (2456).
4. Otero (2571).
5. Prowers (2574).

The five counties have long historical records of the dominant crops grown in each of them and the corresponding acreage. The numbers in parenthesis represent the numbers of (0.5^{o} X 0.5^{o}) cells in the grid of climate data generated by the two GCM's (see section 4.2.3) that each county falls within. The characteristics of each county are listed in Table 4.1 and their location shown on Fig 4.2. The crop and acreage data are from the U.S. Department of Agriculture, agricultural statistical service while the diversion data are from the Colorado State Engineer Office.

4.2.2 Climate Stations

The greatest runoff in the study region comes from snowmelt in the large mountain system at the western border of the region. Substantial water supply (runoff) occurs only where mountain ranges are high enough to receive adequate precipitation.

Therefore, consideration was first given to locating climatic stations on high mountains whose historical records of precipitation are representative to the runoff in the Arkansas River. The stations selected are listed in Table 4.2; locations are shown on Fig 4.2. These are the stations whose precipitation records were used to forecast water supply in the

Table 4-1 Characteristics of the five sub-areas (2002)

Area	Total grown area (hectares)	Irrigated area (hectares)	Dominant crops
Bent	20,250	19,0345	Hay, Sorghum, Corn
Crowley	4,050	4,050	Hay, Corn, Sorghum
Otero	18,630	18,630	Hay, Corn, Wheat
Prowers	68,850	44,550	Hay, Sorghum, Wheat
Pueblo	12,960	10,935	Hay, Corn, Wheat

Table 4-2 Location of precipitation stations (The number listed with each station corresponds to locations of Fig 4.2)

Station	Latitude (deg)	Longitude (deg)	Elevation (m)	Cell # in climate grid
Apishapa (5)	37.33	105.07	3,040	2683
Brumley (2)	39.08	106.53	3,222	2220
Fremont Pass (1)	39.38	106.20	3,465	2221
Prophyry (3)	38.48	106.33	3,271	2451
South Colony (4)	37.97	105.53	3,294	2567
Whiskey Creek (6)	37.22	105.12	3,117	2683

Arkansas river basin (USDA-Natural Resources Conservation Service (NRCS) - National Water and Climate Center). Based on location, each station falls within a (0.5^{o} X 0.5^{o})

cell in the grid of climate data generated by the two GCM's, except for Apishapa and Whiskey creek both of them were found to fall within the same cell (see section 4.2.3).

4.2.3 Climate Scenarios

The Vegetation-Ecosystem Modeling and Analysis Project (VEMAP) (Kittel et al., 1995) provided climate data used in this study. The VEMAP involves the development of climate data sets for the continental United States. The climate data includes historical data from 1895-1993, and projections from two GCM's based transient scenarios for 1994-2099. The two GCM's scenarios are the transient HAD which was developed by the Hadley Center for Climate Prediction and Research, United Kingdom and the transient CCC, which was developed by the Canadian Center for Climate Prediction and Analysis.

The historical time series were derived from: a) variable length data records from 1895-1990 (1200 stations) and b) short data records from 1951-1990 (6000-8000 stations). The two GCM's models generated future climate data (projections) using physics laws, assuming 1% annual increase in CO_2 concentrations.

The National Center for Atmospheric Research (NCAR) as part of VEMAP processed, spatially interpolated (downscaled), and topographically adjusted the historical and the projected climate data to the 0.5^{o} lat/long VEMAP grid (for the VEMAP the conterminous US was divided into $0.5^{o}X0.5^{o}$ grid cells in order to simulate small-scale influences such as local topography and ecosystems on climate) (Kittel et al., 1997). The downscaling process accounted for the effects of local topography on climate parameters. Therefore, this high resolution is partially controlled by the local-scale changes. The characteristics of the two GCMs used in this study compared to other two GCMs

(Geophysical Fluid Dynamics Laboratory (GFDL) and Goddard Institute for Space Studies (GISS)) are listed in Table 4.3 and shown on Fig. 4.4.

4.3 Data Description

The data required for this study include climatic, land cover, and soil type data. Each of these data sets is described in more details in the next sections.

4.3.1 Climatic Data

The historical and scenarios climatic data sets used to design and run the impact simulations were obtained from the Vegetation Ecosystem Modeling and Analysis Project (VEMAP) (Kittel et al., 1995). The data included temperature, precipitation, humidity, and solar radiation. Wind run data sets were compiled from the historical records of the Colorado Climate Center. The stations shown on figure 4.2 (red triangles) are used for measuring the precipitation on the high mountains that provides water (snow-melt) to the Arkansas River. The stations are Apishapa, Brumley, Fremont Pass, Prosphyry, South Colony, and Whiskey Creek. Each station represents a cell in the grid of climate data generated by VEMAP.

Table 4-3 Characteristics of four general circulation models

GCM Model	Horizontal resolution (lat/long)	USA average temperature (^{o}C) increase from CO_2 doubling
GFDL	4.5^{o} X 7.5^{o}	4.0
GISS	7.8^{o} X 10^{o}	4.2
HAD	2.5^{o} X 3.75^{o}	2.0
CCC	3.75^{o} X 3.75^{o}	4.5

Arkansas River Valley

Precipitation

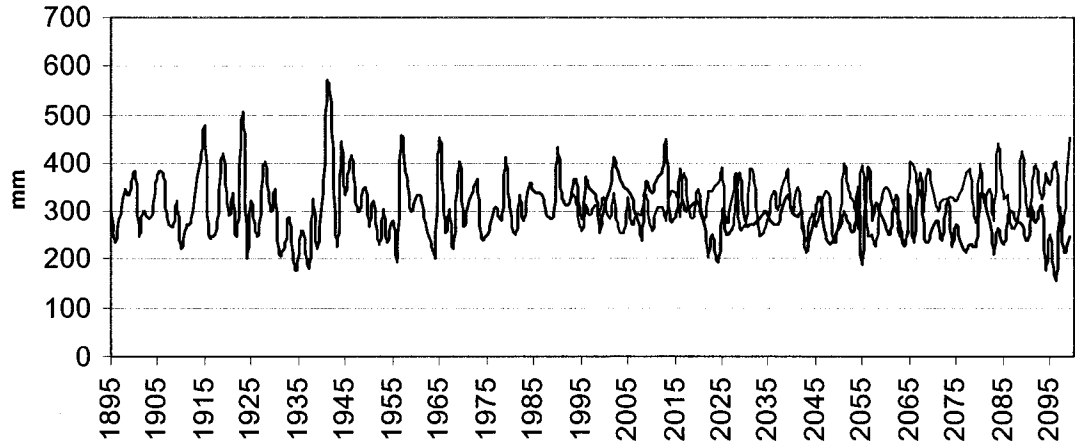

Minimum Temperature

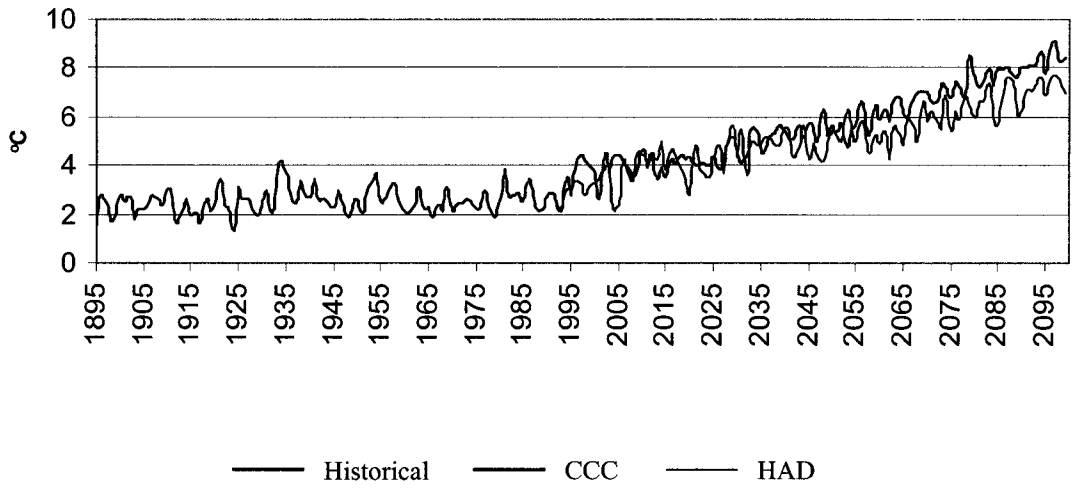

Figure 4-4 Time series of annual precipitation and minimum temperature; the figure includes both historical data from 1895-1993, and projections for 1994-2099.

Station below Pueblo reservoir was selected as streamflow gauging site (Fig 4.2). This station was selected because the length of its record is sufficient to allow assessment of the water supply model behavior; and streamflow correlates well with water diversion records.

4.3.2 Land Cover Data

Land cover is used to describe the features on the land such as houses, water, forest, etc. USGS classified land covers to sub-categories called levels. Each level has a certain degree of detail. Based on these details, agricultural land categorized as level I has two more levels: II (e.g. crop land) and III (e.g. specific crops, such as corn). This study was interested in individual crops such as alfalfa, corn, wheat, and sorghum. Crop type, crop parameters (e.g. LAI), and crop acreage are important factors involved in estimating actual crop consumptive use. Fortunately, the National Agricultural Statistics Service (NASS) in the Department of Agriculture (USDA) has long records of acreages of dominant crops in each county. Historical records of crop acreage were used to infer the crop acreage in the future.

4.3.3 Soil Data

The soil data was obtained from a cooperative study conducted by the Colorado Water Conservation Board (CWCB) and the US Department of Agriculture (USDA) on the Arkansas River basin in the early 1980's. Only the major soil bodies were described. Each major soil body contains different kinds of soils. Different kinds of soils are closely associated and characteristically occur together within particular types of landscape settings. Based on the soil map presented by the CWCB-USDA study the dominant soil type in the study area is nearly level loamy.

4.4 Models Development

Since the basic objective of this study was to estimate water supply and demand for irrigation from future climatic parameters, the type of data available governed the model structure.

A model was developed to evaluate the effects of climatic changes on water supplies. Precipitation is a main indicator of climate change. Changes in precipitation are expected to change river flow regimes the prime determinant of water diversions (water supply). Therefore, these parameters were used as inputs into the model developed to estimate effects of climate change on water supply. The modeling system included an artificial neural network (ANN) trained to approximate the relation between precipitation amounts and river flow and the amount of water diverted for irrigation (water supply). The model was then used to simulate irrigation water diversions under both historical (baseline) and future climate scenarios. Monthly estimates of water supplies were estimated from precipitation and river flow scenarios for the region.

An ANN model was developed to generate future scenarios, of river flow under climate change, to be used as an input into the model that will be used to estimate the water supply. Historical and future precipitation scenarios were used to calibrate and validate the model and simulate the behavior of river flow under future climate scenarios.

A model was developed to evaluate the effects of changes in climate and plant on irrigation water demand. Temperature, precipitation, humidity, solar radiation and wind data are the climatic variables needed to estimate irrigation demand. Using these climatic parameters as inputs the model developed was used to simulate ET under baseline and

future climate scenarios. Daily estimates of ET were made using the Penman-Monteith equation, which accounts for changes in plants in terms of bulk canopy resistance.

4.4.1 Modeling Water Supply

Two kinds of different model structures were compared to test their ability to model the precipitation-water supply process. The two model structures are (1) Artificial Neural Network (ANN) model and (2) Multiple Linear Regression (MLR) model.

4.4.1.1 Artificial Neural Network

Artificial Neural Network (ANN) is a technique able to learn, estimate and generalize a relationship between inputs and outputs of the same pattern in a system. The data set is usually divided into two parts. The first part is used to train the network to estimate the relationship between the inputs and outputs while the second part is used to validate that relationship.

4.4.1.1.1 Network Structure

Network architecture is the key to a successful network. Network architecture includes number of interconnected layers in the network and number of neurons in each layer. The dimension of the input and output data set presented to the network for training, dictates the number of neurons in each related layer (input and output) while trial and error is the common method used to determine the number of hidden layers, number of neurons and activation (transfer) function in each one. In this study a feedforward neural network was used to map the relation between the water diverted for irrigation in the region (output) and the streamflow/precipitation (input). A feedforward ANN having a finite number of neurons in the hidden layer was proved to be a universal function that can approximate any multivariate function (Hsu et al., 1995).

4.4.1.1.2 Artificial Neural Network Training

Training is the process in which the ANN acquires the knowledge of the relationship between the inputs and outputs. Training involves weighting, updating, and passing inputs from the input layer through the hidden layers to an output layer. Training starts by assigning initial weights to interconnections and passing the inputs through the interconnections to hidden layers. Neurons in the hidden layers compute and adjust the interconnection weights of the inputs and pass them, through the activation functions, to the output layer. Weights are estimated and adjusted in the hidden layer based on the relative importance of each input. Back-propagation is the technique used to adjust weights, such as a gradient decent procedure in which the error is propagated backwards to each node throughout the whole network and hence the weights are adjusted. The training process continues through the network for a number of cycles (epochs) until a preset defined criterion is achieved. Minimum squared error between the network output and the target output was the criterion used in this study.

One of the problems with ANNs is that they tend to overfit the data used for training. Overfitting is indicated by the large error that occurs when new data sets are presented to the network even though a very small error resulted during the training process, in other words the network failed to generalize. Early stopping of the training process is a technique used to avoid overfitting and improve generalization. When the network starts to overfit the data presented to it, the error in the validation stage starts to compound; early stopping is based on a certain criterion (number of epochs) for that error when the error starts to rise or remains unchanged for a number of consecutive epochs the

training process stops and is repeated. The training process is repeated until a predefined criterion is satisfied and the target output layer is achieved.

In the feedforward neural network the input layer passes an input x_i to the hidden layer, the interconnections between the input and hidden layer associate weight (w_{ji}) with each input x_i, each node in the hidden layer receives a weighted sum ($\sum w_{ji}\, x_i$) of inputs, passes the weighted sum through a nonlinear activation (transfer) function to produce the output (y_j), following the same procedure y_j is passed to the output layer, the output layer passes the weighted sum ($\sum w_{kj}\, y_j$) through a linear transfer function to produce the final output (z_k). The outputs from the input-hidden layer (y_i) and the hidden-output layer (z_k) were estimated using the nonlinear function log-sigmoid (logsig) and the linear function pure line (purlin) respectively. The mathematical formulations take the following forms:

$$y_i = \text{logsig}(\sum w_{ij}\, x_i + \beta_j) \tag{4.1}$$

$$\text{logsig}(\sum w_{ij}\, x_i + \beta_j) = \frac{1}{1+\exp(-(\sum w_{ij} x_i + \beta_j))} \tag{4.2}$$

$$z_k = \sum w_{jk}\, y_i + \beta_k \tag{4.3}$$

where x, w, and β are the input, the weight, and the bias respectively. The i, j, and k subscripts denote the number of neurons in the input, hidden, and output layers respectively. In the validation stage, the network after having been trained is used to check if it still performs satisfactorily with data that have not been used during the training.

4.4.1.1.3 Performance Statistics

In order to evaluate the performance of the network model, the following performance statistics are used:

$$\text{Root Mean Squared Error (RMSE)} = \sqrt{\frac{\sum (y - \hat{y})^2}{N}} \quad \textbf{(4.4)}$$

$$\text{Correlation Coefficient (R)} = \frac{\sum (y - \bar{y})(\hat{y} - \bar{\hat{y}})}{\sqrt{\sum (y - \bar{y})^2 (\hat{y} - \bar{\hat{y}})^2}} \quad \textbf{(4.5)}$$

In all of which $\bar{y}$ denote the mean of the observed data y_1, y_2, ... y_N; $\bar{\hat{y}}$ denote the mean of the simulated values $\hat{y}_1, \hat{y}_2$, ... $\hat{y}_N$; and N is the sample size. While R is used to measure the association between the observed and simulated values, R^2 is used to measure the goodness of the model. The relation indicative values of R^2 range from 0 (poorest) to 1(best).

4.4.1.1.4 Data Processing

All processes from data preparation to validation through training were performed using MATLAB. Several scripts were used to accomplish all processes performed in this study (provided in Appendix B). The MATLAB package includes efficient toolboxes such as the neural network one. In the training and validation phases, before using the network, the values in the data sets were transformed to the interval of [0.05, 0.95]. This is due to the fact that artificial neural networks use logistic activation functions whose output asymptotically approaches the interval of [0, 1] but never reach it. Other built in functions are used to transform the output data from the network values, back into the original values.

4.4.1.1.5 Model Identification

The output Z(t) was related to the inputs x(t) using the following formula:

$$Z(t) = \delta(x(t)) + \epsilon(t) \quad \textbf{(4.6)}$$

Where $\delta(\ )$ is an unknown mapping function and $\epsilon(t)$ is the mapping error.

To identify the sought model, the number of hidden layers and the associated neurons should be selected and weights should be estimated accordingly so that the mapping error is minimized. Different model (network) architectures were tried using a trial and error procedure. The first model (ANN1) selected for this research is a four-layer neural network: one input layer, two hidden layers, and one output layer. The inputs to the model were the precipitation on the mountains (PPT_m), the precipitation on the basin area (PPT_b), and the river flow (Q_r); with the amount of water diverted for irrigation (D) as the output. The diversion D at time (t) is treated as a function of Q_r, PPT_m and PPT_b at time (t) and (t-1) as follows:

$$D(t) = f(Q_r(t), PPT_m(t), PT_m(t-1), PPT_b(t), PPT_b(t-1)) \quad \textbf{(4.7)}$$

The second model (ANN2) is a three-layer neural network: one input layer, one hidden layer, and one output layer. The diversion D at time (t) is treated as a function of accumulated precipitation on the mountains PPT_{am} at time (t) as follows:

$$D(t) = f(PPT_{am}(t)) \quad \textbf{(4.8)}$$

4.4.1.2 Multiple Linear Regression

Multiple linear regression (MLR) is a technique in which a predictand (D (t)) is expressed as a function of predictors ($Q_r(t)$, $PPT_m(t)$, $PPT_m(t-1)$, $PPT_b(t)$, $PPT_b(t-1)$) as follows:

$$D(t) = a_0 + a_1Q_r(t) + a_2PPT_m(t) + a_3PPT_m(t-1) + a_4 PPT_b(t) + a_5 PPT_b(t-1) \quad \textbf{(4.9)}$$

where the ai's are the regression coefficients that are determined from observed data using least squares method. Statistics that were presented in section 4.4.1.1.3 are used to evaluate the performance of the MLR model.

4.4.2 Modeling Precipitation-River flow Process

The model selected for modeling precipitation-river flow processes (ANNR) is a three-layer neural network: one input layer, one hidden layer, and one output layer. The river flow $Q_r(t)$ at time (t) is treated as a function of accumulated precipitation on the mountains PPT_{am} at time (t) as follows:

$$Q_r(t) = f\ (\ PPT_{am}(t)\ ) \qquad \textbf{(4.10)}$$

Historical precipitation scenarios were used to calibrate and validate the model. Statistics that were presented in section 4.4.1.1.3 are used to evaluate the performance of the ANNR model. Future precipitation scenarios were used to generate scenarios of river flow under changing climate.

4.4.3 Modeling Water Consumptive Use

Evapotranspiration (ET) is the prime factor controlling the irrigation water consumptive use or irrigation demand. Estimation of regional ET is required in assessing the regional impacts of climate change on irrigation. Global warming may change the cloudiness, the patterns of humidity, rainfall as well as temperature. All these factors have an effect on ET. Carbon dioxide (CO_2) affects plant growth and transpiration. Therefore, analysis of climate change impacts on ET must consider all of these climatic and plant factors. For this purpose the consumptive use model IDSCU is used. The IDSCU model used was developed by the Integrated Decision Support group (IDS) part of the Civil engineering department at Colorado State University. The model incorporates monthly and daily ET estimation methods. The model applies the available water supply and weather data to determine the water use of various crops during the growing season. The computation of ET includes an option for calculating a soil moisture budget. The

model estimates the ET from weather data files and applies crop and area information to determine the consumptive use. Surface water supplies can be specified. If there is additional CU beyond the surface supplies; wells can be assumed to supply the additional CU. Weights can be assigned to weather stations, reflecting their relative influence. The IDSCU model can compute monthly CU using Blaney-Criddle, calibrated Blaney-Criddle, Pochop, and Hargreaves methods. Daily CU can be computed using the Penman-montieth, Kimberly-Penman, and ACSE methods. The Penman-montieth daily method is used to estimate ET from climate data for this study. The methods in the model can be used to develop scenarios of CU from scenarios of climate and plant data. This makes IDSCU capable of estimating as well as evaluating the impacts of climate change on irrigation water demand.

In modeling evapotranspiration (ET), many water balance models have ignored the variability of the crops and soils within a modeling area. In this research, we are modeling the ET using a model that is capable of accommodating the variability of the crops and soils within the modeling area. The model is also flexible enough to be used to project the combined impacts on irrigation demand from the general warming and plant physiological responses to elevated atmospheric CO_2 as explained in the next section.

4.4.3.1 Estimating Crop Evapotranspiration

The term evapotranspiration has been used to describe the loss of water from the earth's surface through the combined processes of evaporation (from soil and plant surfaces) and plant transpiration (internal evaporation). There are several terms to describe ET such as potential, reference, and crop ET.

Potential ET (ET_P) is the maximum rate at which evaporation occurs when the moisture available is abundant. Meteorological conditions are the main factor controlling ET_P.

Reference crop ET (ETr) is the rate of water loss from a reference vegetated surface of known characteristics. The reference surface has recently been expressed as a hypothetical crop or vegetative surface characterized as uniform, dense, actively growing, not short of soil moisture, having specified height and surface resistance, and expand at least 100 meters of the same or similar vegetation (Allen et al., 1989).

Actual or crop ET (ETc) is the rate of water evaporation from a surface of a specific crop grown under natural conditions of soil moisture and climate. ETc is controlled by plant and soil type as well as meteorology conditions. The analysis in this study is concerned with ETc.

Generally, the main approach followed in calculating ETc is calculating reference surface ET (ETr) and then applying consistent crop coefficients to estimate specific surface ETc. This approach is represented as follows:

$$ETc = K_c\, ETr \qquad \textbf{(4.11)}$$

where

ETr = reference crop (alfalfa) ET in mm per day (mm/d).

K_c = specific crop coefficient.

Crop coefficients are generally empirical ratios of ETc to ETr that have been derived from experimental data according to the relationship:

$$Kc = ETc/ETr \qquad \textbf{(4.12)}$$

In this work, alfalfa is selected as a suitable reference surface for the region being modeled. Alfalfa was suggested as a reference surface for arid climates (Jensen et al., 1971) and has frequently been used since. Alfalfa is preferable for arid regions because alfalfa is capable of near maximum ET rates when there is considerable advective sensible heat input from the air. Also, because of an extensive root system, alfalfa ET is less subject to decreasing soil water effects under high ET rates compared with a shallow-rooted crop.

Proper use of an ET method with reliable crop coefficients increases the accuracy of ET estimates (Jensen and Wright, 1978). Therefore, different crop coefficient curves were developed and have been used with associated methods to estimate ET_c. Mean crop coefficients (K_{cm}) have been used to estimate daily ETc when it is necessary to estimate total seasonal water requirements for a general area from historical climatic data (ASCE manual #70, 1990). Since this is the case in this research, therefore the mean crop coefficients were selected to estimate the ETc.

4.4.3.2 Selection of ET Method

The ET estimation method selected for this work is the Penman-Monteith Combination Method (ASCE – manual #70, 1990). The climate and plant parameters that influence ET are well represented by this ET method. The equation includes plant and air resistance terms that allow for evaluation of the combined effect of climate and plant change on irrigation. Aerodynamic resistance (r_a) and the bulk canopy resistance (r_c) are included in the equation to evaluate important climate and plant factors that influence ET.

The equation can model the ET under optimal or limited water supply. This method requires a high number of data inputs but it is the most accurate method. The

method has been ranked number one ahead of all other daily methods (Jensen et al., 1990). It is suited for use in simulation because it successfully estimates ET from different ecosystems (Rosenberg et al., 1990).

Daily estimates of ET for alfalfa, corn and wheat were made using the Penman-Monteith (P-M) model with variable bulk canopy resistance. The direct application of the P-M equation (ASCE – manual #70, 1990) takes the form:

$$ET = \frac{\left[\frac{\Delta}{\Delta+\gamma^*}(R_n - G) + \frac{\gamma}{\Delta+\gamma^*} K_1 \frac{0.622\lambda\rho}{P} \frac{1}{r_a}(e_s - e_a)\right]}{\lambda} \quad \textbf{(4.13)}$$

$$\gamma^* = \gamma(1+\frac{r_c}{r_a}) \quad \textbf{(4.14)}$$

Where:

ET : crop evapotranspiration (m/day)

R_n : calculated net radiation at the crop surface (MJ/m^2·day)

G : soil heat flux density at the soil surface (MJ/m^2·day)

e_s : saturation vapor pressure at 1.5 to 2 m height (KPa), calculated for daily time as the average of saturation vapor pressure at maximum and minimum air temperature.

e_a : mean actual vapor pressure at 1.5 to 2.5 m heights (Kpa)

Δ : slope of saturation vapor pressure-temperature curve (Kpa/°C)

γ : psychrometric constant (Kpa/°C)

r_a : aerodynamic resistance to sensible heat and vapor transfer (air resistance) (s/m)

r_c : surface resistance to vapor transfer (canopy resistance) (s/m)

ρ : air density (Kg/m^3)

P : mean atmospheric pressure at site elevation (Kpa)

K_1 : dimension coefficient ($8.64X10^4$ s/day).

λ : latent heat of vaporization (MJ/Kg)

The formulations of the parameters in the equation are described in detail in **appendix A**.

Bulk stomatal resistance of alfalfa, sm^{-1}, was computed as:

$$r_c = \frac{100}{0.5LAI} \quad \textbf{(4.15)}$$

$$LAI = 1.5\ln(h_c) - 1.4 \quad \textbf{(4.16)}$$

where:

LAI : leaf area index

h_c : mean crop height (cm)

Fifty centimeters was taken as a mean height for alfalfa (Allen et al., 1989). The bulk canopy resistance (r_c) for corn and wheat were estimated from published literature, and they take the values: 294 sm^{-1} for corn (Farahani and Bausch, 1995) and 300 sm^{-1} for wheat (Hydrology Handbook, 1996). Daily estimates of ET for the other crops (corn silage, and sorghum) were estimated by multiplying the ET values for alfalfa (reference crop) by the respective mean crop coefficients (K_{cm}).

The effects of elevated CO_2 on plants were evaluated in terms of changes in plant bulk canopy resistance (r_c). Since the direction and magnitude of changes in r_c under climate change conditions is uncertain, four levels of increases (20%, 40%, 60%, 80%) over the current r_c values were assumed and evaluated (Allen et al., 1991).

4.5 Models Testing and Validation

Usually, part of the data is used to validate the neural network model. In the validation stage, the network after having been trained is checked to see if it still performs satisfactorily with data that was not used during the training. The performance statistics described above were used to summarize the relationships between the output of the network and the target values being modeled.

Generally, neural network configuration consists of three layers: an input layer, a hidden layer, and an output layer. The numbers of parameters in the input and output layers dictates the number of neurons in each corresponding layer while the number of neurons in hidden layers is determined by trials in pursuance to optimize the network performance. The network is optimized to ensure its capability to reproduce the target output. Different network structures (number of hidden layers and neurons) were evaluated in trying to optimize the network output. The goal was to find the appropriate number of neurons in the hidden layer. The appropriate number of neurons in the hidden layer determines the successful neural network structure. To escape local minima, training can be started with a small number of neurons in the hidden layer and progressively increase their number until there is no further significant increase in the network's performance as indicated by the training statistics (Hirose et al., 1991). Training, in this study, started with one hidden layer containing one neuron and the network structure was modified until training statistics indicated optimal performance. The network that was found to perform the best was a four-layer network: one input layer, two hidden layers, and one output layer. The input layer has 5 neurons corresponding to each input parameter while the output layer has only one neuron.

Mehrotra et al., 1997 reported that a large number of neurons in the hidden layer may produce a neural network that performs very well during the training stage while it performs very poorly during the validation and testing stages (overtraining). To ensure that the network is not overtraining the data, the number of neurons in the hidden layers was limited to a maximum equal or less than the number of parameters in the input layer (Sahai et al., 2000). Therefore, each hidden layer in the developed network has 5 neurons.

Extensive correlation analysis and numerous data sets were used to select predictors that maximize the potential of the ANN model. Five predictors: $Q_r(t)$, $PPT_m(t)$, $PPT_m(t-1)$, $PPT_b(t)$, and $PPT_b(t-1)$ were used to predict the water diversions (D(t)) at time t. Q_r, PPT_m, and PPT_b are streamflow, precipitation on the mountains and precipitation on the river basin area respectively. Precipitation is selected as the main source of water and a strong indicator of climate variability. Changes in streamflow in response to climate change will have impacts in many areas including water resources (Frederick, 2002). Moreover, streamflow is the prime determinant of water diversions in the region (NRCS, National Water and Climate Center). The main purpose of training the network using streamflow was to improve performance and accuracy by increasing the information content with which the network trains. This assumption has merit since there is a significant correlation between streamflow and water diversions (Table 4.4) and has yielded a significant improvement in the ANN performance. Table 4.4 summarizes the predictors and their respective correlation coefficient with monthly water diversion.

Ninety years of data records (1911 – 2000) were used in training and validating the neural network. The data was portioned into three parts: 1) 1911-1960 for training, 2) 1961-1975 for validation, and 3) 1976-2000 for testing.

Table 4-4 The predictors and their respective correlation coefficients with water diversions (R was calculated for 50 years of data records 1911-1960)

Month	Q_r	$PPT_m(t)$	$PPT_m(t-1)$	$PPT_b(t)$	$PPT_b(t-1)$
April	0.95	0.23	0.30	0.20	0.25
May	0.90	0.24	0.29	0.07	0.30
June	0.92	0.02	0.29	0.07	0.3
July	0.93	0.37	0.35	0.51	0.2
August	0.92	0.35	0.58	0.05	0.29
September	0.94	0.56	0.23	0.35	0.21

The validation process was used to control the network generalization behavior. Testing is a post-analysis process to check the performance of the network, in which a regression analysis is made between the network output and the target output. The relation between the two outputs is indicated by the best line fit and the correlation coefficient (R). If the slope of the best line fit and the correlation coefficient approach the value 1, this is an indication of the ability of the network to map the target output very well.

The neural network (ANN1) was applied to estimate the water diverted for irrigation in each month of the agricultural season (April – Sept.). Results are shown in Table 4.5 and represent the combination of mean input values that provided the closest match between the modeled and actual water diversions (water supplies) as well as the percentage error between the two.

The performance of this model (ANN1) is compared to that of the Multiple Linear Regression model (MLR) identified using the same inputs to ANN1 and the other neural network model (ANN2) identified using accumulated precipitation as an input. The

statistical performance of the identified models for the fifty year training period and twenty five year testing period, respectively, are summarized in Table 4.6. The ANN1 model is shown to provide a better statistical performance than the MLR or the ANN2 model. Therefore, the simulation results of the ANN1 model are presented and discussed below.

The Root Mean Square Error (RMSE) statistic measures the residual variance where the optimal value is 0.0. From Table 4.6, it can be observed that the ANN1 model tends to have small RMSE values during both the training and testing.

The correlation statistic (R) measures the linear correlation between observed and simulated diversions. The R value is smaller during testing than during training, as expected. The ANN1 model performs well as measured by this statistic.

Scatter plots better represent linear correlation between observed and simulated diversions. Fig 4.5 shows scatter plots of simulated versus observed monthly diversions for the testing periods. Data are presented using transformed values.

Generally, the outcome of the results in Table 4.5 shows that the ANN1 model has the tendency to underestimate diversions except for July, where overestimation was observed.

Time series plots for each month are shown in Fig. 4.6. The figure shows the ability of the ANN1 model to match the time series for the training and testing data sets. The results are presented using transformed data so that the model performance over the whole data range can be clearly seen. The main feature of the results is that the model tends to fit the actual data quite well (on R and RMSE basis). The discrepancies in the results may indicate some structural inadequacy of the model. Therefore, there is still a

Table 4-5 Comparison of actual water diversion to that predicted by ANN1 model

Month	**Actual Mean (ha-meter)**	**Predicted Mean (ha-meter)**	**Percent error**
April	8,107	7,889	2.69
May	15,398	14,569	5.38
June	18,165	17,719	2.46
July	15,912	16,613	-4.40
August	12,768	12,677	0.72
September	7,765	7,283	6.21

Table 4-6 Training and Testing Statistics

	ANN1				MLR				ANN2			
	R		RMSE		R		RMSE		R		RMSE	
	Training	Testing	Training	Testing	Training	Testing	Training	Testing	Training	Testing	Training	Testing
April	0.972	0.910	0.04	0.09	0.962	0.892	0.05	0.09	0.680	0.600	0.19	0.16
May	0.958	0.816	0.15	0.19	0.877	0.715	0.25	0.22	0.850	0.790	0.59	0.21
June	0.908	0.856	0.14	0.18	0.909	0.775	0.15	0.22	0.780	0.740	0.49	0.31
July	0.944	0.860	0.06	0.13	0.940	0.813	0.08	0.14	0.910	0.850	0.17	0.17
August	0.935	0.902	0.06	0.11	0.926	0.875	0.08	0.11	0.780	0.750	0.15	0.15
Sept.	0.988	0.900	0.04	0.12	0.945	0.868	0.05	0.14	0.850	0.770	0.13	0.18

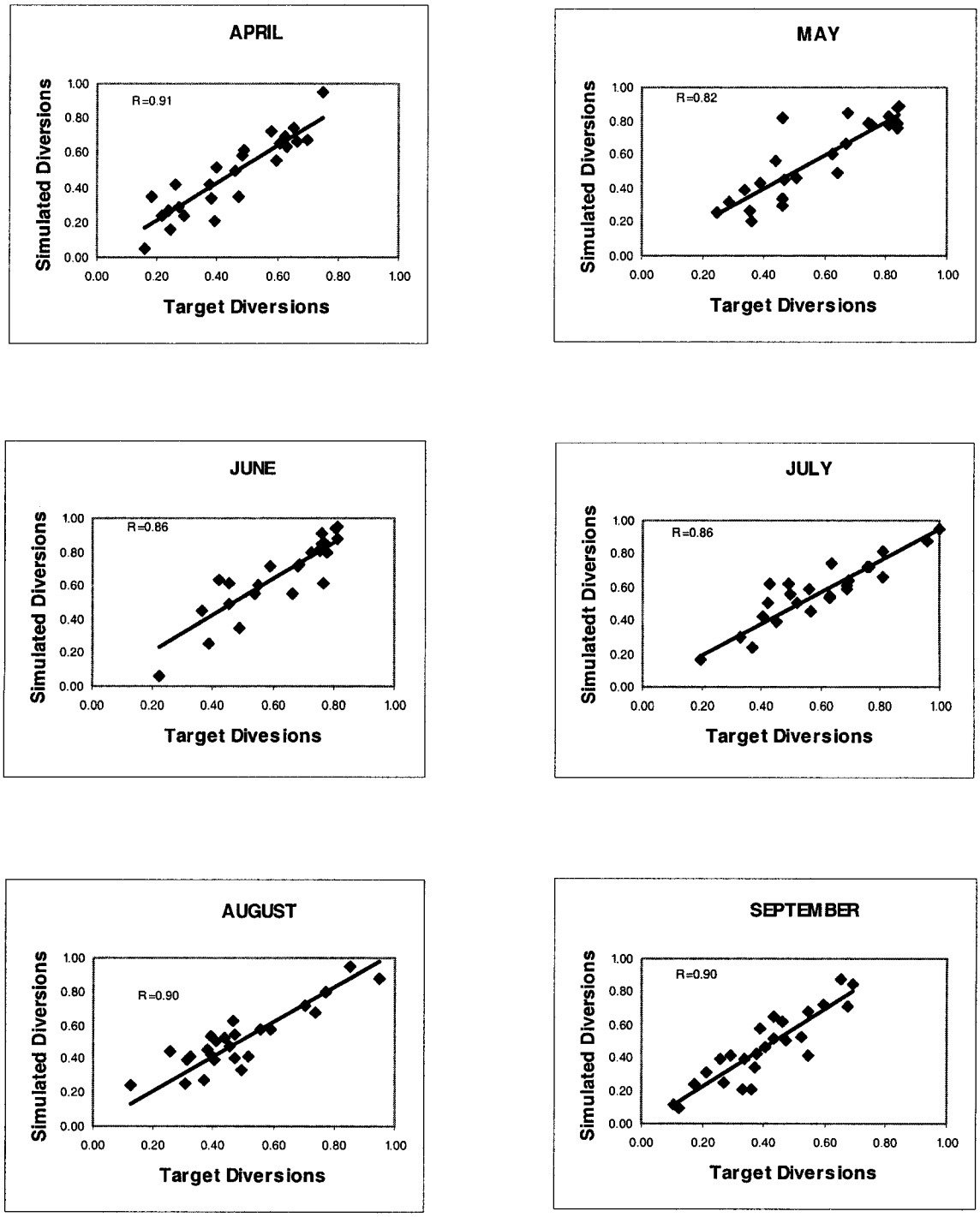

Figure 4-5 Scatterplots comparing simulated and measured diversions for 25 years of testing data

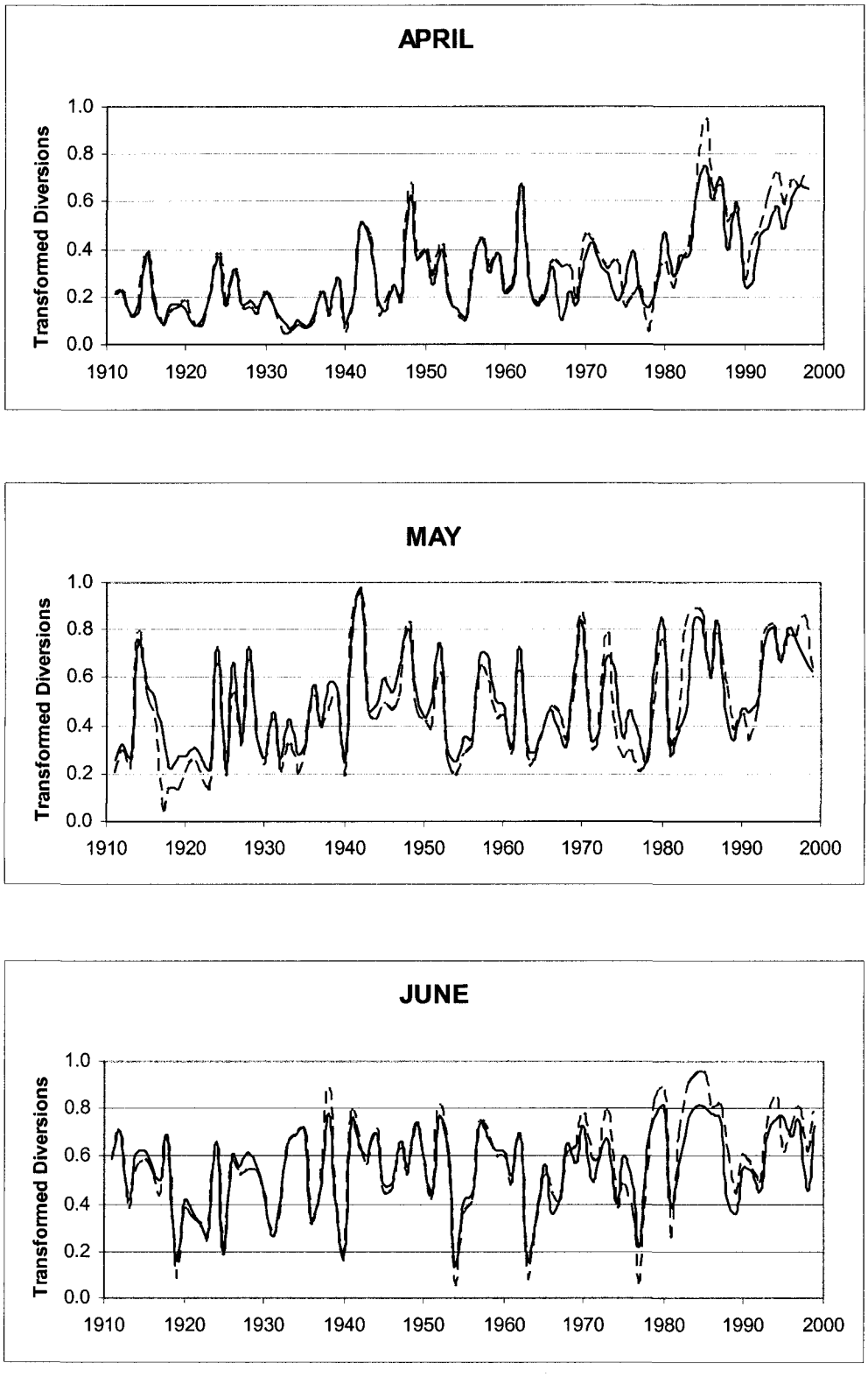

Figure 4-6 Comparison between measured (black line) and predicted (red dash line) diversions for training, validation and testing data

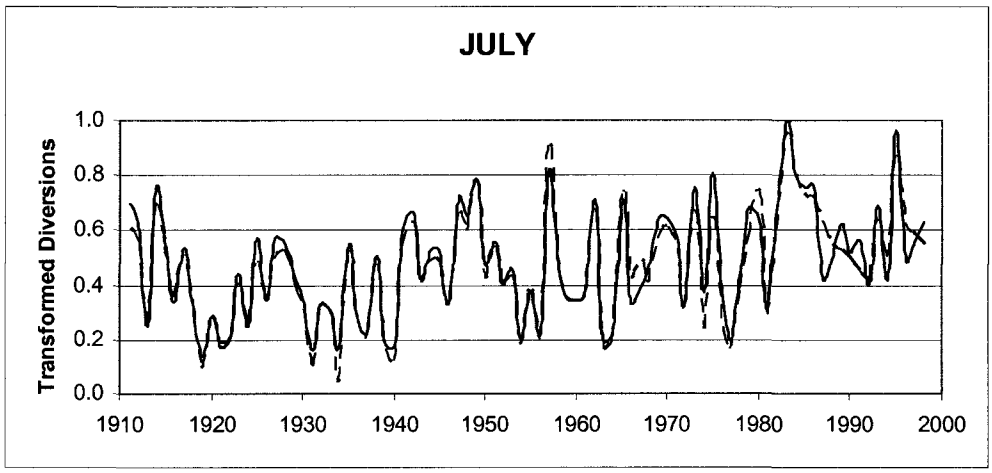

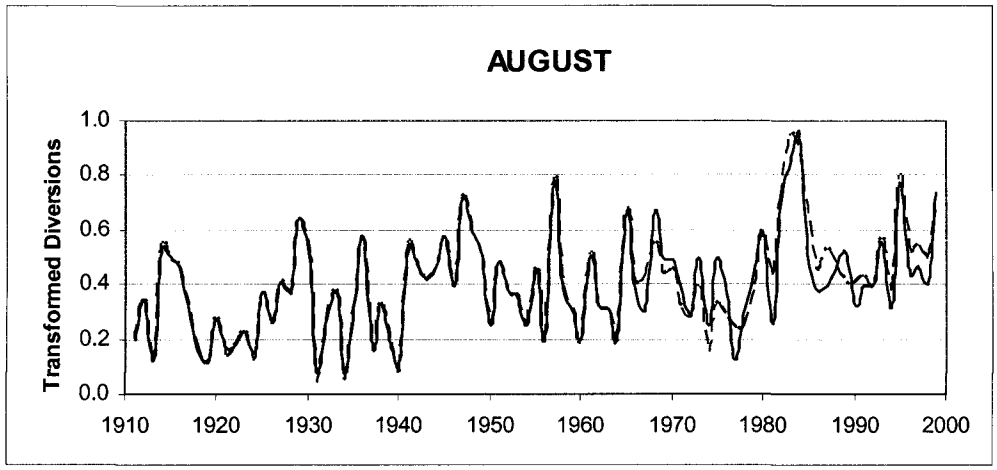

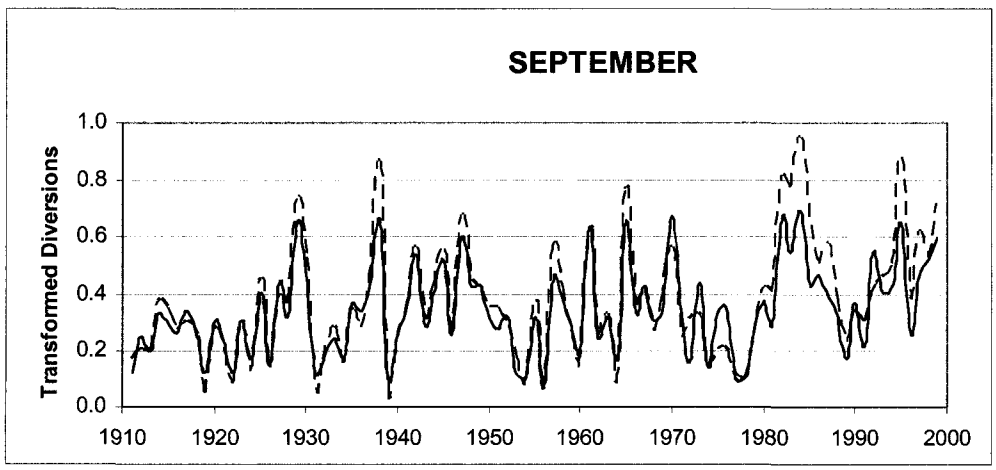

Fig. 4.6 (Continued)

room for improvement.

The residual autocorrelation functions for the ANN1 model for the training and testing periods are presented in Figs. 4-7 and 4-8 respectively. The plots indicate that the residuals that are generated by the ANN1 model are independent. The performance statistics of the ANNR model for the training period (fifty years) and the testing period (twenty five years) are summarized in Table 4.7.

Table 4-7 Training and testing statistics for ANNR model

	R		RMSE	
	Training	Testing	Training	Testing
April	0.634	0.562	0.17	0.24
May	0.790	0.770	0.10	0.18
June	0.863	0.847	0.11	0.15
July	0.899	0.740	0.06	0.13
August	0.852	0.781	0.06	0.12
Sept.	0.904	0.769	0.07	0.17

The method (Penman-Monteith) that was used to estimate ET is already calibrated under different climatic conditions including the ones that prevail in the study area. Currently several scientific agencies (e.g. COAGMET) use this method to estimate the ET in the study area. However, the reference ET (alfalfa) values computed by the model were compared to measured and computed data, for the same period of time from different sources to evaluate the accuracy of the ET method used (Table 4.8). The measured data is part of a project to determine the salinity levels and sources in lower Arkansas River basin. In this project they used Atmometers (www.ext.colostate.edu) to measure ET values in fields of alfalfa and other crops. The model (P-M) reliably produced results in a good agreement with the results of the other sources.

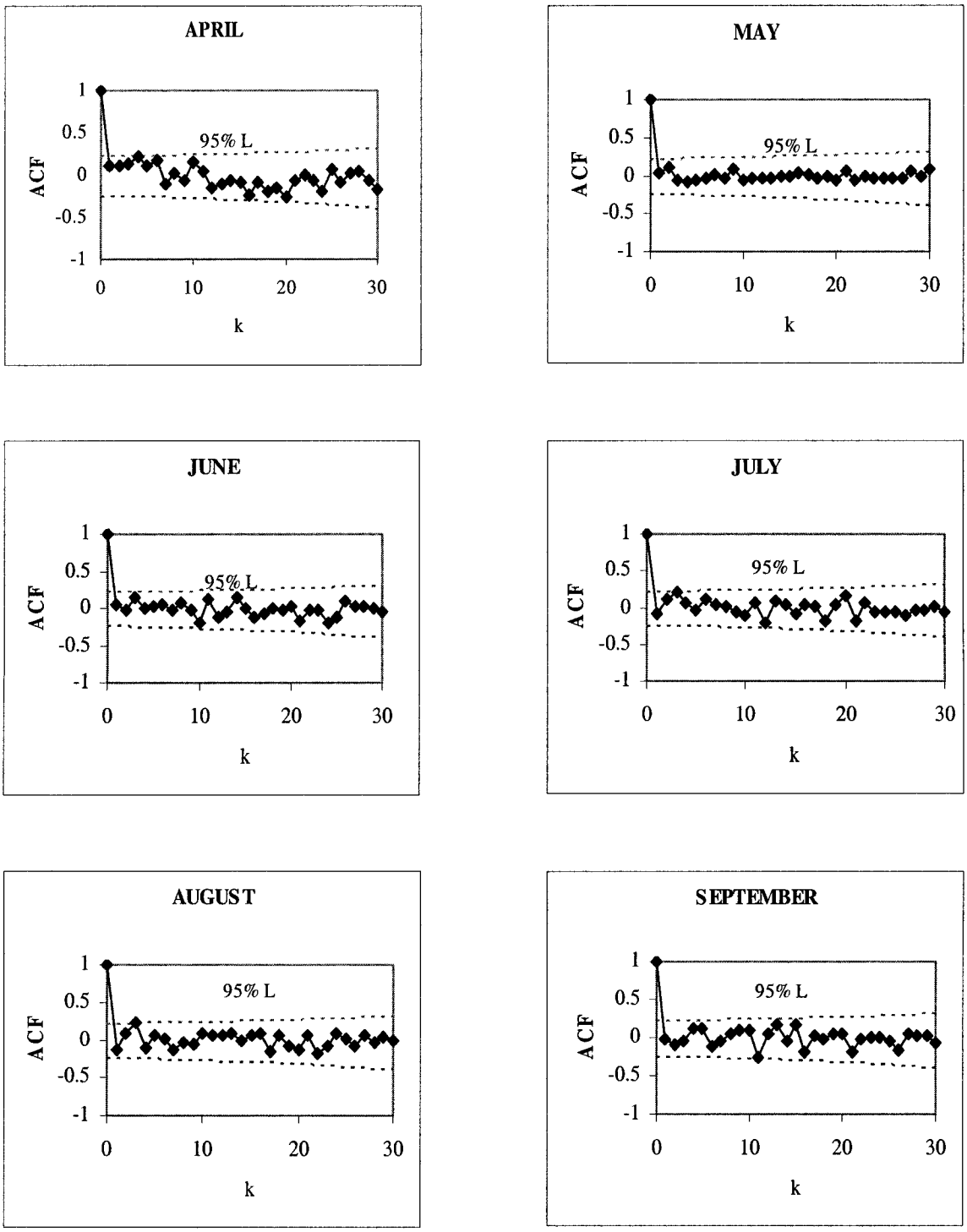

Figure 4-7 Autocorrelation (ACF) function of ANN1 model residuals (training)

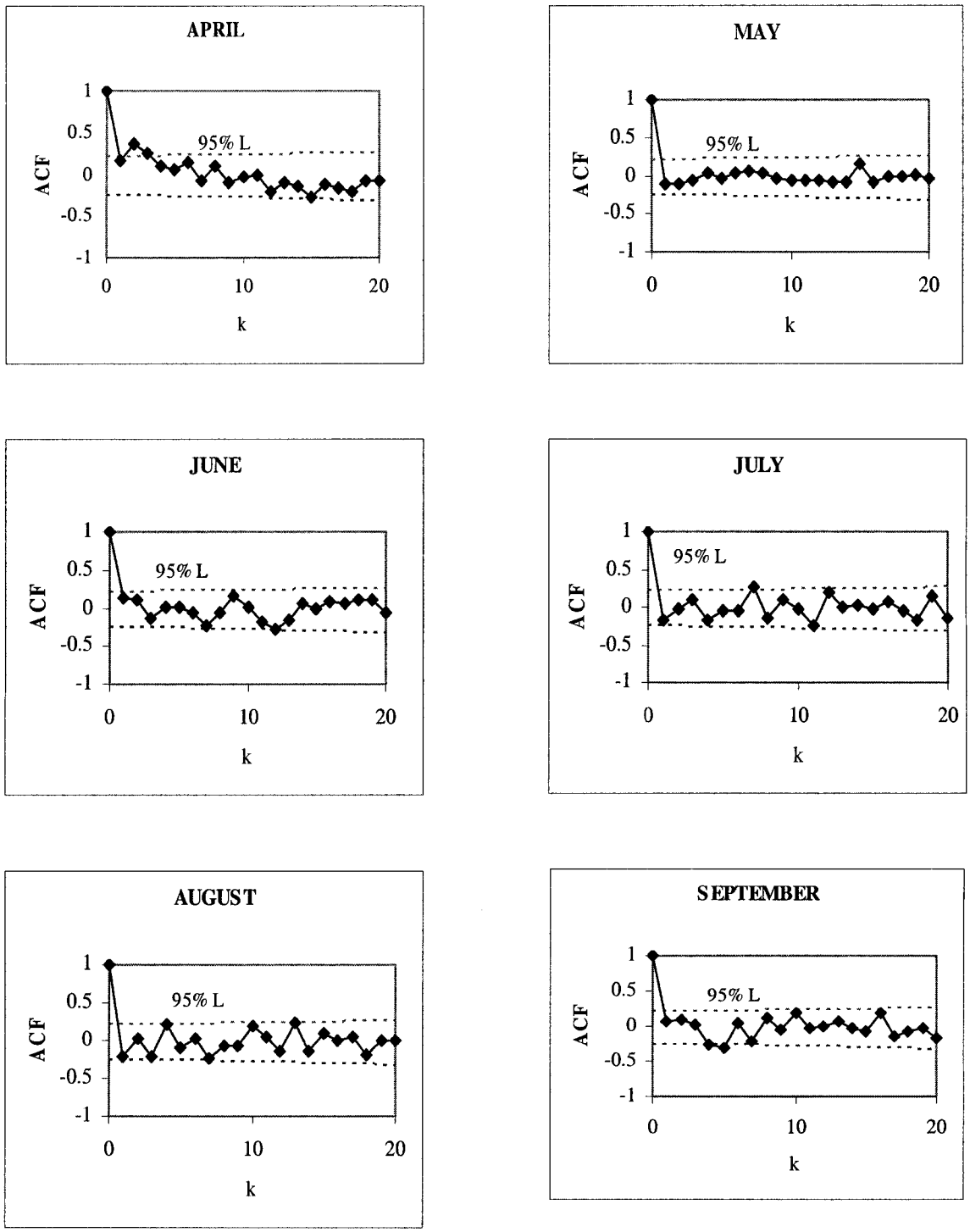

Figure 4-8 Autocorrelation (ACF) function of ANN1 model residuals (testing)

Table 4-8 Comparison of ET values

Source	ET mm (inches)
COAGMET	1165 (45.89)
Model (P-M)	1175 (46.25)
Atmometers	1135 (44.68)

5. RESULTS AND DISCUSSION

The analysis approach in this research was to compare the behavior of the components of the irrigation water budget under climate change to a case under no climate change (baseline). The results are presented in the following sections.

5.1 Changes in Climate

Two climate scenarios were used, in this study, to assess the effects of climate change. The scenarios are series of daily climate data covering the period of time 1895-2099. The baseline data was a daily climate record for 30 years (1960-1990). The main features of these scenarios are presented in the following tables and figures.

Figure 5.1 shows, in decades, the deviations from the baseline of monthly mean temperatures under the HAD and the CCC scenarios in the Arkansas River basin. The projections show that the region is expected to be warmer due to climate change. The decade mean temperature increases gradually over the time toward the end of this century with the 2090s as the warmest decade. The average departure of temperatures from the baseline ranges from 0 °C change in the 1990s up to 5 °C change in the 2090s for the months presented (April – September). The average rate of temperature change is 0.45 °C per decade. Based on the temperature projections the region is expected to be warmer under the CCC scenario than under the HAD scenario.

Tables 5.1 presents the projected changes (rounded) in monthly mean temperatures compared to baseline levels. The statistics in the table are presented in decades to show the trends and the variability in magnitude and direction of the changes.

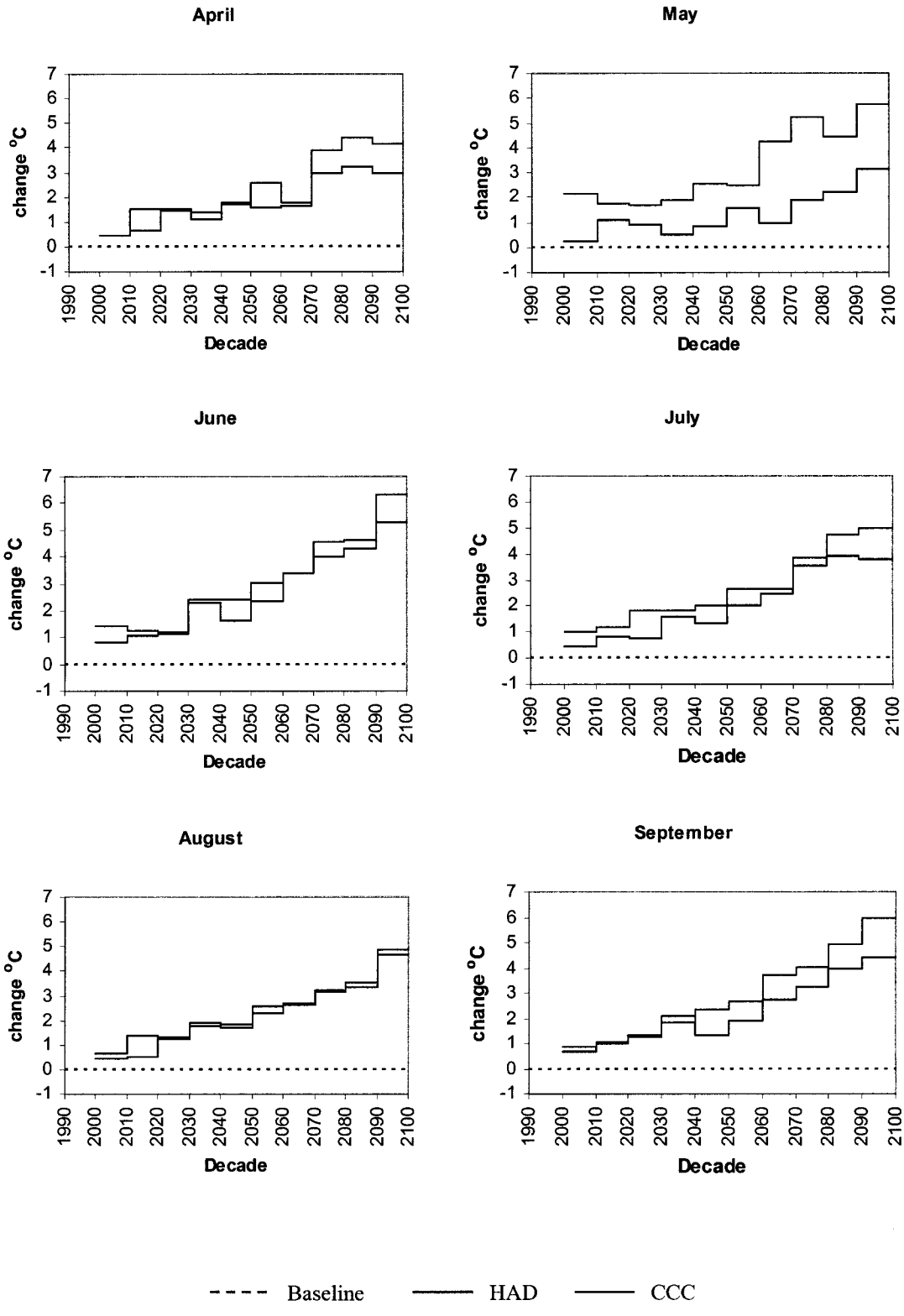

Figure 5-1 Change in monthly mean temperature by decade

Table 5.1 Monthly baseline temperature and deviations from baseline under the HAD and the CCC scenarios

		Baseline (°C)	1990s (ΔT)	2000s (ΔT)	2010s (ΔT)	2020s (ΔT)	2030s (ΔT)	2040s (ΔT)	2050s (ΔT)	2060s (ΔT)	2070s (ΔT)	2080s (ΔT)	2090s (ΔT)
October	HAD	3	1	1	1	2	2	2	2	3	4	4	4
	CCC		0	1	2	1	1	2	2	4	4	4	5
November	HAD	-4	-1	1	2	1	1	2	3	2	3	3	4
	CCC		-1	1	1	1	1	1	1	2	3	4	4
December	HAD	-9	0	1	3	3	3	3	4	4	4	6	6
	CCC		1	2	3	2	4	4	5	4	5	5	6
January	HAD	-10	2	3	3	3	5	4	6	4	5	6	9
	CCC		2	3	3	4	5	6	6	8	8	9	9
February	HAD	-7	1	1	3	2	3	4	4	3	4	5	6
	CCC		2	2	2	3	4	6	5	6	7	8	9
March	HAD	-4	1	1	2	2	3	3	3	3	4	5	4
	CCC		1	1	1	2	3	3	3	4	4	5	5
April	HAD	2	0	0	2	2	1	2	2	2	3	3	3
	CCC		1	0	1	1	1	2	3	2	4	4	4
May	HAD	7	0	0	1	1	0	1	2	1	2	2	3
	CCC		0	2	2	2	2	3	3	4	5	4	6
June	HAD	13	1	1	1	1	2	2	3	3	4	4	5
	CCC		0	1	1	1	2	2	2	3	5	5	6
July	HAD	16	0	0	1	1	2	1	2	2	4	4	4
	CCC		0	1	1	2	2	2	3	3	4	5	5
August	HAD	15	0	1	1	1	2	2	3	3	3	3	5
	CCC		0	0	1	1	2	2	2	3	3	4	5
September	HAD	10	0	1	1	1	2	1	2	3	3	4	4
	CCC		1	1	1	1	2	2	3	4	4	5	6

The deviations from the baseline projected by the two scenarios for the region are indications of the magnitude and direction of the climate changes. The temperatures during the winter months are projected to have relatively larger changes than during summer months. The winter temperatures are projected to increase by up to 9 °C in January of the 2090s, while for summer a maximum increase of 5 °C is expected in July of 2090s. The large increases in winter temperature projections are attributed to the fact that the winter baseline temperatures are very low.

In general the two GCMs scenarios, the HAD and the CCC, have shown a fair agreement on the direction and the magnitude of change in average annual temperature. Regarding the direction and magnitude of change in average annual precipitation, there is very little agreement between the two GCMs.

As discussed in chapter two, most of the surface water supply in the Arkansas River basin comes from precipitation that falls on the mountains. Table 5.2 presents the baseline and the changes in the monthly mean accumulated precipitation in the mountains. The values that are presented in the table (table 5.2) are the accumulated precipitation from October (beginning of the water year) to each following month. For example for April the precipitation amount presented is the accumulated precipitation from October to April. Figure 5.2 shows the baseline and changes in monthly mean accumulated precipitation under the HAD and the CCC scenarios, by decade. Fig. 5.2 shows the variability and general pattern of changes in the decade mean precipitation. Under the HAD scenario, precipitation projections show large differences and abrupt changes in monthly decade mean. Even though there is a variation in the monthly decade mean, a pattern is apparent. The decade mean precipitation increases gradually from the

Table 5-2 Monthly mean accumulated precipitation, by decade, for baseline climate and percent deviations from baseline for the HAD and CCC scenarios (mountains)

		Baseline (mm)	1990s (%)	2000s (%)	2010s (%)	2020s (%)	2030s (%)	2040s (%)	2050s (%)	2060s (%)	2070s (%)	2080s (%)	2090s (%)
October	HAD	37	1	-16	-12	3	5	-32	-20	-29	57	6	-1
	CCC		-8	-31	-23	-8	-33	-47	-35	-18	-43	-40	-30
November	HAD	76	2	-18	-7	2	10	-3	-9	-5	36	12	15
	CCC		-6	-18	-11	-10	-28	-19	-20	-15	-22	-19	-11
December	HAD	114	-1	-11	0	3	12	-3	-1	-1	36	33	21
	CCC		-8	-8	-9	1	-18	-14	-14	-10	-5	-2	1
January	HAD	146	0	-9	9	6	22	6	5	5	38	32	40
	CCC		-6	-5	-7	0	-12	-8	-12	-5	-4	-1	2
February	HAD	184	1	-9	10	8	22	13	10	8	37	35	41
	CCC		-5	-1	-7	-1	-13	-7	-11	-4	-1	3	5
March	HAD	236	5	-6	12	8	19	12	10	14	35	34	39
	CCC		-1	0	-5	-3	-11	-8	-6	-5	1	7	10
April	HAD	282	6	-4	10	10	17	13	9	12	32	31	36
	CCC		0	0	-3	0	-7	-7	-4	-3	3	10	11
May	HAD	321	4	-5	9	12	17	10	7	14	29	30	33
	CCC		-1	-1	-3	2	-6	-5	-4	-2	1	11	7
June	HAD	351	1	-5	10	12	15	8	6	15	25	26	31
	CCC		-3	-1	-2	0	-2	-5	-4	-2	1	10	6
July	HAD	401	3	-5	9	8	14	5	3	14	23	23	25
	CCC		0	2	2	-2	-2	-5	-1	0	0	11	3
August	HAD	453	3	-6	5	7	10	0	1	12	21	21	20
	CCC		1	4	-1	-3	2	-4	0	-2	-3	6	0
September	HAD	490	1	-6	4	8	11	0	3	12	22	21	24
	CCC		0	5	1	-3	1	-6	-2	-2	-6	7	-1

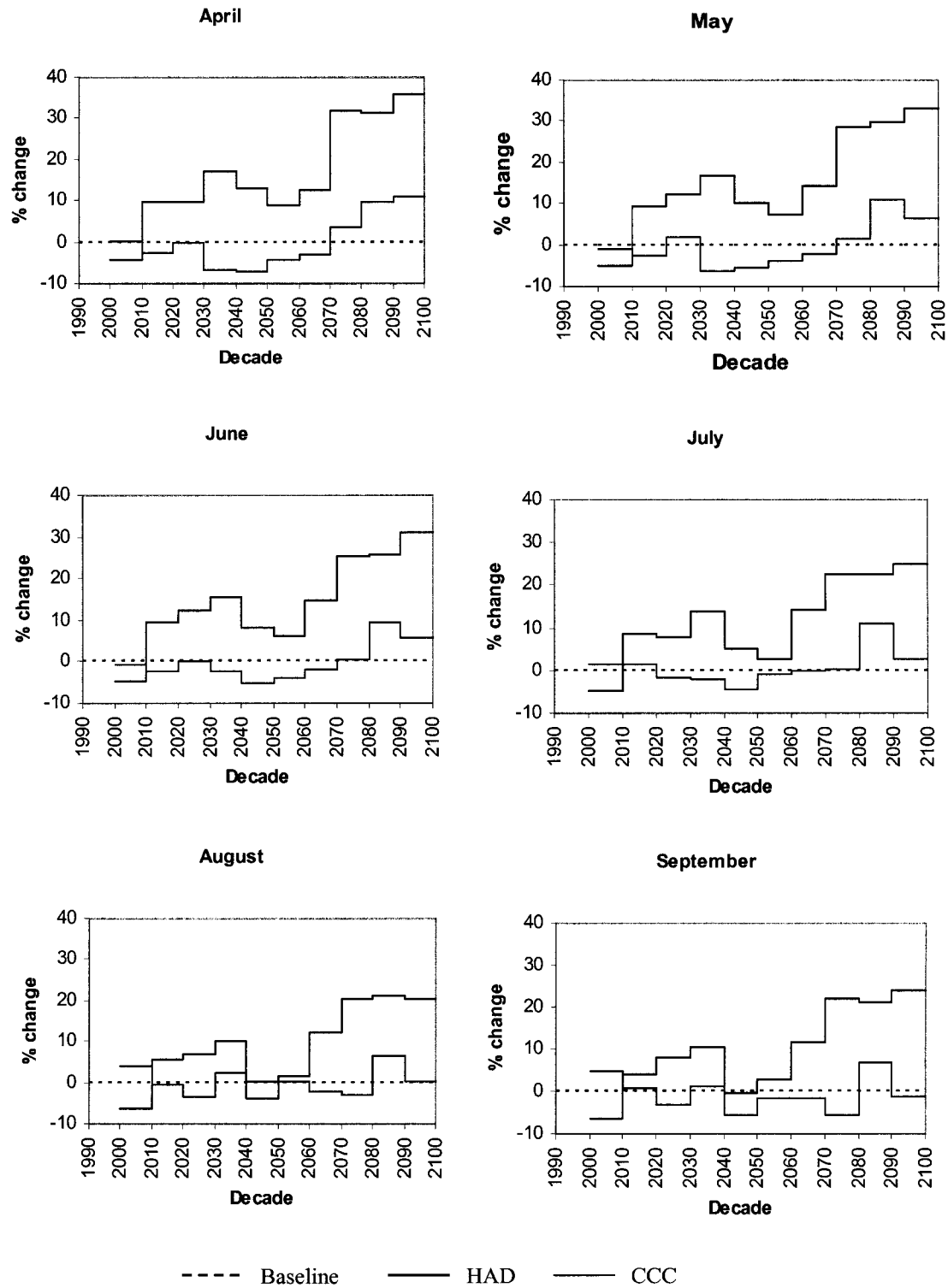

Figure 5-2 Percent change in accumulated precipitation by decade: Mountains

2010s to 2030s with an average increase rate of 1.4% per decade and decreases in the 2040s and 2050s with an average decrease rate of 1.04% per decade and gradually increases from 2060s to 2090s with an average increase rate of 2.16% per decade. In general, the HAD scenario projects a wetter climate regime in the region. Precipitation is expected to increase throughout the year with the greater increase in the winter. These increases are up to 40% during the winter of the 2090s and only 36% and 25% during the spring and summer respectively. The highest increase (41%) is projected for February and 36% increase is projected for April while the lowest increase (20%) is projected for August. The CCC simulations project a considerably drier climate regime for the region. The projections of the decade mean precipitation are at or below the baseline level except for the 2080s where an abrupt increase is projected for the region (average of 9% above the baseline). The variation in the decade mean precipitation is less than that of the HAD with no apparent pattern. Precipitation is projected to decrease throughout the year with the largest percentage change in spring and summer. The 2040s decade is projected to be the driest decade, with the largest decrease (47%) being projected for October and 7% decrease is projected for April while the smallest decrease (4%) is being projected for August.

Based on this analysis the region is expected to experience an increase in winter precipitation and a decrease in summer precipitation. The decreases are relatively small under the HAD scenario compared to the CCC scenario under which the climate in the region is expected to be warmer and drier.

5.2 Effects on Water Supply

Sensitivity Analysis

Figure 5.3 illustrates the sensitivity of water diversion (water supply) to each factor involved in the model developed to estimate the water supply. Each factor is displayed to show the effect of changes in its value on the water diversions. The results presented are for April and July to represent the spring and summer periods. The values presented are an average of twenty-five years of monthly means. Water diversions respond most to changes in streamflow and are less responsive to monthly precipitation in the mountains and least responsive to monthly precipitation in the basin area. Clearly, river flow is the prime factor that affects surface water supplies in the study region.

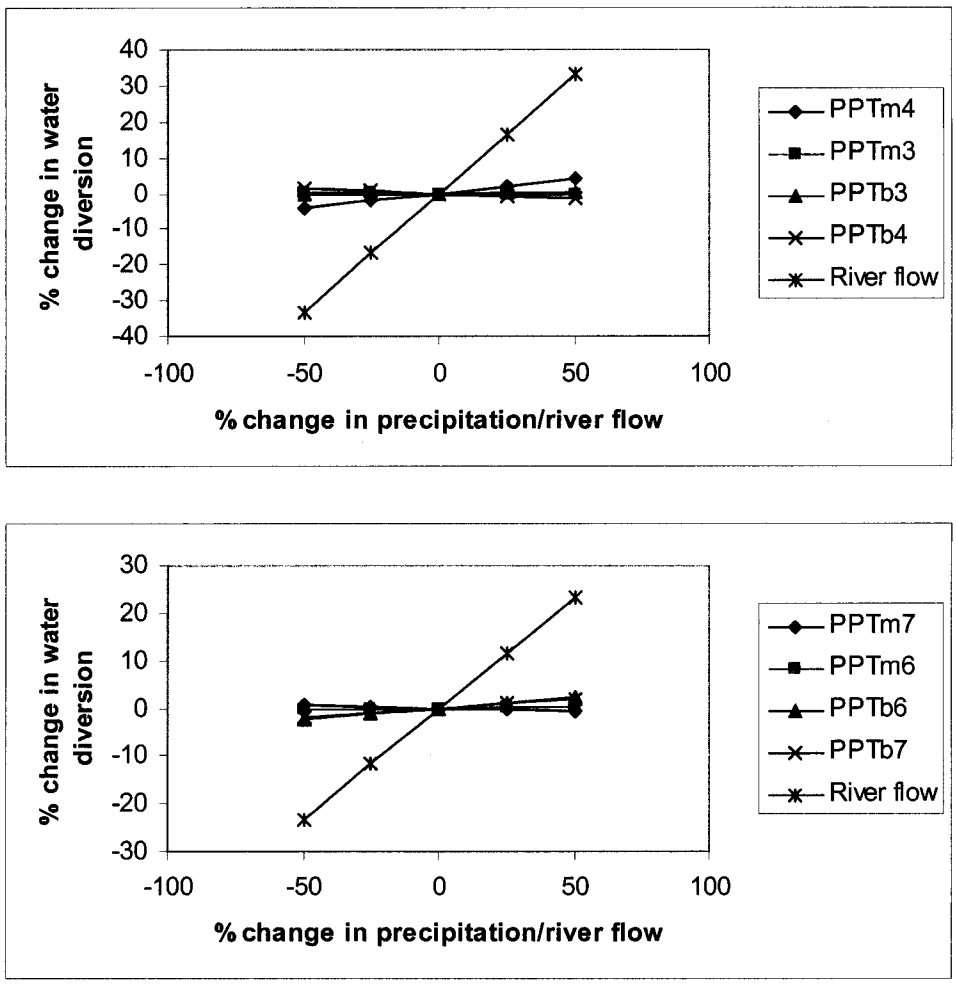

Figure 5-3 Predicted change in water diversions in response to changes in river flow and precipitation.

Figure 5.3 shows that the sensitivities in the spring (April) are greater than those in the summer (July). Figure 5.3 provide some indications of the sensitivity of water supplies in the study region to changes in climatic inputs, but scenario-based studies are more helpful in assessing the effects of climate change (Arnell, 1996).

Scenarios Study

Climate change is expected to have an effect on the distribution of flow through the year, and changes in flow are expected to have the greater impact on the water supplies in the region. Therefore, river flow scenarios were generated from precipitation scenarios using a neural network model to quantify the changes that might happened to the water supplies under climate change. Two precipitation (the HAD and the CCC) and river flow scenarios were applied using the ANN model described earlier in chapter 4 to investigate the sensitivity of irrigation water diversions (water supply) to changes in climate. Responses of water supplies to changes in these factors were estimated for the whole growing season and each month in the season. The results are presented and discussed below.

Results are presented by decades because, due to year to year variability, it was difficult to present changes at an annual scale and changes in longer-term averages are more obvious.

Changes in water diversions, accumulated precipitation and river flow are shown in Fig. 5.4 a-c. The results show the changes in monthly water supplies compared to changes in precipitation and river flow. The figures depict averages of 10 years of historical baseline (1960-1990) and projected monthly water diversions (water supplies).

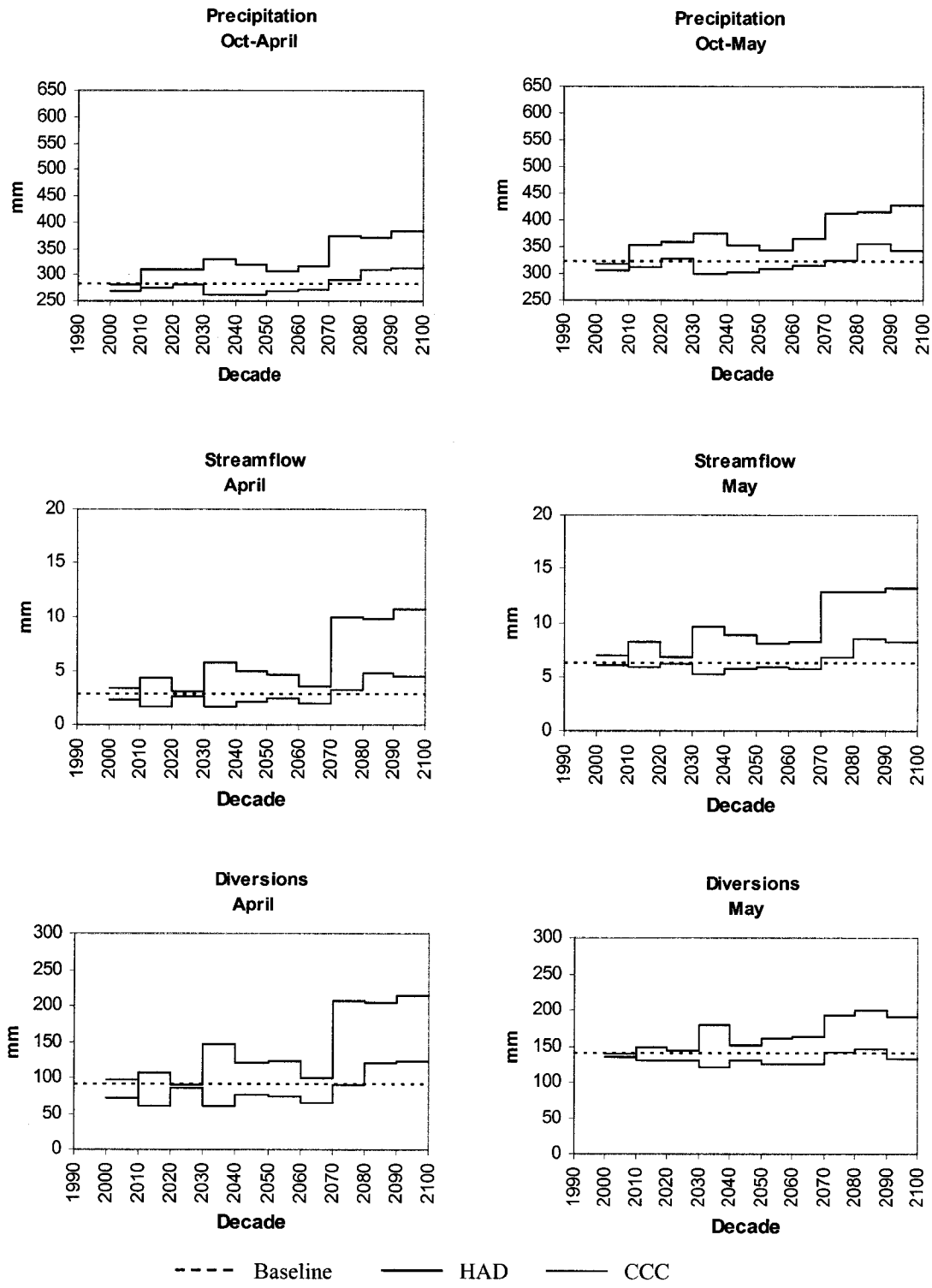

Figure 5-4 a Accumulated precipitation, monthly streamflow, and water diversion under the HAD and the CCC scenarios compared to baseline level

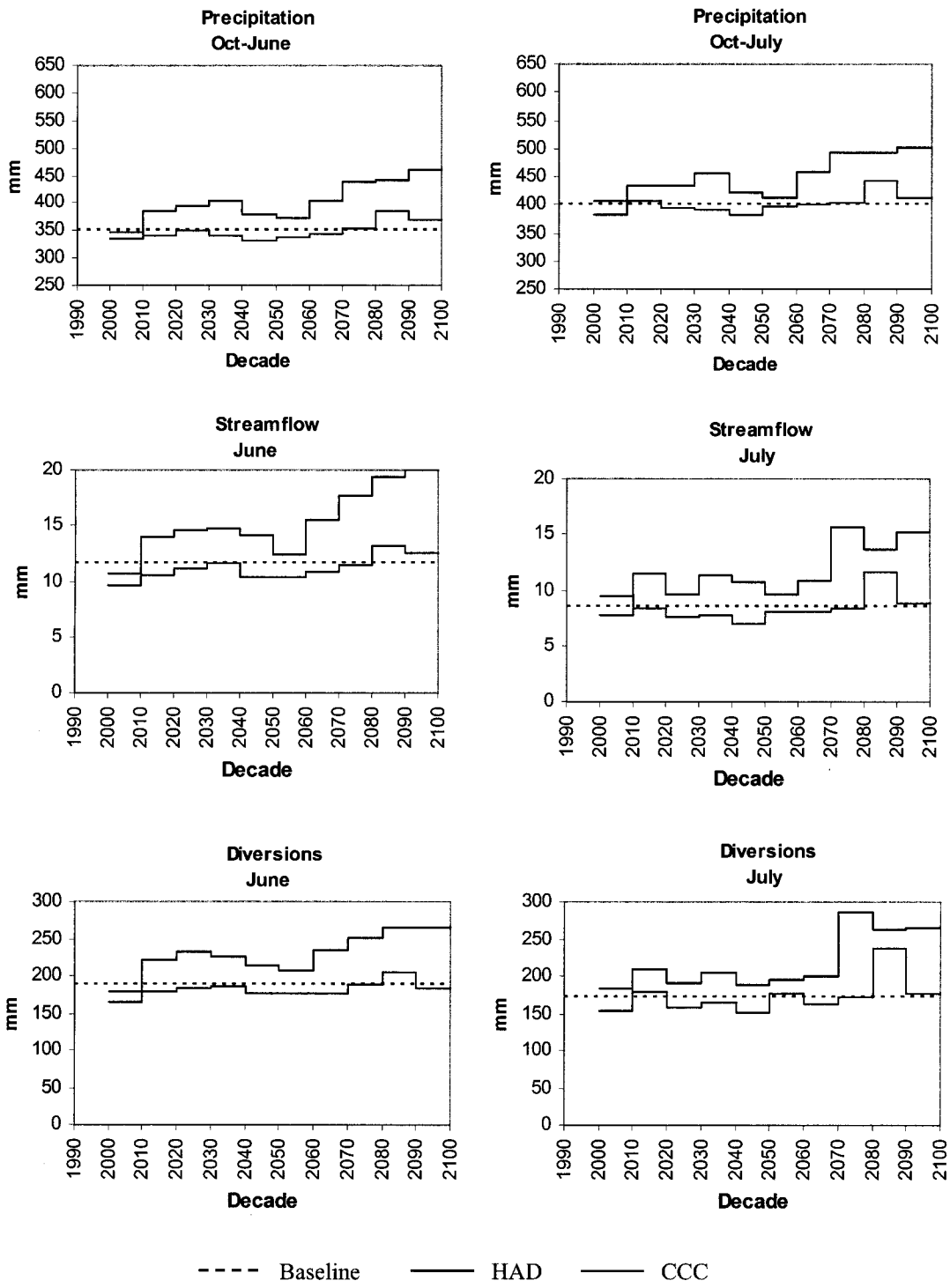

Figure 5-4 b Accumulated precipitation, monthly streamflow, and water diversion under the HAD and the CCC scenarios compared to baseline level

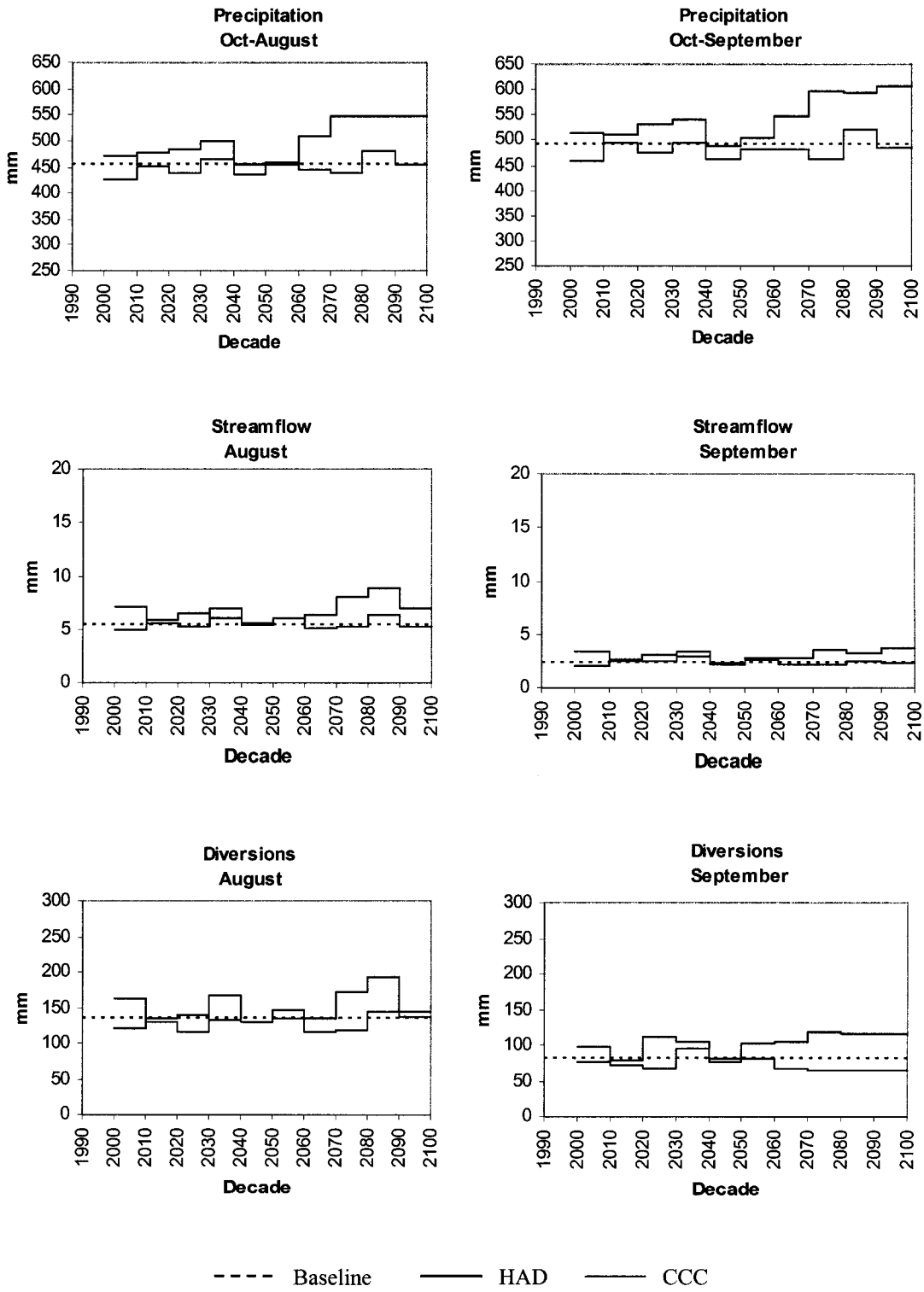

Fig. 5-4 c Accumulated precipitation, monthly streamflow, and water diversion under the HAD and the CCC scenarios compared to baseline level

Table 5.3 Baseline and changes in projected monthly surface water supply

	April		May		June		July		August		September		Season	
	HAD %	CCC %	HAD %	CCC %	HAD %	CCC %	HAD %	CCC %	HAD %	CCC %	HAD %	CCC %	HAD %	CCC %
Baseline(mm)	90		140		188		173		136		81		810	
1990s	39	39	27	27	12	12	12	12	17	17	26	26	20	20
2000s	-21	9	-4	-1	-12	-5	-11	7	-11	20	-4	20	-11	6
2010s	18	-34	7	-6	18	-5	21	3	-2	-5	-1	-10	12	-7
2020s	1	-4	4	-7	23	-3	10	-9	2	-14	38	-18	13	-8
2030s	64	-32	28	-14	20	-1	18	-4	-3	22	29	19	23	-1
2040s	35	-14	8	-8	13	-6	9	-13	-5	-5	1	-7	10	-9
2050s	37	-17	15	-11	9	-7	12	2	8	-1	27	0	16	-5
2060s	12	-27	16	-11	25	-6	16	-5	-1	-14	28	-17	16	-11
2070s	130	2	38	2	33	0	65	-1	26	-12	46	-20	52	-4
2080s	127	35	42	4	41	9	51	37	42	6	42	-19	53	14
2090s	137	38	36	-5	41	-2	53	2	7	0	44	-20	48	1

Generally, in this region climate is projected to be wetter under the HAD scenario and drier under the CCC scenario compared to the historical averages. Changes in hydrologic flow have changed commensurately because they are a result of one input (precipitation). Temporal patterns of river flow are shown to follow fairl ose of precipitation. Water supplies are shown to be more sensitive to changes in river flow (as indication of changes in accumulated precipitation) than monthly precipitation. In general, under the HAD scenario the region is expected to have an average wet period extended from the 2010s to the 2030s followed by a relatively dry period (2040s-2050s) and then a relatively wet period (2060s-2090s). Under the CCC scenario the region is expected to experience water shortages all the time.

The results show that, short term (decade-to-decade) and between months variability are considerably more apparent than any long term trend of change. However, under the HAD scenario, irrigation water diversions are expected to increase in all months of the growing season and expected to decrease in all months under the CCC scenario except for the summer of the 2080s when the scenario projected wet climate for the region.

Table 5.3 show statistics of changes in water supply. for example, according to the HAD scenario an average increase of 8% in annual precipitation (April – September) in the 2010s (average wet), will result in an increase in seasonal water supply of 12%, while it is expected to decrease by 7% when annual precipitation is projected to decrease by 1% under the CCC scenario.

The 2040s decade is projected to be relatively dry in which the annual precipitation is expected to increase by 6% under the HAD scenario and decrease by 5%

under the CCC scenario. These changes in precipitation are expected to be followed by an increase of 10% (HAD) and a decrease of 9% (CCC) in the seasonal water supplies in the region.

During the 2090s decade which is expected to be relatively wet under both scenarios (the HAD and the CCC), seasonal water supply is expected to increase by 48% and 1% due to increases of 24% and decreases of 1% in precipitation under the HAD and CCC scenarios, respectively.

On a monthly basis, water supply signals (responses to climate change) are clearer than those of the season. For example, under the CCC scenario, the high increase in water supply (38%) that is projected for April in the 2090s offset the shortage of water supply that projected for the rest of the months of the growing season and resulted in an increase of 1% in water supply for the whole season. However, under the HAD scenario water supply is expected to increase during all months. Increases in water supply during spring months (April-May) are projected to be more than those during the summer (June-July), this is due to larger increases in winter precipitation. August and September are shown to experience relatively small changes and this is due to the fact that more than 60 percent of the average annual runoff occurs during April through July, and 20 percent during August through October.

Based on this analysis there are several points to be emphasized. The responses of the water supply system follow the changes in the model inputs (monthly precipitation and river flow). The fluctuations (decrease and increase) in projected precipitation that are attributed to inter-annual and decade-to decade variability of imposed climatic changes are reflected on the projections of the water supplies. For example in May the

water supply was projected to increase during several decades although the results show a decrease in river flow for the same decades. This is attributed to the effect of changes in the magnitude of the monthly precipitation (increase). In general water supplies were projected to fall above the historical level (baseline) under the HAD scenario and below the baseline under the CCC scenario.

The projections of the river flow and hence of the water supply, might be relatively higher than what was expected. This is attributed to the fact that the effect of temperature was not included in the water supply model. The temperature, which is expected to be higher in the future, might have a different effect on the evaporation regime in the region. As a result, interaction between precipitation and evaporation and hence the response of water supply might be different. For example, high enough evaporation might offset increases in precipitation and result in small changes in water supply, or, due to higher temperatures, water supply regime might change from a snow-dominated one to a rainfall-dominated one and result in non-linear changes in water supply.

5.3 Effects on Water Demand

This section explores the effects of climate change and increases in atmospheric CO_2 on irrigation water demand. The main approach used in this analysis was to compare model predictions to baseline (historical values under no climate change). Therefore, the ET model described earlier in chapter 4 was first used to estimate ET from historical data to provide baseline data sets. Next the sensitivity of ET to multi climatic and plant factors was tested.

ET Sensitivity

ET responds differently, in magnitude and direction, to changes in each climatic and plant factor (e.g. temperature, net radiation, humidity, wind speed, leaf area index, and stomatal resistance). An increase in temperature means that air is able to hold more moisture and this by itself would cause evaporation to increase. Some other changes accompanying the changes in temperature such as the amount of energy available also affect evaporation rate. High temperatures indicate high levels of radiation, which most likely will increase evaporation, but during times of the year cloud cover reduces net radiation while temperatures are still high. Generally, higher temperatures tend to decrease humidity, even though atmospheric moisture content might increase due to the increased evaporation. However, an increase in humidity or a decrease in solar radiation leads to a decrease in evaporation. Changes in wind speed also affect evaporation rates as well as changes in plant parameters. Therefore, changes in all or some of these factors mentioned above are expected to changes ET. Martin et al., 1989 conducted a sensitivity analysis on ET using the Pennan-Monteith formula in a wheat field in Nebraska. Their results showed that ET is highly sensitive to air temperature, solar radiation, humidity, and stomatal resistance. For this study the sensitivity of ET for each climatic factor was analyzed. Figure 5.5 illustrates the results of the sensitivity analysis. The calculations of ET were made daily. The values presented are an average over the simulation period (100 year). As shown in the figure ET is more sensitive to changes in Temperature (T) and wind speed (U) while SR and RH have only slight effect.

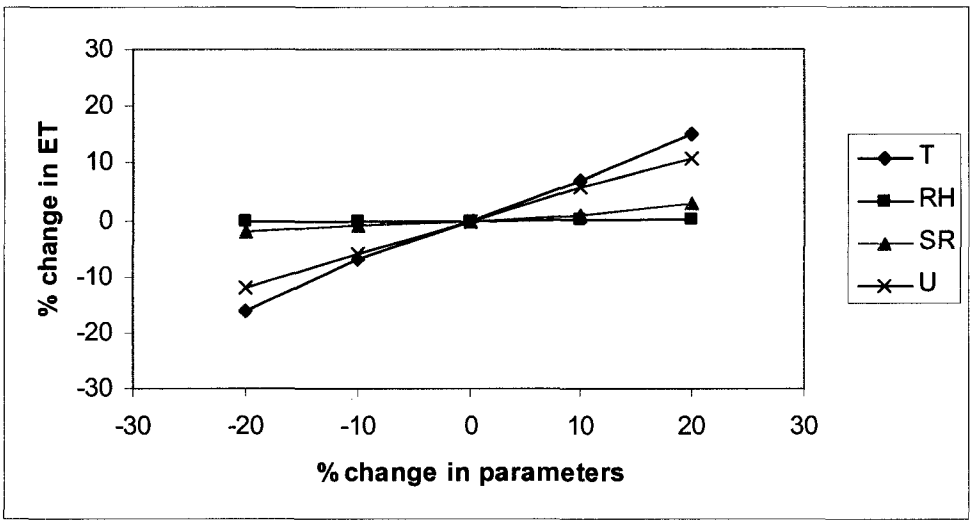

Figure 5-5 Predicted ET in response to changes in climatic factors (temperature T; relative humidity RH; solar radiation SR; wind speed U).

In the scenarios study, the simulations were carried out considering the effects of multi climate factor changes. The climate scenarios used incorporated changes in all factors mentioned above besides the changes in precipitation, and any ET estimates obtained are the result of the combined effects of changes in all of these climatic and plant factors.

5.3.1 Effects on ET

The ET analyses assumed that alfalfa (reference crop) and all other crops used in this study respond in the same manner to changes in climate and CO_2. This assumption permitted the use of crop coefficients to estimate each crop ET while using an alfalfa reference.

Responses of ET to multifactor changes were estimated daily for each crop. Then the daily estimates were aggregated into monthly and seasonal values. By keeping the length of the growing season unchanged, climatic changes are the only cause of changes

in ET. The influences of climatic changes on monthly and seasonal ET are presented in the following sections.

Table 5.4 and Figures 5.6 and 5.7 show the changes in seasonal and monthly ET's for the study region, between 1994 and 2099 under the two transient scenarios. These figures show the changes in decade mean ET for the whole season and each month of the growing season. The results are presented relative to the baseline (1960-1990) to give some insights into the magnitude and direction of the changes. It is very clear in the figures that the effects of the changes in climate influenced both monthly and seasonal ET. There is a gradual increase in the values of ET. These increases are attributed to the influence of temperature. The projected changes in ET under the CCC scenario are larger than those under the HAD, and this is mainly due to the higher temperatures projected by the CCC scenario.

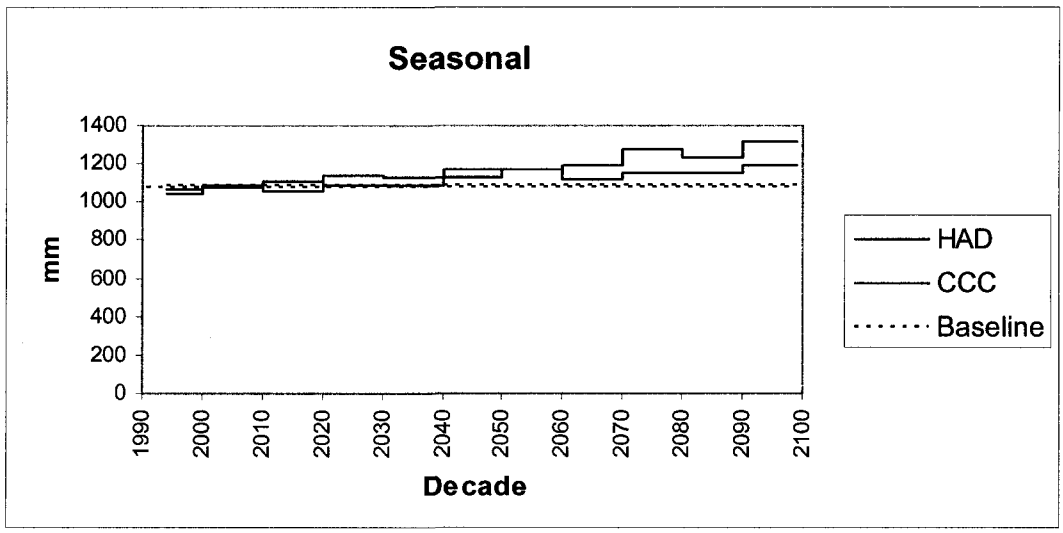

Figure 5-6 Seasonal ET under climate change by decade

Table 5.4 Percentage change in monthly ET from baseline

	April		May		June		July		August		September		Season	
	HAD %	CCC %	HAD %	CCC %	HAD %	CCC %	HAD %	CCC %	HAD %	CCC %	HAD %	CCC %	HAD %	CCC %
Baseline(mm)	10		120		234		268		250		126		1083	
1990s	-27	49	3	17	3	0	-11	-15	-7	-10	10	4	-2	-4
2000s	92	211	15	46	-3	3	-10	-14	-6	-12	7	-8	0	-1
2010s	121	136	23	31	-2	0	-12	-15	-3	-10	3	-2	2	-3
2020s	81	284	10	44	-3	3	-9	-7	-5	-4	3	1	0	5
2030s	7	260	9	53	-1	5	-10	-10	-1	-8	5	-1	0	4
2040s	70	389	22	61	2	7	-11	-8	0	-7	5	3	4	8
2050s	240	512	52	62	5	4	-11	-6	-5	-10	-3	1	8	8
2060s	61	475	23	77	0	10	-10	-9	-2	-8	5	1	3	10
2070s	240	897	31	95	1	7	-6	0	-6	-13	2	2	6	17
2080s	240	739	32	79	3	9	-7	-6	-7	-9	4	1	7	14
2090s	289	1116	45	103	4	10	-7	-1	-2	-13	3	4	10	22

According to the CCC scenario, the seasonal ET increases from values below and crosses the threshold of the historical level in the 2020s. These increases range from 5% above the historical level in the 2020s up to 22% in the 2090s with a rate of increase of 2.6% per decade. Under the HAD scenario, it takes up to the 2040s for ET to cross the threshold of the historical level by an increase of 4%; and ET gradually increases up to 10% above the baseline in the 2090s at a rate of 1% per decade.

As shown in Figure 5.7, changes in monthly ET are more vigorous than those in seasonal ET. Even though within the months, the figure shows a difference between changes in ET in the spring months (April-May) and summer months (June-July). Changes in the spring are more vigorous than in the summer. However, under both scenarios (HAD/CCC) ET is projected to increase above the baseline during the spring months and decrease below the baseline in the summer. According to the CCC scenario, the increases in ET in the spring (May) range from 30% above the historical level in the 2010s up to more than 100% in the 2090s with a rate of increase of 8% per decade, considering that in April increases in ET are more than those in May. Under the HAD scenario, ET increases by 12% in the 2010s and by 45% in the 2090s at a rate of increase of 1% per decade. These large increases in ET in the spring are attributed to the fact that they were estimated from very low historical (baseline) ET values. During the summers, even though ET is projected to fall below the historical average (baseline) a very slight increasing trend can be detected. Under the CCC scenario ET is projected to increase by 14% in the period from the 2010s to the 2090s at a rate of increase of 1.5% per decade, while under the HAD scenario and for the same period of time ET is projected to increase only by 5% with an increasing rate of 0.55% per decade.

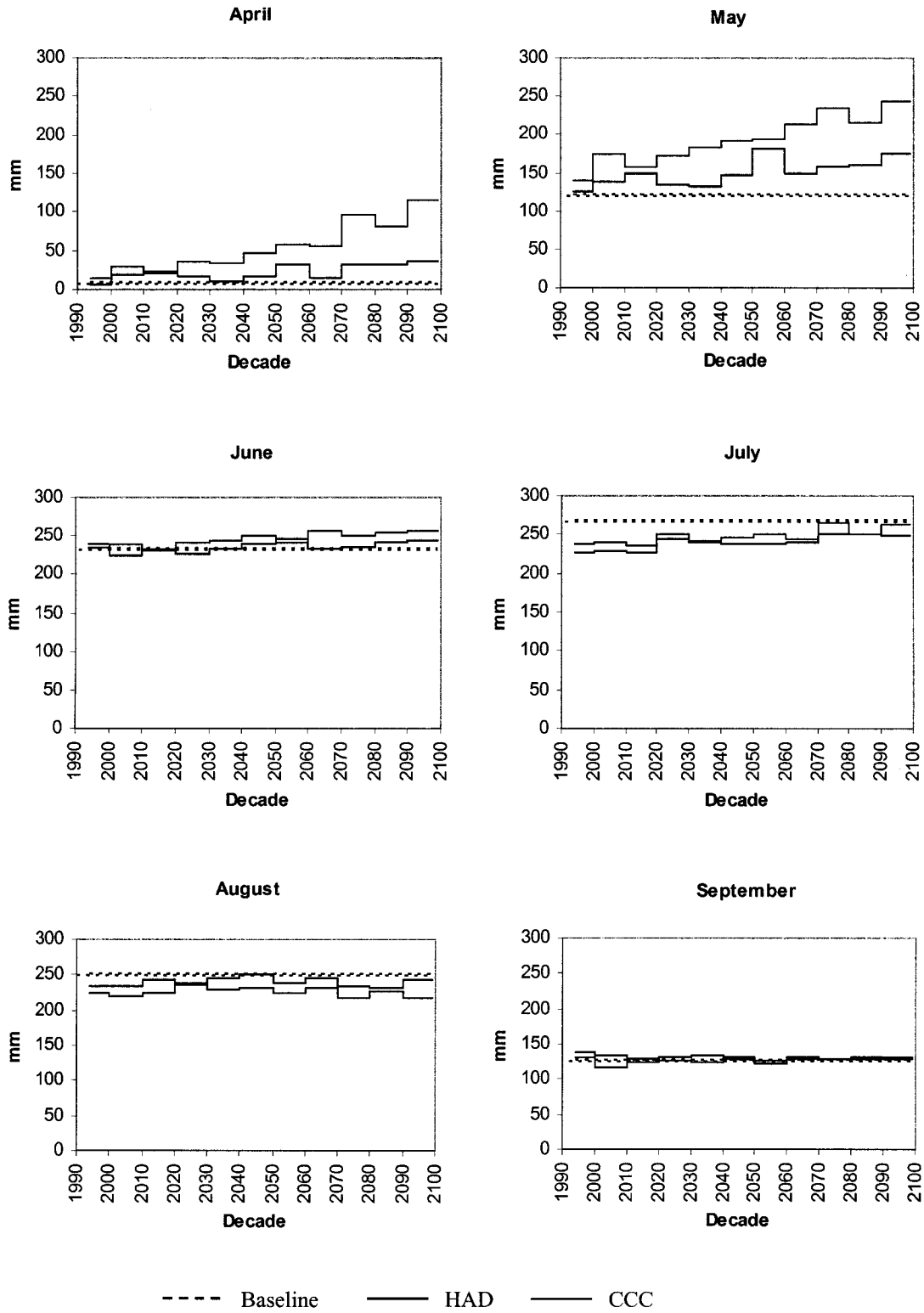

Figure 5-7 Variation in monthly ET under climate change by decades

Based on this analysis there are several points that need to be emphasized. In general, even though there is decade-to-decade variability a trend in ET changes can be identified. It is very clear that ET values increase over time towards the end of the century following the trend of temperature. As shown in Figure 5.7, the rate of change of ET in the summer is less than that in the spring. ET in the summer tends to increase by smaller amounts than in the spring and this is because the wind speed is lower and the relative humidity is higher during the summer than during the spring. In the spring the changes in ET relative to the baseline are higher than those in the summer because the relative change in temperature is higher in the spring than in the summer. In the summer months ET is projected to decrease below the baseline in July and August with almost no change in June. The low projections of ET in the summer are attributed to limited amount of water available for evaporation during the summer as a result of high humidity level and low wind speed. Figure 5.7 shows that the deviations of projected ET from the baseline were larger under the CCC scenario than under the HAD scenario. This is attributed to the effect of higher temperatures projected by the CCC scenario compared to those projected by the HAD scenario.

Figure 5.6 shows that seasonal ET increased above the baseline under both scenarios, although the ET values during the summer were relatively low. This is interpreted by that: the increase in ET during spring was high enough to offset the decrease during summer and resulted in an increase in seasonal ET. Due to warmer and drier climate, projected increases in seasonal ET under the CCC scenario are almost double those under the HAD scenario.

5.3.2 Effects on IWR

Projected changes in irrigation water requirement (IWR) (defined as ET minus effective rainfall, Re) are presented in this section. Besides changes in ET, the change in IWR depends also on the changes in rainfall. Table 5.5 shows the percentage changes in IWR under the two scenarios of climate change. Percentage changes in IWR were very high in April and May due to the very low baseline values. Large changes in precipitation patterns caused large variation in IWR. In general, the projected increases in IWR were higher than ET under the CCC scenario. This is attributed to the effect of drier conditions projected by the CCC scenario. Under the two scenarios, July and August experienced a decrease in both ET and IWR and this is attributed to very high baseline values for both, but still both months showed an increasing trend towards the end of the 21st century where conditions are getting drier (Fig 5.7). Generally, several decades show very little difference in the percentage change in ET and IWR while under drier conditions the percentage change in IWR were slightly higher than those of ET. For example, during the decade of the 2090s, the projected changes, under the CCC scenario, in seasonal IWR show an increase of 24% while ET increases by 22%.

Based on this analysis, under the two climate scenarios applied, seasonal ET and IWR are expected to increase gradually towards the end of this century. Climatic changes are expected to increase ET and IWR during spring months (April and May) and decrease them during summer months (July and August). Even though there were variations in the changes in monthly projections, IWR gradually increased. This is due to the influence of temperature which is projected to gradually increase towards the end of this century.

Table 5.5 Percentage change in monthly and seasonal IWR from baseline

	April		May		June		July		August		September		Seasonal	
	HAD %	CCC %	HAD %	CCC %	HAD %	CCC %	HAD %	CCC %	HAD %	CCC %	HAD %	CCC %	HAD %	CCC %
1990s	-29	50	5	17	4	1	-13	-19	-7	-11	11	4	-2	-5
2000s	98	200	15	46	-5	3	-12	-15	-6	-13	6	-10	0	-2
2010s	123	135	22	32	-2	-1	-13	-17	-2	-9	4	-4	2	-4
2020s	78	289	9	45	-5	5	-8	-7	-6	-2	2	0	-1	6
2030s	5	259	8	56	-2	4	-11	-10	0	-10	4	-2	0	3
2040s	72	393	24	61	3	8	-12	-8	3	-7	5	3	5	8
2050s	228	519	53	65	5	4	-11	-9	-4	-9	-5	0	7	8
2060s	59	476	23	79	-1	12	-11	-11	-2	-5	4	2	2	11
2070s	234	911	31	102	1	9	-5	0	-7	-10	0	3	5	19
2080s	228	749	31	82	3	12	-7	-9	-9	-7	3	0	6	15
2090s	280	1148	45	112	4	12	-7	-1	-2	-12	0	5	9	24

5.3.3 Combined effects

The combined effects of climatic and plant changes on IWR are presented in the following section. Estimates of monthly and seasonal IWR were projected for 0% (climate change only), 20%, 40%, 60%, and 80% increases in plant bulk resistance "r_c". The percentage changes represent scenarios for r_c in environments of doubled CO_2. Since the current levels of CO_2 are expected to double by the 2090s, the projections for the decade of the 2090s are presented here. The rest of the results are presented in **appendix C**.

Figure 5.8 shows a summary of changes in seasonal ET and IWR projected for the doubled CO_2 scenarios from the CCC and the HAD models for a range of stomatal resistances. Figure 5.9 reports the response of seasonal ET and IWR to increases in plant bulk canopy resistance r_c coupled with climatic changes. It is very clear that both of them (ET and IWR) are very sensitive to changes in r_c. Coupling the climate changes with plant changes reduced ET and IWR from the level they were at under climate change only. As shown in Fig. 5.8 both ET and IWR experienced a linear decrease for the increase in r_c.

As shown in Fig. 5.8 the effect of CO_2-induced plant changes (increased stomatal resistance and plant size) decreases ET therefore offsetting any increases due to climate change. The figure shows that a 20% increase in r_c under the CCC scenario only reduces the effect of climate change on IWR, while the same amount of increase in r_c (20%) under the HAD scenario totally offset it. This is because the effects of climate change on IWR were smaller under the HAD scenario than those under the CCC scenario. Under the

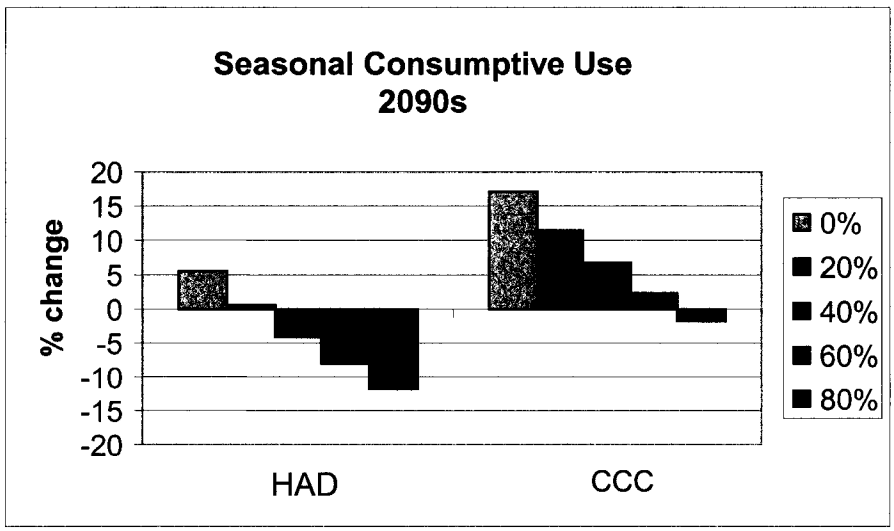

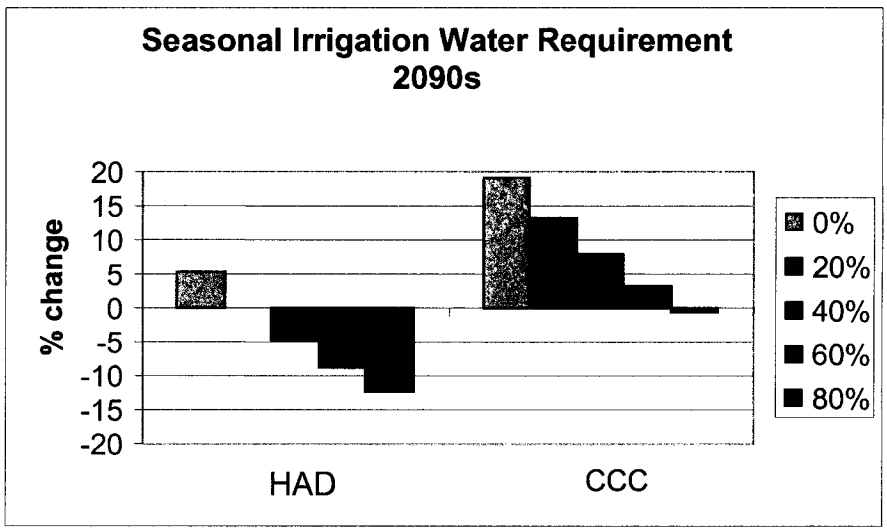

Figure 5-8 Percentage changes in ET and IWR from baseline for percentage increase in bulk plant canopy resistance (r_c).

CCC scenario more than 60% increase in r_c was needed to offset the climate change effect on IWR, and up to 80% increase to negate it.

In general, average increase of 50% in r_c coupled with the HAD scenario is expected to reduce the seasonal ET by 12 % (from 6% above the baseline to 6% below the baseline), and from 17% to 5% above the baseline under the CCC scenario. If r_c increased by the same amount (50%), this would reduce IWR from 19% to 5% under the CCC scenario and from 5% to 7% under the HAD scenario.

5.4 Effects on Irrigation Water Balance

The water resources available for use in a region are determined by the amount of water available (supply) and the amount of water needed (demand). In this region the water supplies determine the amount of water available for use (demand). As discussed in the previous sections, climate change affects both water supply (WS) and water demand (IWR) for irrigation therefore, it is necessary to examine the potential changes in the balance between demand and supply under climate change. This section explores the status of the balance between demand and supply under two scenarios of climate change. The effects of climate change were evaluated using water balance sheets. First, a baseline water balance was established using historical records of water supply and demand. Presented in Table 5.6 is a water demand-water supply balance for historical averages.

The numbers and percentages presented (Table 5.6) show that under the baseline (no climate change) water supplies were already under stress during the summer months. During the summer time of the growing season the region experiences a shortage in water supplies, which can reach up to 28% (on average) of water demand. To fill the gap between demand and surface supply, groundwater supplies have been used conjunctively

Table 5.6 Historical water demand – water supply balance

	Water demand	Water supply	Difference	Difference type	Difference
	mm	mm	mm		%
April	9	90	81	surplus	900
May	109	140	31	surplus	28
June	216	188	28	deficit	13
July	244	173	70	deficit	29
August	230	136	94	deficit	41
September	118	81	37	deficit	31
Season	926	809	117	deficit	13

with surface supplies. Groundwater has been pumped to augment 5-10 % of the deficits presented in Table 5.6. The values show that in June the shortage was up to 13% (28mm) of the water demand, while the percentage varies among the other summer months from 29% (70mm) in July, 41% (94mm) in August, 31% (37mm) in September, and 13% (117mm) during the whole season.

Climate change further stressed surface water supplies and increased water demand especially during the summer time, outweighing the balance of irrigation water. However, there are ways to mitigate the impacts (water shortage) of these effects on agricultural water systems; one of which is the use of groundwater supplies.

As mentioned in the previous paragraph groundwater is used to augment only 5-10% of the historical shortage in surface water supplies. For the purpose of this study, any difference between demand and supply in the future (under climate change) greater than 5-10% is considered a deficit, assuming that we have enough groundwater stored to provide the same current amounts of groundwater supplies (5-10%).

Table 5.7 shows the difference (in percentage) between demand and supply under the two scenarios of climate change. The results show that under the CCC scenario the region is expected to experience a shortage in water supply for long periods of time which extend from the 2010s to the 2090s. Shortages are expected for the whole season and for each month in the season except for April. The maximum shortage for the whole season (30%) is expected during the decade of the 2060s. While no shortage is expected during the decade of the 2080s, the shortage during the decade of the 2090s is expected to be double the current shortage in surface water supply. The shortage during the summer time is greater than that during the spring. The results show that, under the HAD

Table 5.7 Water balance under two scenarios of climate change (HAD and CCC) presented in percentages

	April		May		June		July		August		September		Seasonal	
	HAD %	CCC %	HAD %	CCC %	HAD %	CCC %	HAD %	CCC %	HAD %	CCC %	HAD %	CCC %	HAD %	CCC %
2000s	301	266	7	-13	-20	-19	-29	-11	-44	-19	-38	-9	-20	-14
2010s	434	184	13	-9	5	-16	-1	-12	-41	-38	-34	-36	-2	-26
2020s	472	150	22	-18	13	-19	-15	-31	-36	-48	-7	-43	1	-25
2030s	1471	90	52	-29	6	-17	-5	-24	-43	-19	-15	-17	9	-20
2040s	692	76	12	-27	-4	-24	-12	-33	-45	-39	-33	-38	-6	-29
2050s	322	36	-4	-30	-9	-22	-11	-21	-33	-35	-8	-32	-4	-28
2060s	609	27	21	-36	11	-26	-7	-25	-41	-46	-15	-44	1	-30
2070s	592	2	35	-35	15	-19	24	-29	-20	-42	0	-47	29	-26
2080s	598	60	39	-27	19	-15	15	7	-8	-33	12	-45	32	-13
2090s	528	11	4	-43	1	-24	-7	-26	-36	-33	-14	-38	8	-24

scenario the region is expected to have shortage in water supplies during the summer time (August) of the growing season, while the whole growing season is shown to have no shortage in water supply. This due to the fact that the high water supplies projected for the spring are high enough to offset the shortage expected during the summer assuming that there is enough storage infrastructures to store the large amount of water supplies expected during the spring so that they can be used during the summer time.

6. SUMMARY AND CONCLUSIONS

In this research, two models were developed and applied to estimate the effects of climate change on irrigation in the Arkansas River basin. The first model is an artificial neural network (ANN) model, which was developed to estimate the effects of climatic changes on water supplies for irrigation in the region. The second model was a consumptive use (CU) model developed to estimate the effects of climate change on irrigation water demand. Both models were applied to baseline and transient climatic scenarios predicted by two global GCMs (HAD and CCC). Projections by the two models were used to evaluate the responses of the irrigation system in the study area to climatic and plant changes. In practice, climate is expected to change gradually (transient), therefore, transient climate scenarios were found helpful in assessing the possible effects of transient climate change. Studying the transient effects of climate change provides useful information on the effect of year-to-year variability and long term trend on potential rates of change, which might be very important to decision makers. Should these climatic changes actually occur; several issues discussed in this research will provide, hopefully, a useful contribution towards understanding the extent and magnitude of climate change impacts. However, there are some concluding comments, emphasized by the results of this research which are discussed in the following sections.

6.1 Climate Scenarios

Projections by the transient HAD scenario were compared to baseline data to estimate the direction and magnitude of changes in each component of the irrigation

water balance, and compared to the CCC scenario to assess the importance of differences in projections made by each scenario on different water balance components.

While there are large differences in precipitation projections between the two scenarios, trends of changes in projected air temperature in the study region were similar under both scenarios. Variability in temperature projections is higher in the spring months (April-May) than the summer months with a very clear trend during the summer. The CCC scenario projects higher temperatures than the HAD. Variability dominates precipitation projections. Year-to-year variability in precipitation projections is different across the two scenarios. For example, there were periods of several years in which the direction of change in one scenario is opposite to the direction of the other scenario. However, precipitation projections are higher under the HAD scenario than the CCC.

In general, air temperature was projected to increase by the two scenarios. The CCC scenario projected drier and warmer climate for the region. Trends and patterns of change in climate are more obvious at decadal scale.

It must be noted that there is tremendous uncertainty regarding the regional patterns of precipitation change under global warming. There are large differences across GCM's models in projected precipitation changes (Miller, 1997). The results presented in this study showed that the two scenarios used (HAD/CCC) gave different results regarding the direction of change in water supply in the region.

6.2 Water Supply

The results of this study as intended gave some insights into changes of monthly and seasonal water supplies under two GCM scenarios. Based on the analysis made in this research, the study region is sensitive to climate change. Water supply was sensitive

to changes in precipitation projections. The two GCMs scenarios gave different indications about the direction of the effect of climate change on water supply. The region is expected to be relatively wet under the HAD scenario, with the growing season having enough water supply and relatively dry under the CCC scenario with the growing season having shortages in water supply.

Under the CCC scenario which is dry and warm, projections show that during the growing season (in the study region) shortages are expected to dominate most of the time. Variation in water supply projections within the season are more than those of the projections made for the whole season.

Under the HAD scenario which is relatively wetter and less warm the region is projected to have an increase in water supply compared to the current conditions. Increases in water supply during the spring are more than those during the summer. Moreover, in the late summer (August), crops grown in the region are expected to experience more water shortages.

The results show that the variation in changes that are projected within the growing season (spring and summer) are more than those projected for the whole season. For example, under the HAD scenario the projected changes included an increase in spring water supply and a decrease in summer water supply. As a result the water supply that is projected for spring is expected to be high enough to offset the decrease expected in summer, therefore the growing season is shown to have enough water supply. If the capacity of water storage infrastructures is not enough to store the increase of water supply that is expected in spring, a decrease in summer and hence season water supply is quite possible. This kind of argument reflects some uncertainty on the projected changes

at larger time scales such as a whole growing season or annual scale. For example, Wolock and McCabe 1999 estimated the annual runoff projections in the same region of this study. Due to uncertainties in those estimate, the authors considered their projections unreliable.

The projections reported in this study support the expectation that analysis of climate change effects at smaller scale (monthly) will increase our understanding and help plan for the impacts of climate change. The Projections presented contrasted trends with variability of climate change and gave insights into effects of climate change. The Simulations provided information on when and at what rate increases or decrease in water supply are expected.

6.3 Water Demand

6.3.1 Global Warming effects

Irrigation water requirement (IWR) or water demand was very sensitive to changes in temperature. IWR was projected to increase during spring months under both scenarios. Increases are very high compared to the baseline level and this most probably attributed to an increase in the amount of water available for evaporation as a result of changes in the precipitation regime in the region. Changes in climatic variables caused increases, decreases, and no change in IWR during the summer. Projected increases in air humidity and decreases in solar radiation under the two scenarios reduced the amounts of IWR to a level below the baseline during summer months. The projections also show that IWR during the whole season is expected to increase under both scenarios. This is a misleading indication because the high increases of IWR in spring months offset the decreases of IWR during summer months and the overall effect was that the IWR for the

whole season was projected to increase. This result supports the expectation that analyses at smaller scale (monthly) are more indicative than those at larger scale (seasonal or annual).

Simulations provide information about the magnitude, direction and rate of change in IWR. Under the CCC scenario IWR is expected to increase and water supply to decrease, therefore crops are expected to experience water stress unless the crop cycles shift towards the winter months which are expected to be warmer and the conditions more favorable for crops to grow. Under the HAD scenario the overall effect of climate change is expected to result in an improvement in the supply/demand situation for crop irrigation.

6.3.2 Combined effects

Combined effects of changes in climate and plant, tend to decrease IWR. Under higher concentrations of CO_2 bulk stomatal resistance (r_c) in plants is expected to increase limiting the amount of water transpired by the plant and hence decrease IWR. The amounts of increase in r_c (20%-80%) were large enough to negate the effect of climate change under the HAD scenario and partly offset the effect of climate change under the CCC scenario. This is attributed to larger effects of climate change under the CCC scenario.

Due to limited information, r_c behavior under the effect of increase in CO_2 has not yet been verified in actual field conditions; therefore, sensitivity analysis of the effects of changes in r_c (percentage) on IWR was estimated. The results of this sensitivity analysis support results of a study conducted by Allen, R. G. et al, 1991, which showed that

increases in r_c would offset or negate the increases in IWR that are expected due to climate change (global warming).

6.4 Water Balance

The real impact of climate change in either water supply or water demand can best be evaluated in conjunction with the other. The balance of water supply and demand for irrigation could be affected the differences in temperature and precipitation changes projected by the two scenarios. The results presented show that the region already experiences shortages in surface water supply and a relatively small percentage (5-10%) of these are augmented by groundwater.

Under the CCC scenario the water balance deteriorates in the region because water supplies for the whole season and each month in the season (except for April) are expected to be short to satisfy the demand.

Under the HAD scenario which is wet and less warm than the CCC scenario the changes in the balance between supply and demand range from no significant changes to improvement due to increase in water supply over demand. The high projections of additional water supply during the spring are expected to offset the decreases projected in water supply during summer specifically in August. Therefore, the balance in the growing season under the HAD scenario is projected to improve. As discussed in a previous section (section 6.2) this last result is uncertain in the absence of other factors such as enough water storage infrastructures to store the additional water projected during the spring and use it to offset the decrease of water during the summer.

In general, under the HAD scenario the climate effects on the balance of supply and demand for irrigation would be more favorable in the last three decade of this century

(2070-2090) while the water balance derived from the CCC projections all the time deteriorates.

7. RECOMMENDATIONS FOR FUTURE RESEARCH

1. Adding temperature to the model of water supply might change the projections of the water supply. The temperature, which is expected to be higher in the future, might change the evaporation regime in the region. Therefore, the methodology developed in this research needs to be extended to evaluate what impacts this might have on predictions of water supply in the study region.
2. Reservoirs play a big role in managing water supplies; a further study is needed to investigate the effect of reservoir storage on the water balance.
3. Extend the methodology developed in this research to study the effect of temperature on predictions of water supply.
4. Investigate the frequency of high and low river flows under climate change and their effects on water supply.
5. Study the effect of changes in crop life cycles, that are expected under climate change, on irrigation water requirement and hence on the balance between water demand and supply.
6. Investigate drought or flood events that might happen under climate change and effect of that on water supplies.

BIBLIOGRAPHY

Abu-taleb, M. F., 2000. Impacts of global climate change scenarios on water supply and demand in Jordan. Water International 25(3): 457-463.

Adams, R. M., C. Rosenzweig, R. M. Peart, J. T. Ritchei, B.A. McCarl, J. D. Glyer, R. B. Curry, J. W. Jones, K. J. Boote, and L. H. Allen, Jr. 1990. Global climate change and US agriculture. Nature 345: 219-224.

Allen, S.G., S. B. Idso, B. A. Kimball, J. T. Baker, L. H. Allen, Jr., J. R. Mauney, J. W. Radin, and M. G. Anderson. 1990. Effects of air Temperature on Atmospheric CO_2-Plant Growth Relationships. DOE/ER-0450T. U.S. Department of Energy. Washington, DC. 61pp.

Allen, R. G., F. N. Gichuki, and C. Rosenzweig. 1991. "CO_2-induced climatic changes and irrigation requirements. Journal of Water Resources Planning and Management 117(2): 157-178.

American Society of Civil Engineers (ACSE) Manual No. 70, 1990. Evapotranspiration and Irrigation Water Requirements.

Arnell, N., 1996. Global warming, River Flows and Water Resources. Wiley, West Sussex, England.

Bergstrom, S., B. Carlsson, M. Gardelin, G. Lindstrom, A. Pettersson, and M. Rummukainen, 2001. Climate change impacts on runoff in Sweden – assessment by global climate models, dynamical downscaling and hydrological modeling. Climate Research 16(2): 101-112.

Carter, T. R., M. L. Parry, S. Nishioka, and H. Harasawa, 1994. Technical Guidelines for Assessing Climate Change Impacts and Adaptations. IPCC, University College London, and Center for Global Environmental Research, Tsukuba. pp51.

Chen, C. C., D. Gillig, and B. A. McCarl, 2001. Effects of climatic change on water dependent regional economy: A study of the Texas Edwards Aquifer. Climatic Change 49(4): 397-409.

Chew, F. H. S., P. H. Whetton, T. A. McMahon, and A. B. Pittock, 1995. Sinulation of the Impacts of Climate-Change on Runoff and Soil Moisture in Australia Catchments. Journal of Hydrology 167(1-4): 121-147.

Colorado Water Conservation Board (CWCB) and USDA, 1981. Arkansas River Basin Report.

Cooley, K. R., 1990. Effects of CO2- Induced Climatic Changes on Snowpack and Streamflow. Hydrological Science Journal 35(5): 511-522.

Cure, J. D. and B. Acock. 1986. Crops responses to carbon dioxide doubling: A literature survey. Agriculture and Forest Meteorology 38: 127-145.

Dugan, J. T., T. McGrath and R. B. Zelt. 1994. Water-Level Changes in the High Plains Aquifer-Predevelopment to 1992. U.S. Geological Survey. Water-Resources Investigations Report 94-4027. Lincoln, NE.

Dvorak, V., J. Hlandy, and L. Kasparek, 1997. Climate change hydrology and water resources impact and adaptation for selected river basins in the Czech Republic. Climatic Change 36(1-2): 93-106.

Eldaw, A. K., Long range forecasting of the Nile River flow using large scale oceanic atmospheric forcings, Ph.D. dissertation, Colorado State University, Fort Collins, Colorado, 2001.

Farahani, H. and Bausch, W., 1995. Performance of Evapotranspiration Models for Maize-Bare Soil to Closed Canopy. Journal of the American Society of Agricultural Engineers (ASAE) Soil and Water Division.

Flood, I., and N. Kartam, 1994. Neural networks in civil Engineering. I:Principles and understanding. Journal of Computing in Civil Engineering 8(2): 131-148.

Flood, I., and N. Kartam, 1994. Neural networks in civil Engineering. I: Systems and applications. Journal of Computing in Civil Engineering 8(2): 149-162.

Frederick, K. D. 1993. Climate change impacts on water resources and possible responses in MINK region. Climatic Change 24:83-115.

Frederick, K. D. 1997. Adapting to climate impacts on the supply and demand for water. Climatic Change 37(1): 141-156.

Fyfe, J. C. and G. M. Flato, 1999. Enhanced Climate Change and Its Detection Over the Rocky Mountains. Journal of Climate 12(1): 230-243.

Giorgi, F., C. S. Brodeur, and G. T. Bates, 1994. Regional climate change scenarios over the United States produced with a nested regional climate model. Journal of Climate 7: 375-399.

Glantz, M. H. and J. H. Ausubel. 1984. The Ogallala Aquifer and Carbon Dioxide: Comparison and Convergence. Environmental Conservation 11(2): 123-131.

Goh, A. T. C., 1995. Modeling soil correlations using neural networks. Journal of Computing in Civil Engineering 9(4): 275-278.

Hartig, E. K., O. Grozev, and C. Rosenzweig, 1997. Climate change, agriculture and wetlands in Eastern Europe: Vulnerability, adaptation and policy. Climatic Change 36(1-2): 107-121.

Hsieh, W. W., and B. Tang, 1998. Applying neural network models to prediction and data analysis in meteorology and oceanography. Bulletin of the American Meteorological Society 79(9): 1855-1870.

Hsu, K., H. V. Gupta, and S. Sorooshian, 1995. Artificial neural network modeling of the rainfall-runoff process. Water Resources Research 31(10): 22517-2530.

Hurd, B., N. Leary, R. Jones, and J. Smith, 1999. Relative regional vulnerability of water resources to climate change. Journal of the American Water Resources Association (JAWRA) 35(6): 1399-1409.

Hydrology Handbook, 1996.

IDS. (http://www.ids.colostate.edu)

Idso, S. B. and A. J. Brazel, 1984. Rising Atmospheric Carbon Dioxide May Increase Streamflow. Nature 312(1): 51-53.

IPCC. 1996. Climate Change 1995: The Science of Climate Change. J. T. Houghton, L.B. Meira Filho, B. A. Callander, N. Harris, A. Kattenberg, and K. Maskell (eds.). Intergovernmental Panel on Climate Change. Cambridge University Press. Cambridge.

IPCC, Climate Change 2001: the scientific basis- summary for policy makers and technical summary for the working group 1 report. Cambridge University Press, UK, 2001.

Irmgard F., C. W. Stockton, and W. R. Boggess, 1987. Climatic Variation and Surface Water Resources. Water Resources Bulletin 23(1): 47-57.

Jensen, M. E., 1990. Consumptive use of water and irrigation water requirements. Technical Committee Report on Irrigation Water Requirements, ASCE, Irrigation and Drainage Division.

John, T. C., R. E. Carnell, J. F. Crossley, J. M. Gregory, J. F. B. Mitchell, C. A. Senior, S. F. B. Tett, and R. A. Wood, 1997. The Second Hadley Centre Coupled Ocean-Atmosphere GCM: Model Description, Spinup, and Validation. Climate Dynamics 13:103:134.

Jones, R. N., 2000. Analyzing the risk of climate change using an irrigation demand model. Climate Research 14:89-100.

Kittel, T.G.F., N.A. Rosenbloom, T.H. Painter, D.S. Schimel, and VEMAP Modeling Participants (1995). The VEMAP integrated database for modeling United States ecosystem/vegetation sensitivity to climate change. J. Biogeog. 22:857-862.

Karunanithi, N., W. J. Grenney, D. Whitley, and K. Bovee, 1994. Neural networks for river flow prediction. Journal of Computing in Civil Engineering 8(2): 201-219.

Kuligowski, R. J., and A. P. Barros, 1998. Using artificial neural networks to estimate missing rainfall data. Journal of American Water Resources Association 34(6): 1437-1447.

Lane, M. E. P. H. Kirshen, and R. M. Vogel, 1999. Indicators of impacts of global climate change on US water Resources. Journal of Water Resources Planning and Management-ASCE 125(4): 194-204.

Leavesley, G. H., 1994. Modeling the Effects of Climate Change on Water Resources- A Review. Climatic Change 28:159-177.

Li, P. J., 1999. Variation of snow water resources in northeastern China, 1951-1997. Science in China Series D-Earth Sciences 42:72-79.

Loaiciga, H. A., D. R. Maidment, and J. B. Valdes, 2000. Climate change impacts in a regional Karts aquifer, Texas, USA. Journal of Hydrology 227(1-4): 173-194.

Manne, A., R. Mendelsohn, and R. Richeeis, 1993. MERGE- A Model for Evaluating Regional and Global Effects of GHG Reduction policies. Paper presented at the International Workshop on Integrated Assessment of Mitigation, Impacts and Adaptation to Climate Change, 13-15 October 1993, International Institute for Applied Systems Analysis. Laxenburg, Austria. 14pp.

Martin. P., N. J. Rosenberg, and M. S. Mckenney, 1989. Sensitivity of Evapotranspiration in a Wheat field, a Forest, and a Grassland to Changes in Climate and Direct Effects of Carbon dioxide. Climatic Change 14:117-151.

Mauser, W., and S. Schadlich, 1998. Modeling the spatial distribution of evapotranspiration on different scales using remote sensing data. Journal of Hydrology 21(1-4): 250-267.

Mehrotra, K., C. K. Mohan, and S. Ranka, Elements of artificial neural networks. The MIT press, Massachusetts, 344 pp. 1997.

Meigh, J. R., A. A. McKenzie, and K. J. Sene, 1999. A Grid-Based Approach to Water Scarcity Estimates for Eastern and Southern Africa. Water Resources Management 13:85-115.

McFarlane, N. A. G. J. Boer, J. P. Blanchet, and M. Lazare, 1992. The Canadian Climate Centre Second-Generation General Circulation Model and Its Equilibrium Climate. Journal of Climate 5: 1013-1044.

Miller, K. A., 1997. Climate Variability, Climate Change and Western Water. Report to the Western Water Policy Review Avisory Commission. NTIS: Springfield, Virginia.

Mitchell, G., 1999. Demand forecasting as a tool for sustainable water resources management. International Journal of Sustainable Development and World Ecology 6(4): 231-241.

Nash, L. L. and P. H. Gleick, 1993. The Colorado river Basin and Climatic Change: The Sensitivity of Streamflow and Water Supply to variations in Temperature and Precipitation. Report Prepared for the U.S. Environmental Protection Agency, Office of Policy, Planning and Evaluation – Climate Change Division, EPA 230-R-93-009, Pacific Institute for Studies in Development, Environment, and Security, Oakland, California, 91 pp.

National Agricultural Statistics Service (NASS)-USDA 2002

Natural Resources Conservation Service (NRCS) - National Water and Climate Center (NWCC)-USDA 2003.

Ojima, D., L. Garcia, E. Elgaali, K. Miller, T. G. F. Kittel, and J. Lackett, 1999. Potential Climate Change Impacts on Water Resources in the Great Plains. Journal of the American Water Resources Association 35(6): 1443-1454.

Parton, W. J., J. M. O. Scurlock, D. S. Ojima, T. G. Gillmanov, R. J. Scholes, D. S. Schimel, T. Kirchner, J. C. Menaut, T. Seastedt, E. Garcia Moya, A. Kaamnalrut, and J. L. Kinyamario, 1993. Observations and modeling of biomass and soil organic matter dynamics for the grass biome worldwide. Global Biochem. Cycles 7: 785-809.

Parton, M. Hartman, D. S. Ojima, and D. S. Schimel, 1998. DAYCENT and its land surface submodel: description and testing. Global Planetary Change 19:35-48.

Peart, R. M., R. B. Curry, C. Rosenzweig, J. W. Jones, K. J. Boote, and L. H. Allen, Jr, 1995. Energy and irrigation in south eastern U.S. agriculture under climate change. Journal of Biogeography 22: 635-642.

Peterson, D. F. and A. A. Keller. 1990. Irrigation. In P. E. Waggoner (ed.). Climate Change and Water Resources. Wiley. New York. pp 269-306.

Quinn, N. W. T., N. L. Miller, J. A. Dracup, L. Brekke, and L. F. Grober, 2001. An integrated modeling system for environmental impact analysis of climate variability and extreme weather events in the San Joaquin Basin, California. Advances in Environmental Research 5(4): 309-317.

Rango, A., and V. Van Katwijk, 1990. Water Supply Implications of Climate Change in Western North American Basin. International and Transboundary Water Resources Issues, American Water Resources Association 27th Annual Conference Proceedings. AWRA, Bethesda, Maryland.

Rango, A., 1992. Worldide Testing of the Snowmelt Runoff Model with Applications for Predicting the Effects of Climate Change. NORDIC Hydrology 23(3): 155-172.

Rango, A., 1995. Effects of Climate Change on Water Supplies in Mountainous Snowmelt Regions. World Resources Review 7(3): 315-325.

Revelle, R. R. and P. E. Waggoner, 1983. Effects of Carbon Dioxide-induced Climatic Change on Water Supplies in the Western United States. In: Changing Climate. Report on the Carbon Dioxide Assessment Committee, National Academy Press, Washington, D.C., pp 419-432.

Ritschard, R. L., J. F. Cruise, and L. U. Hatch, 1999. Spatial and temporal analysis of agricultural water requirements in the Gulf Coast of the United States. Journal of the American Water Resources Association (JAWRA) 35(6): 1585-1596.

Rosenberg, N. J., B. A. Kimball, P. Martin, and C. F. Cooper. 1990. From climate and CO_2 enrichment to evapotranspiration. In P. E. Waggoner (ed.). Climate Change and Water Resources. Wiley. New York. PP 151-175.

Rosenberg, N. J., P. R. Crosson, K. D. Frederick, W. E. Easterling, III, M. S. McKenney, M. D. Bowes, R. A. Sedjo, J. Darmstadter, L. A. Katz, and K. M. Lemon 1993. The MINK Methodology: Backgound and Baseline. Climatic Change 24: 7-22.

Rosenberg, N. J., D. J. Epstein, D. Wang, L. Vail, R. Srinivasan, and J. G. Arnold, 1999. Possible Impacts of Global Warming on the Hydrology of the Ogallala Aquifer Region. Climatic Change 42(2): 677-692.

Rosenzweig, C. and D. Hillel. 1993. The dust bowel of the 1930s: Analog of greenhouse effect in the Great Plains? Journal of Environmental Quality 22(1): 9-22.

Rosenzweig, C. and D. Hillel. 1998. Climate Change and the Global Harvest: Potential Impacts of the Greenhouse effect on Agriculture. Oxford University Press. New York.

Sahai, A. K., Soman, M. K. and Satyan, V., All India summer monsoon rainfall prediction using an artificial neural network. Climate Dynamics, 2000, 16, 291–302.

Salas, J. D., D. W. Delleur, V. Yevevich, and W. L. Lane, Applied modeling of hydrologic time series, Water Resources Publications, Littleton, CO., USA, 1980.

Schaake, J. C., 1990. From climate to Flow. In P. E. Waggoner (ed.). Climate Change and Water Resources. Wiley. New York. PP 177-206.

Schulze, R., J. Meigh, and M. Horan, 2001. Present and potential future vulnerability of eastern and southern Africa's hydrology and water resources. South African Journal of Science 97(3-4): 150-160.

Shigidi, A. M. T., Solving the inverse problem in groundwater flow by iterative inversion of a neural network, Ph.D. dissertation, Colorado State University, Fort Collins, Colorado, 2000.

Stockton, C. W. and W. R. Boggess, 1979. Geohydrological Implications of Climate Change on Water Resources Development. Report prepared for the U.S. army Coastal Engineering Research Center, Fort Belvoir, Virginia, Contract Rpt. No. CACW 72-78-c0031, 206 pp.

Strzepek, K. M., D. C. Major, C. Rosenzweig, A. Iglesias, D. N. Yates, A. Holt, and D. Hillel, 1999. New method of modeling water availability for agriculture under climate change: The US Cornbelt. Journal of the American Water Resources Association (JAWRA) 35(6): 1639-1655.

Sureerattanan, S., and H. N. Phein, 1997. Backpropagation networks for daily streamflow forecasting. Water Resources Journal, St/ESCAP/SER.C/195, pp.1-7.

Wilson, K. B., T. N. Carlson, and J. A. Bunce, 1999. Feedback significantly influences the simulated effect of CO_2 on seasonal evapotranspiration from two agricultural species. Global Change Biology 5(8): 903-917.

Wolock, D. M. and G. J. MacCabe, 1999. Estimates of Runoff Using Water-Balance and Atmospheric General Circulation Models. Journal of the American Water Resources Association (JAWRA) 35(6): 1341-1350.

APPENDIX A
Parameters Required for Daily Time-Step Calculations of ET

Parameters Required for Daily Time-Step Calculations of ET

Many of the equations presented here are the same as those reported in ASCE Manual 70 (Jensen et al., 1990) and used in FAO-56 (Allen et al., 1998).

Psychrometric and atmospheric variables

Latent Heat of Vaporization (λ)

The value of the latent heat of vaporization, λ, varies only slightly over the ranges of air temperature that occur in agricultural or hydrologic systems. Therefore, a constant value of $\lambda = 2.45$ MJ kg^{-1} is used.

Mean Air Temperature

The mean air temperature, T, for daily time step is calculated as the mean of the daily maximum and daily minimum air temperature.

$$T = \frac{T_{max} + T_{min}}{2}$$

Where:

T = daily mean air temperature (^{o}C)

T_{max} = daily maximum air temperature (^{o}C)

T_{min} = daily minimum air temperature (^{o}C)

Atmospheric Pressure (P)

The mean atmospheric pressure at the weather site is predicted from site elevation using the following formulation:

$$P = 101.3\left[\frac{293 - 0.0065Z}{293}\right]^{5.26}$$

Where:

P = mean atmospheric pressure at station elevation Z (KPa)

Z = weather site elevation above mean sea level (m)

Slope of the Saturation Vapor Pressure-Temperature Curve (Δ)

$$\Delta = \frac{2504 \exp\left(\frac{17.27T}{T+237.3}\right)}{(T+237.3)^2}$$

Where:

Δ = slope of the saturation vapor-temperature curve (KPa $^{o}C^{-1}$)

T = daily mean air temperature (^{o}C)

Saturation Vapor Pressure (e_s)

$$e_s = \frac{e^o(T_{\max}) + e^o(T_{\min})}{2}$$

Where:

e^o(T) = saturation vapor pressure (KPa) at temperature T (^{o}C).

$$e^o(T) = 0.6108 \exp\left[\frac{17.27T}{T+237.3}\right]$$

Actual Vapor Pressure (e_a)

$$e_a = \frac{RH_{mean}}{100}\left(\frac{e^o(T_{\max}) + e^o(T_{\min})}{2}\right)$$

Psychrometric Constant (γ)

$$\gamma = \frac{C_p P}{0.622\lambda}$$

Where:

γ = Psychrometric constant (KPa $^{o}C^{-1}$)

C_p = specific heat of moist air at constant pressure =1.013 KJ $Kg^{-1o}C^{-1}$

Aerodynamic Resistance

$$r_a = \frac{\left[\ln\frac{Z_w - d}{Z_{om}}\right]\left[\ln\frac{Z_p - d}{Z_{ov}}\right]}{(0.41)^2 U_z}$$

Where:

r_a = aerodynamic resistance (s m^{-1})

Z_w = height of wind speed (U_z) measurement

Z_p = height of temperature measurement

d = crop height displacement

Z_{om} = roughness length for momentum transfer

Z_{ov} = roughness length for vapor transfer

and

$Z_{om} = 0.123\ h$

$Z_{ov} = 0.1\ Z_{om}$

$d = 2/3\ h$

Where:

h = mean crop height

For wind speed (U_z) in m s^{-1}:

$$K_1 \frac{0.622\lambda\rho}{P} = 1710 - 6.85T\ ,\ \text{T in } ^\circ\text{C}$$

APPENDIX B
MATLAB SCRIPTS

Script to train, validate and test the ANN

```
%This file contain the training instructions for the matlab file
clear;
clear epochs;
clear err_goal;

load input_file;
x=(input_file);
x1=rot90(x);
x2=flipud(x1);
pn=x2;

load output_file;
y=(output_file);
%my=max(y);
%y1=y/my;
y1=y;
y2=rot90(y1);


% n= number of the data sets used to train the network
n=50;
kk=15;
nn=89;
d=1;
% r=total number of inputs in the problem 1FLOW,2SWE, 2RAIN
r=5;
ro=1;
%month for whic training is considered

%Transform input and output vectors to fall between 0 and 1

%set the s matrix to intialize the weights
s(1:r,1)=0.05;
s(1:r,2)=0.95;


% pt=matrix containing the output FLOW data  assigned for training and testing

in=pn;
out=y2;

%define input matrix "i"
i=in(1:r,:);
```

```
%define the target matrix "t"
t=out(1:ro,:);

%pt=matrix containing the data assigned for training
pt=i(:,d:n);

% g=matrix containing the output data assigned for training
g=t(1,d:n);

% v.P=matrix containing the input data assigned for validation
v.P=i(:,n+1:n+kk);

% v.T=matrix containing the output data assigned for validation
v.T=t(:,n+1:n+kk);

%test.P=matrix containing the input data for testing
test.P=i(:,n+kk+1:nn);

%test.T=matrix containing the output data for testing
test.T=t(:,n+kk+1:nn);

%Number of neurons in the hidden layer
nhl=5;
nh2=5;
%nh3=5;
%nh4=5;
net=newcf(s,[nhl,nh2,ro],{'logsig','logsig','purelin'},'trainlm');

%net.trainParam.lr= 0.05;
%net.trainParam.lr_inc= 1.1;

net.trainParam.show=200;
net.trainParam.epochs=100000;
net.trainParam.goal=1e-4;
[net,tr]=train(net,pt,g,[],[],v,test);

YY=sim(net,test.P);
YT=YY';
save YTT YT  -ascii;
T = test.T';
save TT T -ascii;
YY1=sim(net,pt);
YTR=YY1';
save YTTR YTR  -ascii;
TR = g';
save TTR TR -ascii;
```

```
YV=sim(net,v.P);
YV1=YV';
save YVV YV1  -ascii;
TV = v.T';
save TVV TV -ascii;
```

Script for post-analysis of ANN

```
% This file is to perform a post-training analysis on the network.

a=sim(net,test.P);

for j=1
figure(j)
[slope(j),intercept(j),coeff(j)]=postreg(a(j,:),test.T);
End
```

Script for simulation ANN

```
load input_file;
x=(input_file);
x1=rot90(x);
x2=flipud(x1);
pnew=x2;
pnewn = tramnmx(pnew,minp,maxp);
%[pn,minp,maxp] = premnmx(p); %Rescale between -1 and 1
%load aproo_out.dat;
%y=(aproo_out);
%y1=rot90(y);
%Newdata  x
% x1=2*(x-minp)/(maxp-minp)-1;
%t=y1;

%[tn,mint,maxt] = premnmx(t);
Y=sim(net,pnewn);
[Ytt] = postmnmx(Y,mint,maxt);
YF= Ytt';
save MF YF -ascii
```

APPENDIX C
SENSITIVITY OF ET AND IWR TO CHANGES IN STOMATAL RESISTANCE

Fig. C Percentage changes in ET and IWR from baseline for percentage increase in bulk plant canopy resistance (r_c).